

Article

Earthquake-Triggered Landslides in Greece from Antiquity to the Present: Temporal, Spatial and Statistical GIS-Based Analysis

Spyridon Mavroulis * , Andromachi Sarantopoulou and Efthymios Lekkas

Department of Dynamic, Tectonic, Applied Geology, Faculty of Geology and Geoenvironment, School of Sciences, National and Kapodistrian University of Athens, 15784 Athens, Greece; asaranto@geol.uoa.gr (A.S.); elekkas@geol.uoa.gr (E.L.)

* Correspondence: smavroulis@geol.uoa.gr

Abstract: This research provides a detailed analysis of earthquake-triggered landslides (ETLs) in Greece, spanning from antiquity to the present, with an emphasis on their temporal, spatial, and statistical characteristics. Supported by published scientific sources and geographic information systems (GIS) tools, we detected 673 landslides triggered from 144 earthquakes in Greece. With 166 ETLs associated with historical earthquakes and 507 with recent ones, the analysis reveals that regions in western Greece, including the Ionian Islands and the Peloponnese, exhibit the highest ETL frequencies, a trend strongly related to their seismotectonic regime. Most ETLs have occurred in geotectonic units belonging to the External Hellenides. Limestone-dominated lithologies and post-alpine deposits were identified as particularly susceptible to ETLs. These are strongly associated with earthquakes with magnitudes ranging from 5.5 to 7.0. Rockfalls constitute the most frequent type of ETLs in Greece, accounting for nearly half of all documented events. Coastal and offshore landslides, though less frequent, still pose unique risks for Greece. ETLs have mainly been observed in the very high and high susceptibility areas. The impacts of ETLs on both natural and built environments are profound, with destruction of buildings and infrastructure exacerbating the public health impact and socio-economic toll of such events.

Keywords: earthquakes; Greece; landslides; rockfalls; earthquake-triggered landslides; GIS; landslide dataset



Academic Editor: Faccini Francesco

Received: 20 December 2024

Revised: 22 January 2025

Accepted: 29 January 2025

Published: 2 February 2025

Citation: Mavroulis, S.; Sarantopoulou, A.; Lekkas, E. Earthquake-Triggered Landslides in Greece from Antiquity to the Present: Temporal, Spatial and Statistical GIS-Based Analysis. *Land* **2025**, *14*, 307. <https://doi.org/10.3390/land14020307>

Copyright: © 2025 by the authors. Licensee MDPI, Basel, Switzerland. This article is an open access article distributed under the terms and conditions of the Creative Commons Attribution (CC BY) license (<https://creativecommons.org/licenses/by/4.0/>).

1. Introduction

Earthquakes are considered as geophysical hazards [1,2] and can cause a multitude of impacts on the natural environment, on elements of the built environment (buildings, networks and infrastructure) and consequently on humans and their activities. Earthquake environmental effects (EEEs) comprise various phenomena, which can be divided into (i) primary effects, strongly related to the seismic energy and surface expression of the seismogenic fault and (ii) secondary ones, which are associated with the strong ground motion [3].

The secondary EEEs include eight categories of effects, as follows: (i) hydrological anomalies; (ii) sea waves/tsunamis; (iii) ground cracks; (iv) slope failures; (v) tree shaking; (vi) liquefaction phenomena; (vii) dust clouds; and (viii) jumping stones [3]. Among these effects, earthquake-triggered landslides (ETLs) are characterized by a high potential to cause some of the greatest impacts on adjacent human structures and subsequently on the affected population [4–9].

Casualties caused by ETLs result from the rapid mobilization of unstable geological materials and the subsequent crushing impact and collapse of buildings and infrastructure due to slope failures [8]. Additionally, they are linked to the high-velocity transport of debris across terrains with gentle slopes [10]. ETLs account for 70% of all earthquake-related fatalities not directly caused by ground shaking but instead by secondary effects [4]. Among these, at least 90% of fatalities are attributed to rockfalls, rock avalanches, and rapid soil flows, despite the rarity of rock avalanches and rapid soil flows [10].

The societal impacts of ETLs extend beyond direct effects, such as the destruction of buildings and infrastructure, to indirect effects, which involve damage to critical lifelines like road networks, dams, and utilities [11–13]. Such damage significantly increases the likelihood of disruptions to socio-economic activities, including transportation and communication failures. These disruptions can affect emergency response and recovery efforts, leading to increased casualties due to delays in administering first aid and transporting injured individuals to healthcare facilities.

ETLs have been documented as far back as 1789 BC in China [14,15]. The most widely adopted ETLs classification was proposed by Keefer [10], who studied data from 40 historical earthquakes across the globe, with magnitudes ranging from 5.2 to 9.5 and occurring in diverse geographic, geological, and seismotectonic settings. Keefer's classification considers the type of movement, the extent of internal disruption in the mobilized material, and the morphological, lithological, and geological characteristics of the impacted regions [10].

ETLs are categorized into 14 distinct types, grouped into three main categories, as follows: (i) disrupted slides and falls, (ii) coherent slides, and (iii) lateral spreads and flows [9]. The first category includes falls, slides, and avalanches in both rocks and soils; the second consists of slumps, block slides in rock and soil, and slow earth flows; while the third encompasses soil lateral spreads, rapid soil flows, and subaqueous landslides [9]. The most prevalent ETLs are highly disrupted landslides, which involve falls, slides, and avalanches of rock or soil, originating on steep source slopes and extending onto gentler slopes [10,16]. The total number of ETLs generally correlates with earthquake magnitude, ranging from a few dozen for most earthquakes with $M < 5.5$ to several thousand for those with $M > 8.0$ [10].

Since the extensive research on ETLs worldwide conducted by Keefer in 1984 [10] and Rodriguez et al. in 1999 [17], several ETL studies have been performed both at the national and the local level. Among others, Hancox et al. in 1997 and 2002 [18,19] and Rosser et al. in 2007 [20] have published relevant research and databases for New Zealand; Papadopoulos and Plessa in 2000 [21] for Greece; Bommer and Rodriguez in 2002 [22] for Central America; Rodriguez in 2006 [23] for Colombia; Devoli et al. in 2007 [24] for Nicaragua; Chen et al. in 2012 [25] for southwest China; and Prestinizi and Romeo in 2000 [26] and Martino et al. in 2014 [27] for Italy. Several studies draw upon published scientific sources, e.g., [10,21,22], providing a foundation of contemporary research and analysis. Other studies place significant emphasis on the use and reevaluation of historical sources, e.g., [24], highlighting their value in uncovering critical insights about the nature, timing, and spatial distribution of landslides. Such insights are particularly valuable for countries where the investigation of landslides is still an emerging field, as they support the development of a more comprehensive understanding of past events to inform current and future research efforts.

Recording these landslide locations and, by extension, highlighting landslide-prone areas, is an important tool in the efforts of scientists and stakeholders to protect the built environment, to reduce human and economic losses and to build resilient societies against earthquakes and the resulting geohazards. The knowledge gained from such studies enables all those involved in preventing and managing the effects of disasters and reduc-

ing disaster risk to support policy making, urban planning, construction practices and emergency response strategies, contributing to a much safer and more prepared society in earthquake-prone regions affected by ETLs among other adverse effects.

The research on systematically cataloging ETLs in Greece is not widespread. The research of landslides in Greece primarily consists of studies that offer maps of landslides across the country [28–31] and maps of settlements affected by landslides [32], alongside several studies that provide findings from field surveys in regions impacted by both earthquakes and ETLs, where the latter are documented among other consequences.

The first attempt to establish a comprehensive landslide recording system in Greece was made by Koukis and Ziourkas in 1991 [28]. They performed a statistical analysis of 800 landslide case histories in Greece from 1949 to 1986. The data were collected from 1500 coded engineering reports and studies conducted by various public institutions, including the Hellenic Authority of Geological and Mining Research (formerly the Institute of Geology and Mineral Exploration of Greece) and the Central Union of Greek Municipalities. Their study covered cases from villages and surrounding areas, as well as along the road network, examining the frequency of landslides and their effects on various geological formations, altitudes, rainfall, slope angles, etc. They also explored certain interrelationships and produced an engineering geological map, along with maps of landslide distribution and frequency zones.

A similar methodology was adopted by Koukis et al. in 1994 [29], who expanded the dataset from Koukis and Ziourkas [28] by analyzing 1116 landslide case histories from 1949 to 1991. They focus on the frequency distribution of landslide controlling factors, presenting their results in tables and charts. Further updates and expansions to the number of landslides and the time period covered were made by Koukis et al. in 1997 [30], with data on 1200 landslides from 1949 to 1995; by Koukis et al. in 2005 [31], with 1300 landslides from 1950 to 2004; and by Sabatakakis et al. in 2013 [33], with 1635 landslides up to 2010.

While these studies identify landslide locations, they do not provide additional qualitative or quantitative landslide information regarding their causes, the timing of their occurrence or the volume of the mobilized material. As a result, the landslides recorded in these studies cannot be linked to specific triggering factors and events, such as earthquakes, rainfall, or human activity. Therefore, the maps produced in these studies are not particularly useful for investigating ETLs in Greece, as they do not indicate the causative event.

In addition, Papadopoulos and Plessa in 2000 [21] compiled data on 47 earthquake-induced landslides from 1650 to 1995, with magnitudes ranging from 5.3 to 7.9. Their analysis led to magnitude–distance relationships for ETLs in Greece, which are consistent with global models. They also examined the spatial distribution of ETLs, their size distribution, and the maximum epicentral distances of landslides. However, the data they collected were neither sufficient nor precise enough to be used for analyzing other factors, such as the geomorphology and geology of the affected sites, the lithology and age of the mobilized geological formations and the mechanical properties and the geotechnical behavior of the affected formations. According to Papadopoulos and Plessa [21], the historical descriptions of ETLs in Greece are often too vague to serve as a reliable foundation for modern scientific analysis. After reviewing hundreds of documents, they concluded that a database containing data from the 16th century onward could be valuable for further research.

During the last fifteen years, various efforts have been made to assess and map the landslide susceptibility in several earthquake-prone areas of Greece, aiming to highlight regions most susceptible and vulnerable to ETLs. The most prominent examples come from the central part of the Ionian Islands (western Greece), particularly the studies of Papathanassiou et al. [34] and Polykretis et al. [35] for Lefkada and Mavroulis et al. [36] for Cephalonia. In these studies, new earthquake-triggered landslide inventories were

compiled and then compared with landslide susceptibility maps to validate the applied models and to highlight the most susceptible areas. On a national scale, Sakkas et al. [37] considered various factors that favor landslide occurrence, including landslide locations for model validation, without categorizing them based on the triggering factor.

In this article, we initially review and reevaluate all available scientific literature on ETLs and their causative seismic events in Greece (Figure 1) and present new data on the most recent occurrences. The study further examines the geographical, qualitative, and quantitative characteristics of ETLs on a national scale, encompassing both continental and island regions and spanning a broad temporal range from antiquity to the present. The analysis generated a rich dataset of hundreds of ETLs in Greece that have never been published before, offering a comprehensive perspective and providing the first in-depth temporal, spatial and statistical analysis of these phenomena. All detected information about ETLs in Greece were then analyzed temporally, spatially and statistically, based on (i) geological properties of the affected sites (geotectonic unit, geological formations, lithology and age of formations); (ii) morphological characteristics (elevation and slope); (iii) land cover data; (iv) seismic hazard; and (v) landslide susceptibility indices.

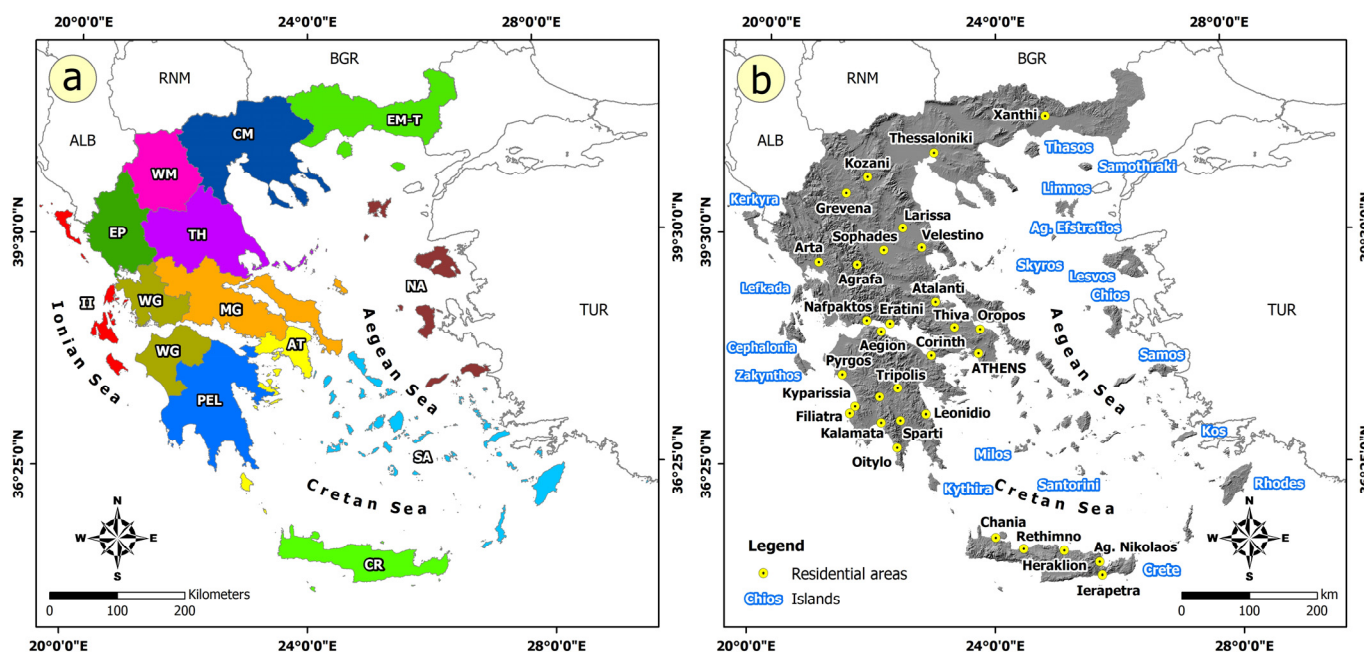


Figure 1. (a) Map of the regions of Greece. EM-T: Eastern Macedonia and Thrace; CM: Central Macedonia; WM: Western Macedonia; EP: Epirus; TH: Thessaly; WG: Western Greece; II: Ionian Islands; PEL: Peloponnese; NA: North Aegean; SA: South Aegean; CR: Crete. Greece is bounded to the north by Albania (AL), Republic of the North Macedonia (RNM), and Bulgaria (BG) from W to E, respectively; to the east by Turkey (TUR); to the west by the Ionian Sea; and to the south by the Eastern Mediterranean Sea. (b) Residential areas of Greece affected by earthquakes and ETLs and described in the text.

At the same time, through the review of existing literature and the search for information on ETLs in Greece, a presentation and categorization of the effects of ETLs on the natural environment, including changes in riverbeds, stream valleys and mountain slopes among other landforms, is carried out. Impacts on several elements of the built environment, such as buildings, networks and infrastructure, are also presented, as well as impacts on the population, including direct effects (human losses and injuries) and indirect health effects (sporadic cases, outbreaks and epidemics of infectious diseases).

The temporal, spatial and statistical analysis in this research is supported by a wider range of tools in a geographic information system (GIS) environment, providing functions for spatial analysis and summary statistics, management of geospatial information and the creation of new dataset based on analytical procedures. These tools focus on the collection of earthquake- and landslide-related information and data, the creation of new data and the correlation between different features and attributes and offer statistical analysis of fields and parameters.

Such studies are of multidimensional importance for mitigating the effects of earthquakes and the triggered landslides. The recording of secondary EEEs and the analysis of their qualitative and quantitative parameters allows for the detection and understanding of the factors controlling the occurrence of ETLs. Moreover, the possible correlation of the effects of landslides with the above factors can contribute to the identification and the emergence of zones that are susceptible to the occurrence of ETLs, reducing the disaster risk by taking the necessary structural and non-structural measures.

2. Methodology

This paper is based on the results of the research conducted in the context of the doctoral dissertation of Mavroulis [38] on the EEEs of historical and recent earthquakes in Western Greece, including the central and southern Ionian Islands (Lefkada, Cephalonia, Ithaki and Zakynthos) and the western Peloponnese and on the Master's dissertation of Sarantopoulou [39] on the spatial distribution and properties of landslides caused by historical and recent earthquakes along the Hellenic Island Arc. The earthquakes and the triggered landslides recorded in the above dissertations were enriched with various scientific sources. All of these ETLs in Greece are presented in the frame of a temporal, spatial and statistical analysis supported by GIS tools and functions.

The applied methodology initially includes a review of the available scientific literature containing information on historical and recently recorded ETLs in Greece. The information provided was obtained from the following sources:

- Articles in scientific journals that included assessment and mapping of EEEs, including ETLs;
- Publications at national and international conferences that included assessing and mapping EEEs, including ETLs;
- Scientific books containing catalogues and information on earthquakes in Greece and the Eastern Mediterranean region and their effects on the natural and built environment, including ETLs among other phenomena and damage;
- Official deliverables of applied research projects containing information on earthquakes and their impact on the natural and built environment;
- Official reports from field and reconnaissance surveys on the earthquake impact and subsequent landslides on the affected areas;
- Doctoral dissertations on EEEs, including ETLs.

For the research on the ETLs in Greece, a total of 85 scientific sources were used. Of these 85 sources, those from which the most information on ETLs was obtained were the scientific books that contained descriptions of many earthquakes in Greece, such as the following:

- The research of Papazachos and Papazachou [40] on earthquakes in Greece (data from 52 earthquakes were used in this study). This publication was preceded by two previous editions in 1989 and 1997 for earthquakes in Greece. In the present study, the most recent and updated edition of 2003 has been used, with data on earthquakes and their subsequent effects up to 2001.

- The scientific research of Ambraseys [41] on seismicity and major earthquakes in the Mediterranean and the Middle East up to 1900 (56 earthquakes);
- The chronicle of earthquakes in Greece from antiquity to the present day by Spyropoulos [42] (52 earthquakes);
- The research on magnitude–distance relations for earthquake-induced landslides in Greece compiled by Papadopoulos and Plessa [21] (36 earthquakes);
- The research of Ambraseys and Jackson [43] on the seismicity of, and related regimes in, central Greece from 1890 to 1998 (24 earthquakes);
- The research of Ambraseys and Jackson [44] on the seismicity of the Corinth Gulf from 1694 and for the next 300 years (12 earthquakes);
- The research of Soloviev et al. [45] on tsunamis in the Mediterranean Sea from 2000 BC to 2000 AD (14 earthquakes).

Another 20 sources provided information on more than two earthquakes, while the remaining 58 sources provided information on only one earthquake event each. In relation to the number of sources exploited, more details are presented in Figure 2. The available sources were reviewed with an emphasis on ETLs. The data extracted, evaluated and used in this research were not only related to the generated landslides but also to the causative earthquakes. Regarding earthquakes, the extracted information includes the origin time, the epicenter coordinates (latitude and longitude), the focal depth in km, the magnitude, the maximum intensity and the affected area.

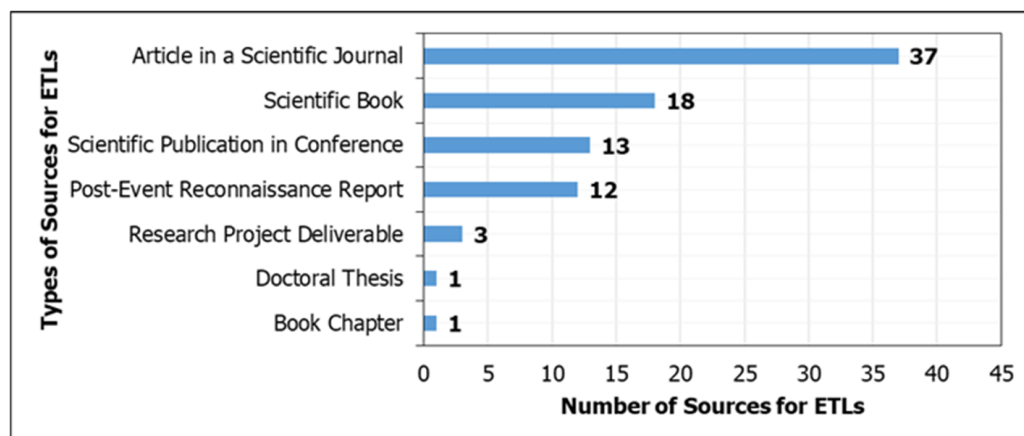


Figure 2. Types and numbers of sources used and evaluated for the temporal, spatial and statistical analysis of ETLs in Greece.

For a more complete and accurate presentation of these data, earthquake catalogues were used, including the updated and expanded catalogue of earthquakes for Greece and adjacent regions from 1900 to 2009 compiled by Makropoulos et al. [46]; the SHARE European Earthquake Catalogue (SHEEC) 1000–1899 presented by Stucchi et al. [47]; and its subsequent version, titled the European PreInstrumental Earthquake Catalogue (EPICA) and updated by INGV [48] and Rovida et al. [49]. For earthquakes from antiquity to 1000, data presented by the catalogue of Papazachos and Papazachou [40] for Greek earthquakes were also used.

The compilation of the SHARE European Earthquake Catalogue (SHEEC) 1000–1899 was undertaken as part of the European Commission-funded project “Seismic Hazard Harmonization in Europe” (SHARE; 2009–2012). This initiative was built on the foundational work and insights gained during the EC I3 project “Network of Research Infrastructures for European Seismology” (NERIES; 2006–2010). This project incorporated a significant component dedicated to the creation of the “European Archive of Historical Earthquake Data” (AHEAD), aiming to systematically collect, archive, and process historical seismic

data. Central to this effort was the development of standardized methodologies for extracting earthquake parameters in a consistent manner from macroseismic data. AHEAD played a pivotal role in finalizing the SHEEC catalogue by resolving duplications, eliminating numerous spurious events, and incorporating the most recent and reliable historical earthquake datasets, ensuring a robust and harmonized seismic record for Europe.

The EPICA version 1.1 includes a total of 5703 earthquakes that satisfy the criteria of either a maximum observed intensity equal or larger than V or a moment magnitude equal or larger than 4.0. This compilation is based on data derived from 160 sources of macroseismic data points (MDPs) and 39 regional catalogues obtained through AHEAD. For 3297 of these earthquakes, parameters have been re-evaluated using standardized methodologies applied directly to the MDPs.

The process of identifying the locations of the ETLs and incorporating them into the results of the present research involved several steps, combining evaluation of existing literature, conducting fieldwork, analyzing relevant data and using geographic information systems (GIS) for further analyzing ETLs. Regarding the availability of the geographic information of landslides in the evaluated sources, many of them included maps of earthquake-triggered landslide locations [e.g., Ambraseys and Jackson [43] for earthquakes generated from 1890 to 1988 in central Greece and in 1997 for earthquakes generated from 1694 to 1821 in the Gulf of Corinth [44]], which made it easy to identify the location in a GIS environment after georeferencing the maps, digitizing the available information and adding relative properties in appropriately selected fields in attribute tables. Identifying the locations of ETLs in sources that did not include landslide maps was accomplished by a combined use and evaluation of all available information and by further exploitation of all available cartographic material, including topographic, geological, engineering geological, seismotectonic, and landslide susceptibility maps.

A large part of the locations of landslides triggered by both historical and recent earthquakes were also verified in the field during fieldwork conducted by Mavroulis [38] and Sarantopoulou [39], especially in western Greece and with an emphasis on the Ionian Islands, Peloponnese, and Crete. Furthermore, ETLs were either detected or verified by the authors of the present study in several earthquake-affected areas of the country during post-event field surveys for assessing the impact of the following:

- the 1986 Kalamata (southwestern Peloponnese) earthquake by Mariolakos et al. [50] and Fountoulis and Mavroulis [51];
- the 1988 Vartholomio (western Peloponnese) earthquake by Lekkas et al. [52];
- the 1992 Milos (Cyclades Island complex) earthquake by Papanikolaou et al. [53];
- the 1993 Pyrgos (western Peloponnese) earthquake by Lekkas et al. [54];
- the 1995 Grevena-Kozani earthquake by Lekkas et al. [55];
- the 1995 Aegion earthquake by Lekkas et al. [56];
- the 1999 Athens earthquake by Lekkas [57];
- the 2006 Kythera earthquake by Lekkas et al. [58] and Lekkas and Danamos [59];
- the 2008 Andravida earthquake by Mavroulis et al. [60,61];
- the 2017 Lesvos (NE Aegean) earthquake by Lekkas et al. [62];
- the 2017 Kos (NE Aegean) earthquake by Lekkas et al. [63];
- the 2020 Samos (eastern Aegean) earthquake by Mavroulis et al. [64];
- the 2021 Thessaly (central Greece) earthquake by Lekkas et al. [65];
- the 2021 Arkalochori (Crete) earthquake by Mavroulis et al. [66];
- the 2021 Zakros and the 2023 Samaria earthquakes in Crete in the frame of the present study.

Furthermore, cartographic material was used to extract geographic, qualitative and quantitative information on ETLs. This source comprises maps with information about the geological structure of the affected areas, the lithology and age of the affected formations and the mechanical characteristics and the geotechnical behavior of the mobilized formations. They also comprise qualitative information on the landslide type, the morphological characteristics of the landslide-affected site (elevation, slope), the land use and the landslide susceptibility of the unstable areas. The cartographic material is presented in detail in Table 1.

Table 1. Raster data used for the temporal, spatial and statistical analysis of ETLs in Greece along with their sources.

Data	Type	Scale/Cell Size	Source
Geological Map of Greece	Raster	1:500,000	[67]
Engineering Geological Map of Greece	Raster	1:500,000	[68]
Seismotectonic Map of Greece	Raster	1:500,000	[69]
Geotectonic Map of Greece: Geotectonic Units and Tectonostratigraphic Terranes	Raster	1:200,000	[70]
Seismic Hazard Zonation Map	Raster		[71]
CORINE Land Cover (CLC) 2018	Raster	1:100,000	[72]
European Landslide Susceptibility Map version 2 (EL SUS v2)	Raster	European scale/200 m	[73]

The Geological Map of Greece, at a scale of 1:500,000 [67] includes the geological formations of the country classified into (i) post-alpine deposits, (ii) alpine formations, (iii) pre-alpine series, and (iv) metamorphic, (v) igneous and (vi) volcanic rocks. The Engineering Geological Map of Greece [68] includes 28 categories of formations with different mechanical properties and geological, hydrogeological, geotechnical and other geo-environmental information. The Seismotectonic Map of Greece [69] comprises seismological and geological information, including the lithology and the mean density of geological formations, the seismic velocity of P waves, tectonic structures including faults ruptured since the Pliocene, and epicenters of earthquakes with magnitudes equal or larger than 6.5 along with the fault-plane solutions. The Geotectonic Map of Greece [70] comprises the geotectonic units and the tectonostratigraphic terranes of Greece.

The Seismic Hazard Zones map of Greece is divided into sub-regions based on the maximum expected peak ground acceleration (PGA) for a 475-year recurrence period [71], as follows: (a) Zone I, with an expected PGA of 0.16 g; (b) Zone II, with an expected PGA of 0.24 g; and (c) Zone III, with an expected PGA of 0.36 g.

CORINE Land Cover (CLC) 2018 is a pan-European land cover and land use inventory with 44 thematic classes, ranging from broad forested areas to individual vineyards [72]. The product is updated with new status and change layers every six years, with the most recent update made in 2018.

The European Landslide Susceptibility Map version 2 (EL SUS v2) covers all European Union member states except Malta, and several neighboring countries [73]. The map has been produced by regionalizing the study area based on elevation and climatic conditions, followed by spatial multi-criteria evaluation modelling using pan-European (i) slope angle, (ii) shallow sub-surface lithology, and (iii) land cover spatial datasets as the main landslide conditioning factors [74]. In addition, (v) the location of over 149,000 landslides across Europe, provided by various national organizations or collected by the authors, has been used for model calibration and map validation [74]. This map shows the distribution of

landslide susceptibility in 5 classes with the following coding: 0 = no data, 1 = very low, 2 = low, 3 = moderate, 4 = high, 5 = very high [74].

Following the map georeferencing and the creation of suitable files for editing and managing landslide geospatial data within GIS environment, we assess the frequency of ETLs across various parameters by utilizing the aforementioned geospatial data. This information, available in both vector and raster formats, was analyzed and processed to extract relevant geographical, qualitative, and quantitative details for each ETL site, thus providing valuable insights into their spatial distribution and underlying patterns. For this analysis, we used a suite of specialized tools in ESRI ArcMap [75], including the following:

- Reclassify (Reclass toolset in Spatial Analyst Toolbox): to reclassify raster files;
- Slope (Surface toolset in Spatial Analyst Toolbox): to convert digital elevation models (DEMs) into slope rasters;
- Spatial Join (Overlay toolset in Analysis Toolbox): to assign properties from thematic layers to the ETLs;
- Summary Statistics (Statistics toolset in Analysis Toolbox): to calculate the frequency of ETLs based on various parameters;
- Near (Proximity toolset in Analysis Toolbox): to calculate the epicentral distances of the detected ETLs.

In addition, data were obtained on the impacts of ETLs on the natural environment (mainly on hillsides, river and stream beds and the coastal zone), on adjacent elements of the built environment (buildings, networks and infrastructure), and subsequently on the affected population (fatalities and injuries).

Using the point geometries of the detected ETLs in Greece and the epicenters of the causative earthquakes as well as the seismological properties derived from the relevant earthquake catalogues, we calculated the epicentral distances for all available landslides and then the maximum epicentral distances of ETLs for each earthquake. The maximum epicentral distances of landslides were paired with the magnitudes of the causative earthquakes and plotted on a graph to visualize their relationship. The distribution of these data points was further compared with the upper-bound curve delineating the maximum observed epicentral distances for disrupted slides and falls, as proposed by Keefer [10,15]. Keefer's curve, derived from a comprehensive dataset of 40 globally distributed earthquakes, represents the theoretical upper limit of epicentral distances at which ETLs are likely to occur for specific magnitudes. This comparison provides a critical benchmark for assessing the spatial extent of landslide impacts in relation to earthquake magnitude.

While searching relevant information, it was found that landslides were triggered by historical earthquakes that occurred before 1900, as well as earthquakes dating back to antiquity (BC). The documentation of these secondary EEEs is limited to very general characteristics, such as the wider area in which the ETLs occurred, or a general description of their type without further details. This makes it difficult to determine the exact location of the event.

For this reason, it was considered necessary to implement a location reliability index (LRI) for the ETLs in Greece. The adopted LRI comprises 4 location approximation classes for the landslide location: (i) 0–100 m; (ii) 0–1 km; (iii) 0–10 km; and (iv) >10 km. Depending on the accuracy of the determination of the landslide location as derived from the available properties, an LRI value was assigned to each landslide location.

These indices have been widely used in studies of recent earthquakes and their impact on the natural and built environment in various seismotectonic settings. Typical examples are the applications of such indices for the primary and secondary environmental effects of the 28 December 1908, $M_w = 7.1$ earthquake in Messina (Italy) by Comerchi et al. [76]; the August 1953 seismic sequence in the central part of the Ionian Islands by Mavroulis

and Lekkas [13], which included three of the most destructive earthquakes in the recent history of Greece; and also historical earthquakes, such as the 4 February 1867 Cephalonia earthquake by Mavroulis et al. [77], which is the largest recorded earthquake in the central part of the Ionian Islands (western Greece).

Due to the inherent uncertainties in historical studies attributed to general descriptions and related interpretations, similar indices could be used for assessing the information reliability [13]. These indices usually comprise three reliability classes: (i) low; (ii) moderate, and (iii) high. Due to the type of sources used, that have been evaluated and widely accepted by the scientific community, the vast majority of the detected and present information for ETLs in Greece is considered reliable (high information reliability class). Where this information has a lower level of reliability, it has already been highlighted in the original sources by the respective researchers and authors and is certainly not taken into account in this research.

The steps of the applied methodology are summarized in Figure 3.

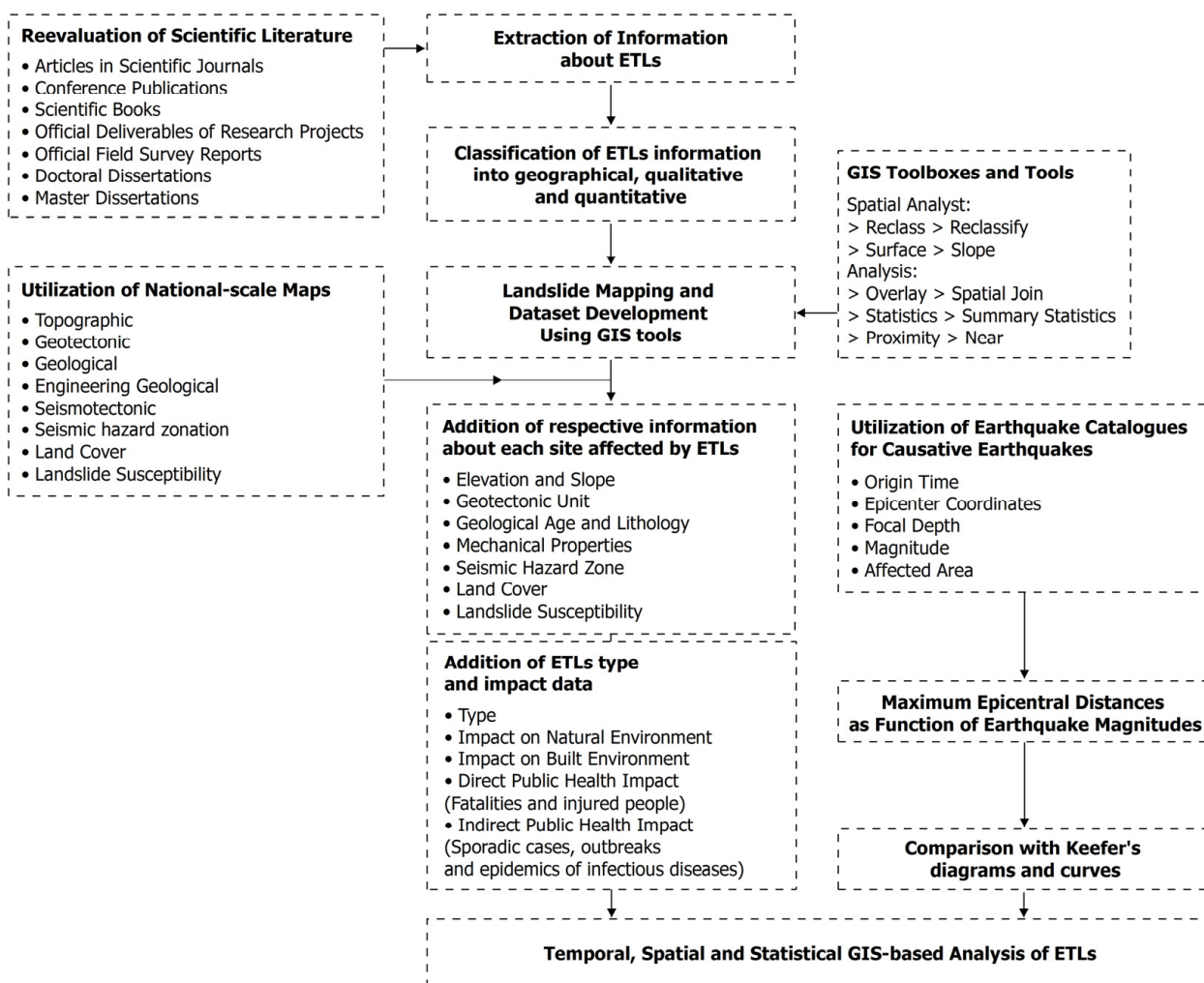


Figure 3. Flow chart of the applied methodology.

3. Regional Setting

3.1. Morphology

Greece is located in the southernmost part of the Balkan Peninsula. It is bordered to the north by Albania, the Republic of North Macedonia, and Bulgaria from W to E, respectively; to the east by Turkey; to the west by the Ionian Sea; and to the south by the Eastern Mediterranean (Figure 4). It has a total area of 131,957 km² with the terrestrial part amounting to 130,647 km² and the remaining 1310 km² being rivers, lakes and other

water bodies within its terrestrial part. A proportion of 80% of Greece is constituted by mountainous terrain. The main mountain range of mainland Greece is Pindos, which, with a NW–SE strike, a length of 230 km and a maximum width of 70 km, separates the wider region of Epirus to the west and the regions of Macedonia and Thessaly to the east (Figure 4).

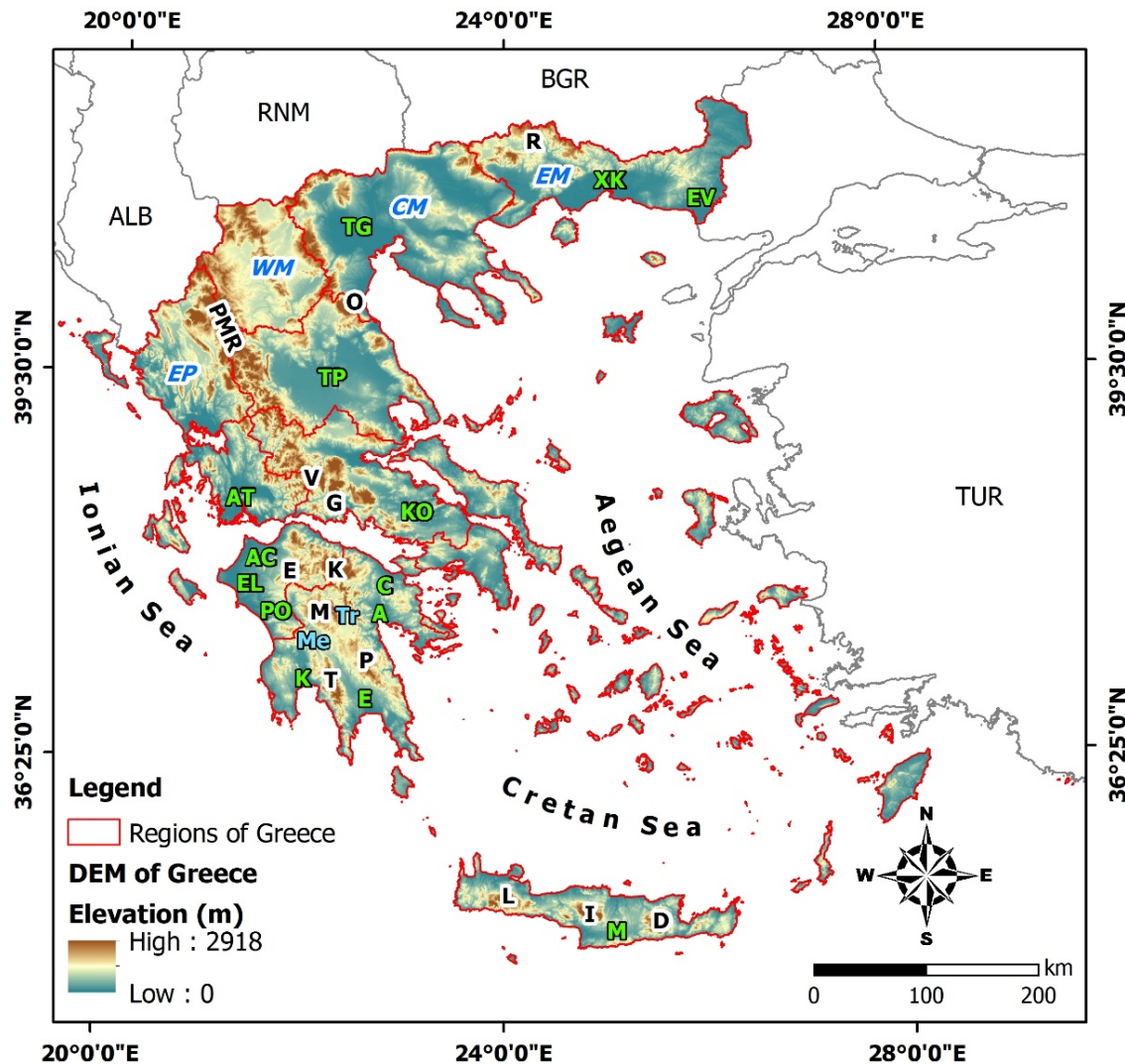


Figure 4. Morphological map of Greece with the main morphological structures, including mountains, plateaus and lowlands. Green letters represent basins and lowlands: EV: Evros; XK: Xanthi-Komotini; TG: Thessaloniki-Giannitsa; TP: Thessalian plain; KO: Kopais; AT: Aetoliko; AC: Achaia; EL: Elis; PO: Pyrgos-Olympia; K: Kalamata; E: Evrotas; A: Argolis; C: Corinth; M: Messara. Black letters represent mountains: R: Rhodope; O: Olympus; PMR: Pindos Mountain Range; V: Vardoussia; G: Ghiona; E: Erymanthos; K: Kyllini; M: Mainalo; T: Taygetos; P: Parnon; L: Lefka; I: Idi (Psiloritis); D: Dikti. Blue letters represent plateaus: Me: Megalopolis; Tr: Tripolis. Italic letters represent regions of Greece: EP: Epirus; WM: western Macedonia; CM: central Macedonia; EM: eastern Macedonia.

Further south, in the Peloponnese, the mountainous terrain is represented by the Peloponnesian Mountains, including, from north to south, Panachaiko, Erymanthos, Kyllini, Mainalo, Taygetos and Parnon Mts, which separate the extensive lowlands of Achaia, Elis and Messinia in the west from the limited lowlands of Corinth, Argolis and Laconia in the east (Figure 4). The mountainous character is also observed further south on Crete and is represented by the Lefka, Idi (Psiloritis) and Dikti (Lassithian) Mts (Figure 4). Large mountains are also found in other regions of Greece, such as the Olympus Mt, which forms

the boundary between Thessaly in the south and Macedonia in the north, with the highest elevation in Greece (2918 m), and the Rhodope Mts, which form the natural boundary between Greece in the south and Bulgaria in the north (Figure 4).

From south to north, the lowland areas are located in the central part of Crete (Messara), in the western Peloponnese (Pyrgos—Olympia basin), in the eastern Peloponnese (Argolis plain), in the eastern part of mainland Greece (Kopais plain), in Thessaly (Thessalian plain), in central Macedonia (Thessaloniki—Giannitsa plain) and in Thrace (Xanthi, Komotini and Evros River plains) (Figure 4). In addition to the lowlands, there are also important plateaus, such as the Megalopolis and Tripolis plateaus in the Peloponnese and the Omalos and Lassithi plateaus in Crete (Figure 4).

Along the margins of the above morphological units, faults and fault zones develop. The majority of these have been classified as active, while many of them are considered seismic [78,79]. The synergy of endogenous forces (tectonic deformation and earthquakes) and exogenous processes (weathering and erosion) form a rugged morphology, prevailed by steep fault scarps and other primary tectonic landforms that make extensive areas susceptible to the generation of primary and the triggering of secondary EEEs, including landslides, among other destructive phenomena.

3.2. Geodynamic Setting

The Hellenides belong to the Alpine system and in particular to the southern branch of the Tethys orogenic system [80]. The Hellenic Arc is about 1500 km long. The main characteristic of the Hellenic Arc is its morphotectonic trend. It initiates with a NNW–SSE trend in Albania and mainland Greece. Then, it bends to E–W from Kythira to Crete and then to NE–SW from the Dodecanese island complex and Lysia of Southwest Asia Minor to Isparta and Antalya, in the intersection zone between the Hellenic and Taurus Arcs [80,81] (Figure 5). Thus, a right angle is formed between the two branches of the Hellenic Arc.

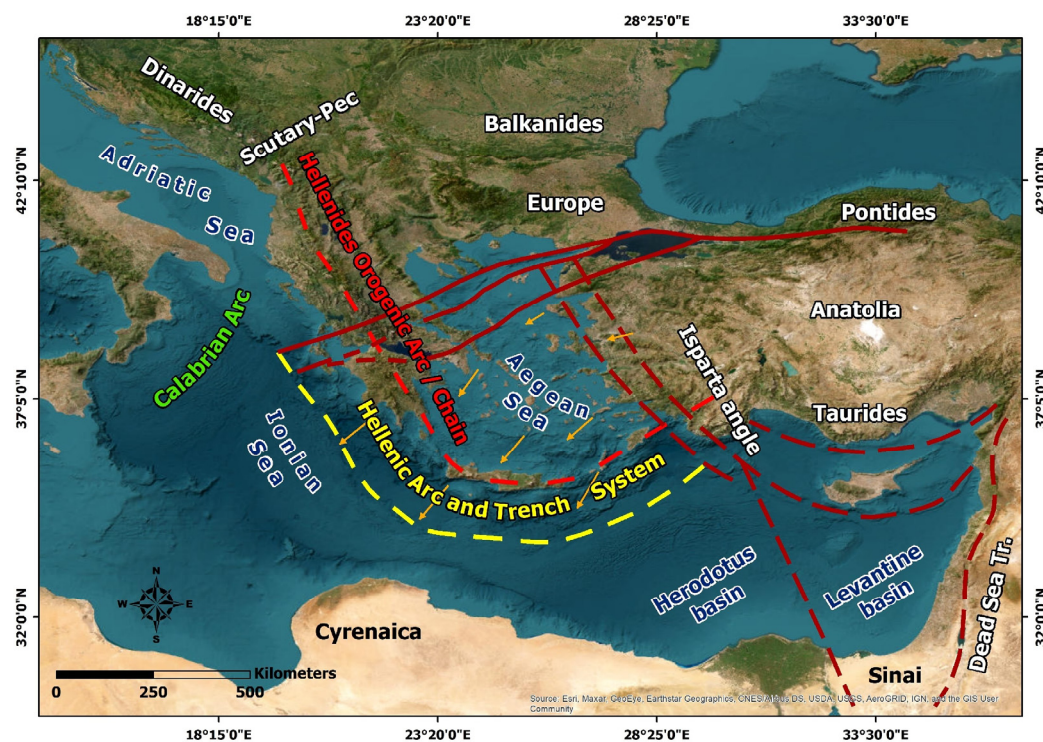


Figure 5. The Hellenides orogenic arc and the modern Hellenic Arc and Trench system, which, since the Late Miocene, is limited to a small segment of the previous structure at the front of the newly formed Aegean microplate. The depicted structures are derived from Papanikolaou [80].

The main characteristic of the Hellenic Arc is that it is the only segment of the entire Tethys system where orogeny due to plate convergence continues and it is characterized by geodynamic characteristics of an evolving orogenic arc. This is because the Eastern Mediterranean, in particular the Ionian Sea area, is the last remnant of the Tethys Ocean that has not yet fully participated in the Alpine orogeny and which represents the still undeformed passive margin of the African plate, whose boundary is close to the present-day coastline of Libya and Egypt [80]. In contrast, along the entire remaining length of the Tethys alpine system, the collision between Eurasia and the various parts of the former Gondwana has already occurred.

The present-day Hellenic Arc and Trench system [82] is restricted to a small arcuate section, which is bounded to the north by the Cephalonia Transform Fault Zone and to the east by complex structures that developed sub-parallel to the coastal zone of western Anatolia (Figure 6).

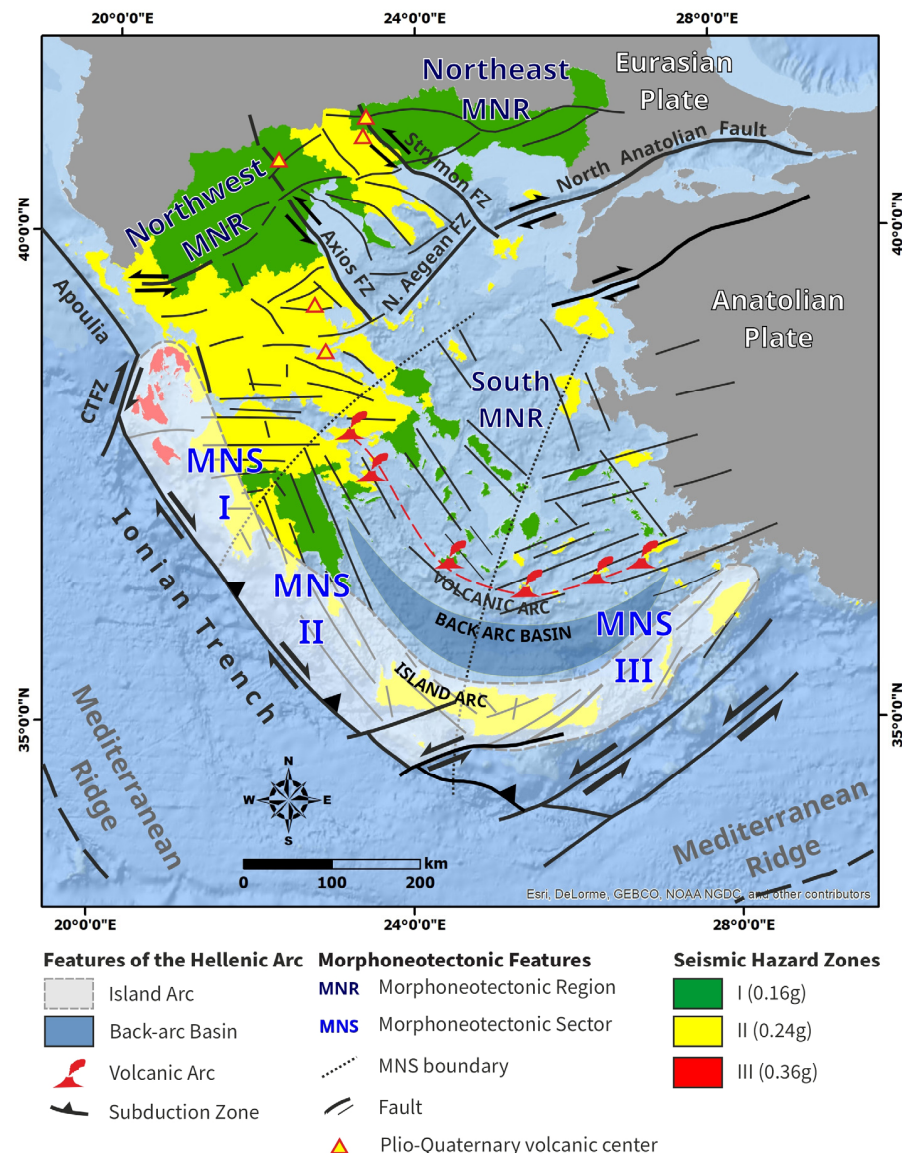


Figure 6. The current geometry of the Hellenic Arc, with its main features (the trench, the island arc, the back-arc basin and the volcanic arc, from S to N). The morphoneotectonic regions (MNR) of Greece based on Mariolakos et al. [83] are also illustrated along with the main faults and fault zones, with different trends and properties resulting in different morphoneotectonic sectors. The seismic hazard zones of Greece based on the expected peak ground acceleration (PGA) for a 475-year recurrence period and compiled by EPPO [71] are also presented.

The current geometry of the Hellenic Arc is characterized by the following structures:

- The Hellenic Trench is a deep basin with a maximum depth of 4500 m in the Ionian Sea, known as the “Oinousses Abyss”, which delineates the convergent plate boundary. The trench exhibits a rectangular bend: its southwestern part trends NW–SE, from Cephalonia to the southeast of Gavdos island, while its southeastern section trends NE–SW, from south of Crete to the east of Rhodes, where it is represented by two parallel trenches, the Pliny and Strabo trenches. According to Le Pichon and Angelier [82,84], the southwestern segment is characterized by subduction (perpendicular motion across the boundary), while the Pliny and Strabo trenches predominantly host dextral strike-slip motions and secondarily, subduction. The Strabo trench acts as a backstop behind the accretionary prism of the Eastern Mediterranean. Within this prism, back-thrusting occurs in the internal section (i.e., thrusting directed NW), along with gigantic mudslides and mud volcanoes [85];
- The Island Arc includes the Peloponnese, Crete, and the Dodecanese. This mountain chain, which develops parallel to the trench, results from the deformation and uplift of mainly sedimentary rocks from the Eurasian plate margin, with folding, imbrications, thrusting, and metamorphic phenomena occurring at depth. On the surface, intense geomorphological processes of erosion are present, depending on the location of each area in relation to faults and ridges;
- The Back-arc Basin is a marine basin (Cretan Sea), typically shallower than the trench, located on the Eurasian plate and behind the island arc. Here, decompression of rocks leads to the formation of extensional structures and classical molasse-type sedimentation, which may visually resemble the simultaneously deposited flysch in the trench but is in a different geodynamic environment, characterized by unconformity on a pre-tectonically deformed substrate. Its maximum depth reaches approximately 2000 m;
- The Volcanic Arc, which is found at a considerable distance from the trench, depending on the subduction angle, often traced by the Benioff seismic zone, is due to the melting of the subducting lithosphere and the subsequent rise of magma. The modern volcanic arc of the Aegean extends for 500 km and is about 20–40 km wide, beginning from the Saronic Gulf, passing through the southern Aegean, and reaching the western coasts of Asia Minor. It is approximately 250 km away from the present-day boundary of the two tectonic plates. As the African plate subducts beneath the European plate, it enters high-temperature zones, leading to its melting. This molten material, being less dense, rises through the overlying European plate, creating volcanic activity. Materials that do not have time to solidify have given rise to the volcanoes of the Lichades Islands, Sousaki, Poros, Methana, Milos, Kimolos, Santorini, Antiparos, Christiana Islands, Kos, and Nisyros, which have been active over the last 3 Ma.

The ridge of the Eastern Mediterranean, located south of the Hellenic Arc, forms the accretionary prism, with the detachment of the thick sedimentary sequence (approximately 8 km) from the underlying oceanic crust. This structure is controlled by the detachment and intercalation of the Messinian evaporites, which are thick and widely developed [85–87].

The current geotectonic regime in the Hellenic Arc and Trench System is characterized by asymmetry in the movement caused by the rectangular geometry of the arc, with normal convergence in the Ionian Sea and sub-parallel horizontal slip in the Pliny and Strabo trenches [80,88]. Compression prevails along the Hellenic Trench in the Ionian Sea, where a NE–SW slip orientation is observed in the focal mechanisms along the subduction zone, in contrast to the dominant left-lateral horizontal slip with a minor reverse component in a NNE–SSW direction observed in eastern Crete and the Dodecanese, north of the Pliny and Strabo trenches.

Another significant characteristic of the Hellenic Arc is its dextral rotation from 40° to 60° from the mid-Miocene, as determined by paleomagnetic measurements [80]. These large rotations have been particularly observed along the western zone within the External Hellenides from measurements in the Miocene–Pliocene sediments, while opposite rotations have been identified in other areas of the southern Aegean and Crete [80].

In the Aegean Plate, extensional structures dominate, often hosting a significant horizontal slip component that creates tilting of blocks around subducting horizontal axes, as seen in the Corinth Canal [89]. Simultaneously, large-scale rotations of fault blocks are observed, showing systematic rotation towards a specific direction, which leads to the creation of tectonic dipoles [90], with opposite vertical motion at the ends (the poles) of the large tectonic dipoles. These dipoles represent transverse structures to the Hellenic Arc and were created during the last few million years.

These fault blocks are bounded by major neotectonic faults, which have generally been active since the Upper Miocene and form the seismogenic structures of the Hellenic Arc [78,79]. The systematic analysis of these structures led to the distinction of three morphoneotectonic regions with the following characteristics [83]:

- The northeast MNR (NE-MNR) is bordered to the south by the large North Aegean Fault Zone (the extension of the North Anatolian Fault into the northern Aegean Sea) and to the west by the Axios fault zone. In contrast to the northwest MNR (NW-MNR), the region does not experience significant vertical movements, leading to a generally smooth topography. However, vertical movements are localized in areas where fault reactivation has occurred, particularly during the Plio-Quaternary period, resulting in localized incision. The majority of the primary tributaries of the drainage network originate from the north, including the Axios, Strymon, Nestos, and Evros rivers. The first-order basins have a NW–SE orientation. Plio-Pleistocene volcanic activity is present along the northern margins of the current grabens (Aridaia, Sidirokastro, and Strymoniko);
- The NW-MNR is bounded by the Axios fault zone to the east and by the continuation of the Malliakos-Amvrakikos Gulf fault zone to the west, with the drainage network predominantly oriented NW-SE. Notable characteristics, particularly in the western sector, include the absence of typical horst–graben structures and the presence of E–W strike-slip fault zones. In the eastern sector, the original strike of the horst–graben structures is NW–SE (Meso-Hellenic Trough, Ptolemais-Servia basin), which were later fragmented into smaller basins by faults with a NE–SW orientation. Plio-Pleistocene volcanic activity is found in the southeastern part of the sector;
- The south MNR (S-MNR) is bounded to the north by the large North Anatolian Fault Zone and the continuation of the Malliakos-Amvrakikos Gulf fault zone, to the west and south by the Hellenic Trough, and to the south–southeast by the Pliny and Strabo Troughs. The Strabo and Pliny Troughs represent the eastern extension of the southern part of the Hellenic Trough. These troughs exhibit different kinematics compared with the Hellenic Trough, which results in variations in brittle tectonics, karstification, and hydrogeological characteristics in the affected areas.

3.3. Main Tectonic Regimes, Seismicity and Seismic Hazard in Greece

The main tectonic regimes in Greece are the dextral strike-slip along the North Aegean Fault Zone (the extension of the North Anatolian Fault into the North Aegean Sea) in the North Aegean Trough, the dextral strike-slip along the Cephalonia Fault Zone in the Ionian Sea, compression along the Hellenic Arc, and extension in northern and central Greece as well as the Peloponnese [90].

From the above observations, it is clear that the deformation of the Hellenic Arc is quite complex and significantly influences the distribution, frequency, and intensity of seismic activity in its individual regions, as will be discussed below.

Regarding seismicity, there is no region in Greece that has not hosted an earthquake epicenter during the last centuries [44] (Figure 7). Approximately 75% of the earthquakes in Greece take place either offshore, away from populated areas, or at a depth of several kilometers, thus reducing the seismic risk [44]. However, several onshore earthquakes have occurred, with significant impacts and extensive damage to elements of the built environment (buildings, networks and infrastructure) as well as primary and secondary EEEs attributed to them [40–42]. Among the secondary EEEs, ETLs have a high potential to cause further impacts on both the built environment and the population, either through direct health impacts (human casualties, injuries, homeless and displaced people) or indirect impacts on the functionality of networks and infrastructure.

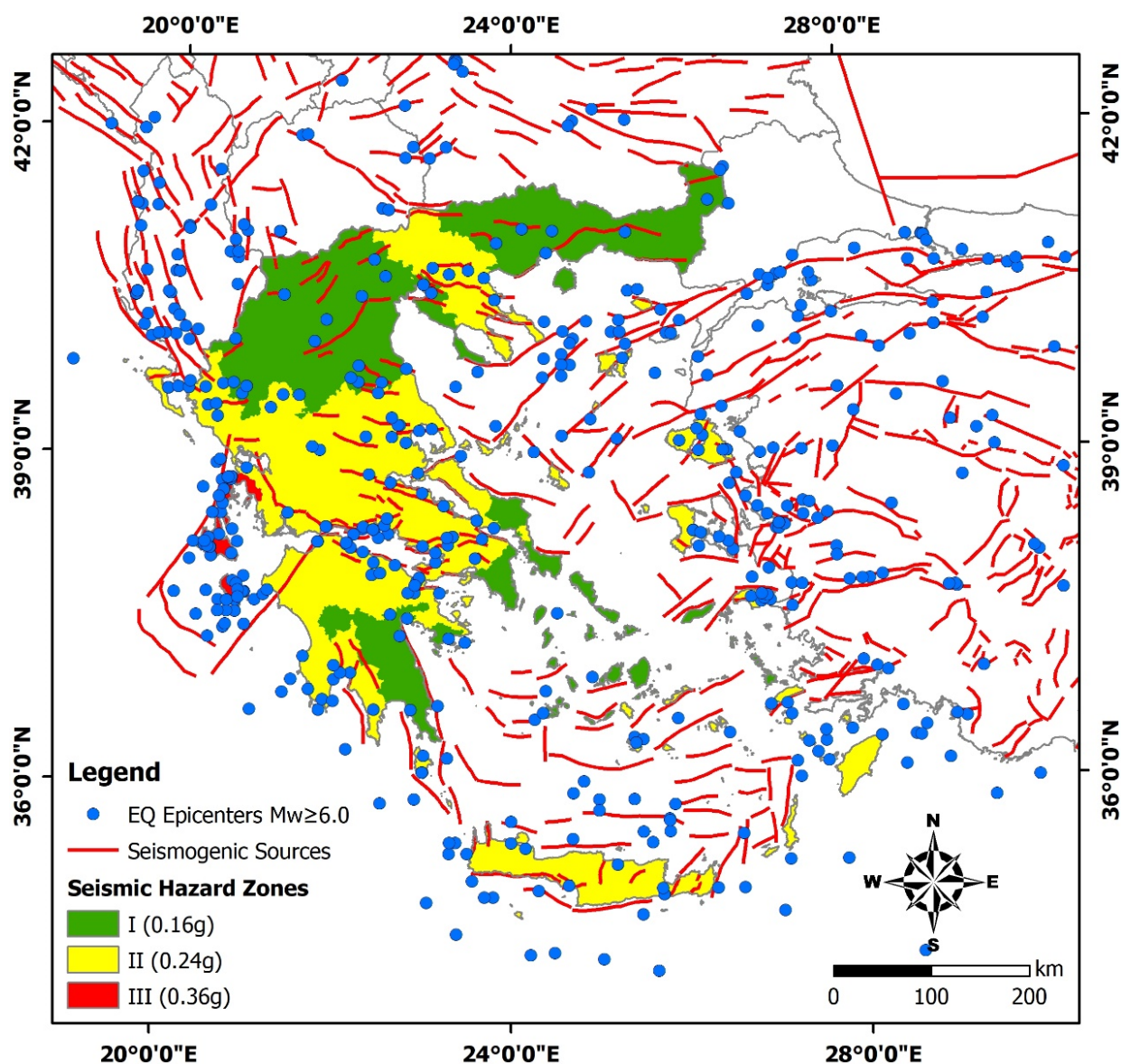


Figure 7. Map with the seismogenic sources of Greece based on the GEM Global Active Faults Database (GAF-DB) compiled by Styron and Pagani [79], the spatial distribution of earthquakes with $M_w \geq 6.0$ based on the aforementioned earthquake catalogues of Makropoulos et al. [46], Stucchi et al. [47] and Rovida et al. [49] and the seismic hazard zones of Greece compiled by EPPO [71].

Regarding seismic hazard in Greece, the first (green) zone includes several parts of northern, central and southern Greece; eastern Macedonia and Thrace; the western part of central Macedonia; western Macedonia; northern Epirus; the southeastern part of the Peloponnese; the westernmost peninsula of Halkidiki area (Kassandra peninsula); and the Cyclades (Figure 7).

The second (yellow) zone includes many areas of island and mainland Greece, such as the northern part of the Ionian Islands (Kerkyra and Diapontian Islands); western and central mainland Greece, including Epirus; Thessaly; mainland Greece and the northern Peloponnese on both sides of the Corinthian Gulf; the Western Peloponnese (Achaia and Elis); Crete; the Dodecanese; the islands of the north and east Aegean (Samothece, Lemnos, Agios Efstratios, Lesbos, Chios, Psara, Oinousses, Ikaria, Fournoi, and Samos); and the end of central Macedonia in the Aegean Sea with the peninsulas of Sithonia and Athos (Figure 7).

The third (red) zone includes the islands of the central and southern part of the Ionian Sea (Lefkada, Cephalonia, Ithaki, and Zakynthos Islands) (Figure 7), where large and destructive earthquakes occurred [13,77,91,92]. These seismic events are attributed to the proximity of the islands to both the CTFZ and the northwestern part of the Hellenic Trench [92].

However, there are areas, which, after recent probabilistic seismic hazard assessment studies, are characterized by higher seismic hazard values than those of the Seismic Hazard Zone Map of Greece, such as in the region of Attica (eastern mainland Greece) [93] or in the Ionian Islands [94], highlighting the need for revision of the active building code in Greece.

Earthquakes with magnitudes greater than or equal to 6.0 are distributed in specific zones (Figure 7), where seismogenic sources exist [78,79] and are located in the Ionian Sea, along the Hellenic Arc and Trench system, on the margins of the plains and plateaus of mainland Greece, and in the northern, northeastern and eastern Aegean Sea [46,78,79,83].

The seismic risk in Greece today is larger than in the past, mainly due to the significant population growth and urbanization and vulnerability due to inadequate infrastructure and building practices of previous decades [95]. Typical recent examples of earthquakes that have highlighted this fact are the 20 June 1978, $M_w = 6.5$ earthquake in Thessaloniki [96–98], which is the metropolis of the region of Central Macedonia and Greece's second largest city; the 1981 Alkyonides (eastern Corinth Gulf) earthquake sequence, which included the events on 24 and 25 February and 4 March with $M_w = 6.7$, $M_w = 6.4$, and $M_w = 6.3$, respectively [99–101], and which affected Athens city; the 13 September 1986, $M_w = 6.2$ earthquake that affected Kalamata City (southwestern Peloponnese) [51]; and the 5 June 1995, $M_w = 6.1$ seismic event with its impact on Aegion city (northern Peloponnese) [102]. These earthquakes caused significant building damage, including partial or total building collapse, resulting in numerous fatalities. The impact on the built environment also comprised damage to infrastructure, mainly to parts of the road network, attributed to triggered rockfalls and slides [50,51], without further effects on the local population and public health.

Until the 1978 Thessaloniki earthquake and the 1981 Alkyonides earthquake, the state's efforts to develop seismic regulations lagged behind significant destructive earthquakes. However, over the past two decades, this approach has changed drastically. Greece's modern seismic code, considered one of the most advanced globally, offers hope that new earthquake-resistant structures will perform significantly better than older ones in future seismic events.

4. ETLs in Greece

4.1. Causative Earthquakes and Triggered Landslides

4.1.1. Introduction

A reevaluation of the available sources identified 144 earthquakes with Mw ranging from 4.0 to 8.3 that have occurred in Greece from 279 BC to 2023 and have triggered landslides. A total of 76 earthquakes (52.78%) have occurred in ancient and historical times (before 1900), while the remaining 68 earthquakes (47.22%) have occurred and been recorded instrumentally (after 1900) (Tables 2 and 3). Due to the limited available information especially for historical effects, it was not possible to determine the exact location of landslides triggered by six of the historical earthquakes. These earthquakes are not excluded from the presentation of the results with a view to identifying further evidence from other types of contemporary or recent sources in future research and related studies. However, they are not further analyzed in the frame of the statistical analysis of the documented landslides. The geographically determined ETLs in the present study amount to 673 events. Of these, 166 (24.66%) were triggered by historical earthquakes, while the remaining 507 (75.33%) by instrumentally recorded ones. Three of them were identified offshore, while one was triggered by an earthquake in Greece, but recorded in Egypt and is therefore considered a far-field effect. Therefore, the total ETLs in Greece taken into account at each stage of the following temporal, spatial and statistical analysis amounted to 669 events. The numbers of ETLs and the studied sources are presented in detail in the following Table 2, while their spatial distribution is illustrated in Figures 8 and 9.

Table 2. Historical and recent earthquakes in Greece and the number of triggered landslides per earthquake, together with the landslide sources evaluated in the present study. The seismological parameters (origin time, coordinates of the epicenter, moment magnitude, and focal depth) are derived from the EPICA catalogue for the historical earthquakes [48,49]; from Makropoulos et al. [46] for the recent earthquakes from 1900 to 2009; and the earthquake catalogue of the Seismological Laboratory of the National and Kapodistrian University of Athens [103] for the recent earthquakes since 2009. The seismic intensities come mainly from Papazachos and Papazachou [40], from the EPICA catalogue for the historical earthquakes [48,49], and from the sources of the last column of the table for the recent earthquakes.

No	Earthquake Origin Time	Epicenter Coordinates		Mw	Imax	D	Most Earthquake -Affected Area	No of ETLs	Sources for ETLs
		Latitude	Longitude						
1	550 BC	36.90	22.40	6.8	IX	-	Sparti (Laconia, Peloponnese)	1	[40,104]
2	464 BC	37.00	22.50	6.8	X	-	Sparti (Laconia, Peloponnese)	1	[40,41,104]
3	279 BC	38.40	22.40	6.4	IX	-	Delphi (mainland Greece)	1	[41,104]
4	1 AD	-	-	-	-	-	Ladon River (Arcadia, Peloponnese)	1	[41]
5	53 AD	-	-	-	-	-	Rhodes Island (Dodecanese)	1	[41]
6	551 AD	38.40	22.70	-	-	-	Schisma (Boeotia, mainland Greece)	1	[40,41,104]
7	8 August 1303	35.717	25.797	8.26	-	-	Crete	1	[105,106]
8	June 1402	38.168	22.272	6.67	IX	-	Xylokastro (Achaia, western Greece)	3	[40]
9	1507	-	-	-	-	-	Santorini Island (Cyclades)	1	[107]
10	29 May 1508	35.02	25.72	7.13	IX	-	Ierapetra (Crete)	1	[41]
11	16 April 1513	37.60	20.80	6.5	VIII	-	Zakynthos Island (Ionian Sea)	1	[42,108]
12	24 April 1544	39.500	22.327	6.52	-	-	Pyli (mainland Greece)	1	[40,41]
13	11 July 1566	39.13	21.65	6.15	VII-VIII	-	Agrafa (Thessaly)	1	[41]
14	28 May 1592	37.70	20.80	-	-	-	Zakynthos Island (Ionian Sea)	1	[42,108,109]
15	2 July 1630	38.809	20.704	6.49	VIII-IX	-	Lefkada Island (Ionian Sea)	3	[42,110]
16	5 November 1633	37.782	20.896	6.57	VIII-IX	-	Zakynthos Island (Ionian Sea)	3	[28–30,33]

Table 2. Cont.

No	Earthquake Origin Time	Epicenter Coordinates		Mw	Imax	D	Most Earthquake -Affected Area	No of ETLs	Sources for ETLs
		Latitude	Longitude						
17	9 September 1636	37.928	20.885	6.62	VIII-IX	-	Cephalonia Island (Ionian Sea)	1	[40–42,110]
18	24 August 1658	38.20	20.42	6.7	IX	-	Cephalonia Island (Ionian Sea)	1	[36,40–42,111]
19	22 November 1704	38.825	20.673	6.38	VIII-IX	-	Lefkada Island (Ionian Sea)	1	[40–42,110]
20	3 September 1705	38.225	23.667	5.99	VII	-	Athens (Attica)	1	[40–42]
21	9 July 1729	37.851	20.808	6.28	VIII	-	Zakynthos Island (Ionian Sea)	n/d	[40–42,112]
22	18 June 1751	37.710	27.008	6.69	IX-X	-	Samos Island (north Aegean)	n/d	[40,41,113]
23	15 June 1754	37.80	22.80	7.0	VIII	-	Nafpaktos (Aetoloakarnania, western Greece)	n/d	[40,41,44]
24	22 July 1767	38.268	20.464	6.65	X	-	Cephalonia Island (Ionian Sea)	1	[36,40,42,114,115]
25	18 September 1776	-	-	-	-	-	Rhodes Island (Dodecanese)	n/d	[41,116]
26	22 March 1783	37.60	21.80	6.1	-	-	Lefkada Island (Ionian Sea)	4	[41,42]
27	23 March 1783	38.65	20.57	6.64	IX-X	-	Lefkada Island (Ionian Sea)	4	[40,42,110]
28	29 June 1798	36.149	22.988	6.38	VIII	-	Kythera Island (Attica region)	2	[21,40,41,117]
29	16 February 1810	35.50	25.60	7.5	IX	90	Heraklion (Crete)	1	[41]
30	23 August 1817	38.241	22.075	6.54	VIII	-	Aegion (Achaia, western Greece)	1	[40,45]
31	1818	-	-	-	-	-	Kerkyra Island (Ionian Islands)	1	[41]
32	19 January 1825	38.834	20.708	6.71	IX-X	-	Lefkada Island (Ionian Islands)	1	[41,42]
33	3 April 1831	37.757	26.976	5.65	VI	-	Samos Island (North Aegean)	1	[40–42]
34	20 March 1837	37.421	23.326	5.99	VII	-	Nea Epidaurus (eastern Peloponnese)	3	[21,40–42,44]
35	15 August 1837	38.00	22.00	4.8	-	-	Pyrgos (Elis, western Greece)	1	[41]
36	30 October 1840	37.794	20.826	6.44	VIII-IX	-	Zakynthos Island (Ionian Sea)	2	[21,40–42,91,108]
37	18 April 1842	37.058	22.150	6.21	VII-VIII	-	Messinia (SW Peloponnese)	2	[41,118]
38	18 October 1843	36.220	27.620	6.47	VIII-IX	-	Chalki Island (Dodecanese)	2	[21,40–42,45]
39	11 October 1845	39.100	26.217	6.28	VIII	-	Lesvos Island (north Aegean)	3	[21,40,41,113,119]
40	25 June 1846	37.757	26.976	6.05	VII-VIII	-	Samos Island (north Aegean)	1	[40–42,113]
41	14 July 1852	38.666	22.433	5.92	VII	-	Gravia (mainland Greece)	2	[40,41,44]
42	18 August 1853	38.319	23.317	6.71	IX-X	-	Thiva (mainland Greece)	1	[40–42,44,45]
43	30 July 1854	39.80	20.20	6.5	-	-	Souli (Epirus)	1	[41]
44	14 February 1855	-	-	-	-	-	Rhodes Island (Dodecanese)	n/d	[41,116]
45	12 October 1856	35.60	25.80	7.7	IX	-	Crete, Rhodes (Dodecanese island complex)	1	[41,116]
46	21 February 1858	37.87	22.88	6.5	IX	-	Corinth (Peloponnese)	5	[21,40–42,44]
47	6 August 1860	40.40	25.80	6.2	VII	-	Samothrace Island (north Aegean)	1	[40–42]
48	29 June 1861	-	-	-	-	-	Nisyros Island (Dodecanese)	1	[41]
49	26 December 1861	38.207	22.126	6.69	IX	-	Valimitika (Achaia, western Greece)	11	[40–42,44,45,120]
50	11 June 1864	-	-	-	-	-	Rhodes Island (Dodecanese)	1	[41,116]
51	4 February 1867	38.233	20.424	7.15	X	-	Cephalonia Island (Ionian Sea)	11	[40,42,77,115,121–123]
52	7 March 1867	39.238	26.264	6.85	IX-X	-	Lesvos Island (north Aegean)	1	[40–42,45,119,124–126]
53	18 April 1869	36.50	27.60	6.8	IX	-	Symi Island (Dodecanese)	1	[40,41]
54	24 June 1870	36.00	25.50	6.61	VI-VII	-	Crete	2	[120]
55	1 August 1870 (mainshock)	38.48	22.55	6.8	IX	-	Fokis (mainland Greece)	10	[21,40–42,44,127]
56	1 August 1870 (aftershock)	38.48	22.55	-	-	-	Fokis (mainland Greece)	1	[40–42,44,127]
57	25 October 1870	38.48	22.55	-	-	-	Fokis (mainland Greece)	1	[41,127]
58	30 November 1870	38.48	22.55	-	-	-	Fokis (mainland Greece)	2	[41,127]

Table 2. Cont.

No	Earthquake Origin Time	Epicenter Coordinates		Mw	Imax	D	Most Earthquake -Affected Area	No of ETLs	Sources for ETLs
		Latitude	Longitude						
59	18 March 1874	38.420	23.807	5.54	VII	-	Eretria (Evia Island)	1	[21,40,42,44]
60	26 June 1876	37.846	22.771	5.85	VII	-	Nemea (NE Peloponnese)	1	[21,40,44]
61	3 April 1881	38.220	26.195	6.47	VII	-	Chios Island (north Aegean)	6	[21,40,41,119,124]
62	28 March 1885	37.125	21.959	6.08	VIII	-	Messini (SW Peloponnese)	n/d	[40]
63	7 July 1885	35.30	24.60	5.58	V	-	Crete	1	[128]
64	14 December 1885	38.80	20.50	5.1	VI-VII	-	Lefkada Island (Ionian Islands)	3	[42,110]
65	27 August 1886	36.988	21.467	7.17	-	-	Filiatra (Messinia, SW Peloponnese)	1	[40,41]
66	3 October 1887	38.053	22.647	6.27	VIII	-	Xylokastro (Achaia, western Greece)	3	[40]
67	9 September 1888	38.250	22.072	6.2	VIII-IX	-	Valimitika (Achaia, western Greece)	2	[40–42,44]
68	25 August 1889	38.517	21.384	6.53	VIII	-	Aegion (Achaia, western Greece)	2	[41,44]
69	26 October 1889	39.194	25.987	6.78	IX-X	-	Lesvos Island (North Aegean)	4	[21,40–42,113,119]
70	31 January 1893	37.68	20.81	6.3	-	-	Zakynthos Island (Ionian Sea)	5	[91,108]
71	9 February 1893	40.589	25.526	6.84	VIII	-	Samothraki Island (north Aegean)	4	[40–42,124,129]
72	17 April 1893	37.732	20.828	6.34	VIII-IX	-	Zakynthos Island (Ionian Sea)	2	[21,42,91,108]
73	23 May 1893	38.31	23.25	6.2	VIII	10	Thiva (mainland Greece)	2	[21,40–43]
74	20 April 1894	38.600	23.209	6.77	IX	6	Atalanti (mainland Greece)	8	[21,40,41,43,130]
75	27 April 1894	38.716	22.959	6.91	IX	11	Atalanti (mainland Greece)	7	[21,40–43,45,130]
76	22 January 1899	37.20	21.60	6.5	VIII	9	Kyparissia (Messinia, SW Peloponnese)	5	[21,41,43,118]
77	28 July 1902	35.40	24.20	5.55	VI	-	Chania (Crete)	1	[42,128]
78	11 August 1903	36.30	23.00	7.6	IX	80	Kythera Island (Attica region)	1	[21,40,42,117]
79	20 January 1905	39.70	22.90	5.5	X	5	Magnesia (Thessaly)	1	[21,40,42]
80	8/9 November 1905	40.30	24.40	7.1	X	17	Athos peninsula (central Macedonia)	3	[21,40,42]
81	30 May 1909	38.25	22.20	5.9	VIII	20	Fokis (mainland Greece)	4	[21,43]
82	15 July 1909	37.90	21.50	5.6	IX	15	Chavari (Elis, Peloponnese)	1	[131]
83	24 January 1912	38.10	20.50	6.1	X	11	Cephalonia Island (Ionian Sea)	1	[36]
84	17 October 1914	38.20	23.50	5.9	VIII+	8	Thiva (mainland Greece)	8	[40,41,43]
85	27 November 1914	38.80	20.60	5.9	IX	6	Lefkada Island (Ionian Sea)	7	[21,40,42,45,110]
86	4 June 1915	39.10	21.10	5.9	VIII	4	Agrafa (Thessaly)	3	[21,43]
87	7 August 1915	38.50	20.50	6.3	-	12	Lefkada Island (Ionian Sea)	3	[40,42,45,110]
88	24 December 1917	38.65	21.86	5.7	VIII	15	Nafpaktos (Aetoloakarnania, western Greece)	1	[40,42,43]
89	26 June 1926	36.75	26.98	7.0	XI	109	Rhodes Island (Dodecanese)	4	[116,132]
90	30 August 1926	36.76	23.16	6.7	VIII	26	Sparti (Laconia, Peloponnese)	1	[40,42]
91	1 July 1927	36.72	22.85	6.3	IX	45	Oitylo (Laconia, Peloponnese)	5	[21,40,42,43]
92	22 April 1928	38.08	23.12	6.3	IX	8	Corinth (NE Peloponnese)	5	[21,43,133]
93	31 March 1930	39.70	23.34	5.9	VIII	10	Magnesia (Thessaly)	1	[21,43]
94	17 April 1930	37.80	23.17	5.9	VIII	66	Corinth (NE Peloponnese)	2	[21,43]
95	23 April 1933	36.76	27.17	6.5	IX	44	Kos Island (Dodecanese)	1	[134]
96	20 July 1938	38.30	23.66	5.9	VIII	42	Oropos (Attica)	1	[21,40,42,43]
97	1 March 1941	39.73	22.46	6.1	VIII	25.0	Larissa (Thessaly)	n/d	[43]
98	6 October 1947	36.71	21.79	6.5	IX	2	Messinia (SW Peloponnese)	7	[21,40,42,43,45,135]
99	22 April 1948	38.73	20.38	6.5	IX	12	Lefkada Island (Ionian Sea)	2	[21,40,42,45]
100	30 June 1948	38.96	20.53	6.5	-	36	Lefkada Island (Ionian Sea)	8	[40,42,136]
101	23 July 1949	38.71	26.27	6.7	IX	17	Chios Island (north Aegean)	3	[21,40,42,45,119,124]
102	9 August 1953	38.24	20.80	5.9	VIII	21	Cephalonia Island (Ionian Sea)	4	[13]
103	11 August 1953	38.35	20.74	6.6	VIII	11	Cephalonia Island (Ionian Sea)	8	[13]
104	12 August 1953	38.13	20.74	7.0	IX	11	Cephalonia Island (Ionian Sea)	41	[13]

Table 2. Cont.

No	Earthquake Origin Time	Epicenter Coordinates		Mw	Imax	D	Most Earthquake -Affected Area	No of ETLs	Sources for ETLs
		Latitude	Longitude						
105	30 April 1954	39.23	22.28	6.5	IX	16	Sophasdes (Thessaly)	5	[21,43,137]
106	8 March 1957	39.34	22.66	6.6	IX	30	Velestino (Thessaly)	3	[21,43]
107	14 May 1959	35.11	24.65	5.9	VIII+	23	Crete	7	[21,40]
108	9 March 1965	39.34	23.82	6.1	IX	18	Alonissos Island (Sporades island complex)	3	[43]
109	5 April 1965	37.75	22.00	5.9	X	34	Apiditsa (Arcadia, Peloponnese)	22	[21,43]
110	6 July 1965	38.37	22.40	6.2	VIII+	18	Eratini (mainland Greece)	4	[21,43,45]
111	5 February 1966	39.10	21.74	6.0	IX	16	Kremasta (mainland Greece)	6	[21,40,42,43]
112	1 May 1967	39.60	21.29	6.0	IX	34	Tzoumerka, Arta (Epirus)	2	[21,43]
113	19 February 1968	39.40	24.94	6.9	IX	7	Agios Efstratios (NE Aegean)	1	[21,42,45,138]
114	8 April 1970	38.34	22.56	6.0	VII	23	Antikyra (mainland Greece)	1	[21,43]
115	30 June 1970	38.80	20.57	4.6	V-VI	22	Lefkada Island (Ionian Sea)	2	[139]
116	29 November 1973	35.18	23.81	5.8	VII+	37	Chania (Crete)	3	[40,42,128]
117	24 February 1981	38.23	22.97	6.4	IX	18	Eastern Corinth Gulf, Athens (mainland Greece)	6	[21,40,43,140,141]
118	17 January 1983	38.07	20.25	6.7	VI	17	Cephalonia Island (Ionian Sea)	2	[36,142]
119	13 September 1986	37.08	22.15	5.7	IX	9	Kalamata (Messinia, SW Peloponnese)	49	[40,50,51,143]
120	16 October 1988	37.93	20.92	5.6	VIII	25	Vartholomio (Elis, western Greece)	6	[52]
121	20 March 1992	36.66	24.49	5.2	-	11	Milos Island (Cyclades island complex)	24	[21,53,144,145]
122	26 March 1993	37.68	21.44	5.3	VIII	10	Pyrgos (Elis, western Greece)	47	[54,146]
123	13 May 1995	40.17	21.69	6.3	IX	14	Grevena–Kozani (western Macedonia)	12	[21,55,147]
124	15 June 1995	38.40	22.27	6.3	VIII	15	Aegion (Achaia, western Greece)	4	[56,148–152]
125	7 September 1999	38.12	23.58	5.8	IX	9	Athens (Attica)	37	[153]
126	26 July 2001	39.10	24.27	6.0	VII	19	Skyros Island (Sporades island complex)	1	[40]
127	14 August 2003	38.99	20.57	5.8	VIII	12	Lefkada Island (Ionian Sea)	17	[154–157]
128	1 March 2004	37.17	22.12	5.4	-	14	Messinia (SW Peloponnese)	7	[158]
129	8 January 2006	36.28	23.27	6.5	VII-VIII	58	Kythera (Attica Region)	9	[58,59,117]
130	6 January 2008	37.26	22.70	6.3	VI	84	Leonidio (eastern Peloponnese)	1	[159]
131	8 June 2008	37.96	21.45	6.3	VIII-IX	16	Andravida (NW Peloponnese)	13	[60,61]
132	15 July 2008	35.92	27.80	6.6	VII	65	Rhodes Island (Dodecanese)	1	[160]
133	26 January 2014	38.21	20.47	6.1	VIII	16	Cephalonia Island (Ionian Sea)	11	[161,162]
134	3 February 2014	38.27	20.41	5.9	VII	5	Cephalonia Island (Ionian Sea)	4	[161,162]
135	6 December 2014	38.905	26.261	4.9	VIII	-	Plomari (Lesvos, NE Aegean)	1	[119]
136	17 November 2015	38.68	20.59	6.4	VIII	14	Lefkada Island (Ionian Sea)	29	[163]
137	12 June 2017	38.86	26.37	6.3	VIII	13	Lesvos Island (NE Aegean)	6	[62]
138	20 July 2017	36.99	27.44	6.6	VI	11	Kos Island (eastern Aegean)	1	[63,140]
139	25 October 2018	37.36	20.50	6.6	VII	20	Zakynthos Island (Ionian Sea)	4	[91,164]
140	30 October 2020	37.92	26.80	6.9	VII	13	Samos Island (eastern Aegean)	17	[64]
141	3 March 2021	39.73	22.18	6.3	VI	12	Thessaly (central Greece)	3	[65]
142	27 September 2021	35.14	25.27	5.9	VIII	14	Arkalochori (Crete)	7	[66]
143	12 October 2021	35.07	26.33	6.3	VII	21	Zakros (Crete)	1	this study
144	13 August 2023	35.257	23.888	4.8	-	-	Samaria (Crete)	1	this study

n/d: not determined.

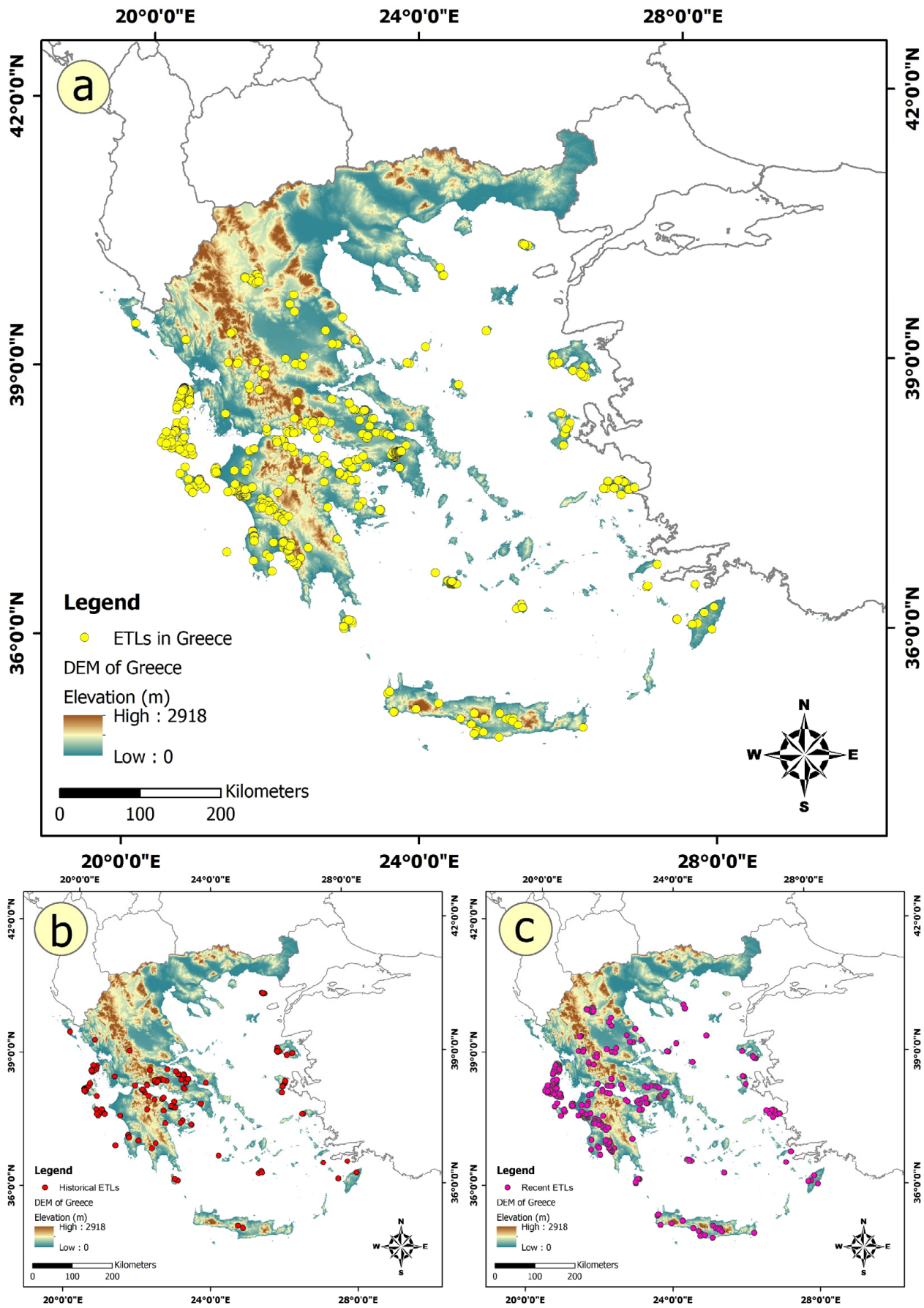


Figure 8. Spatial distribution of all ETLs (a), (b) before 1900 and (c) after 1900 in Greece.

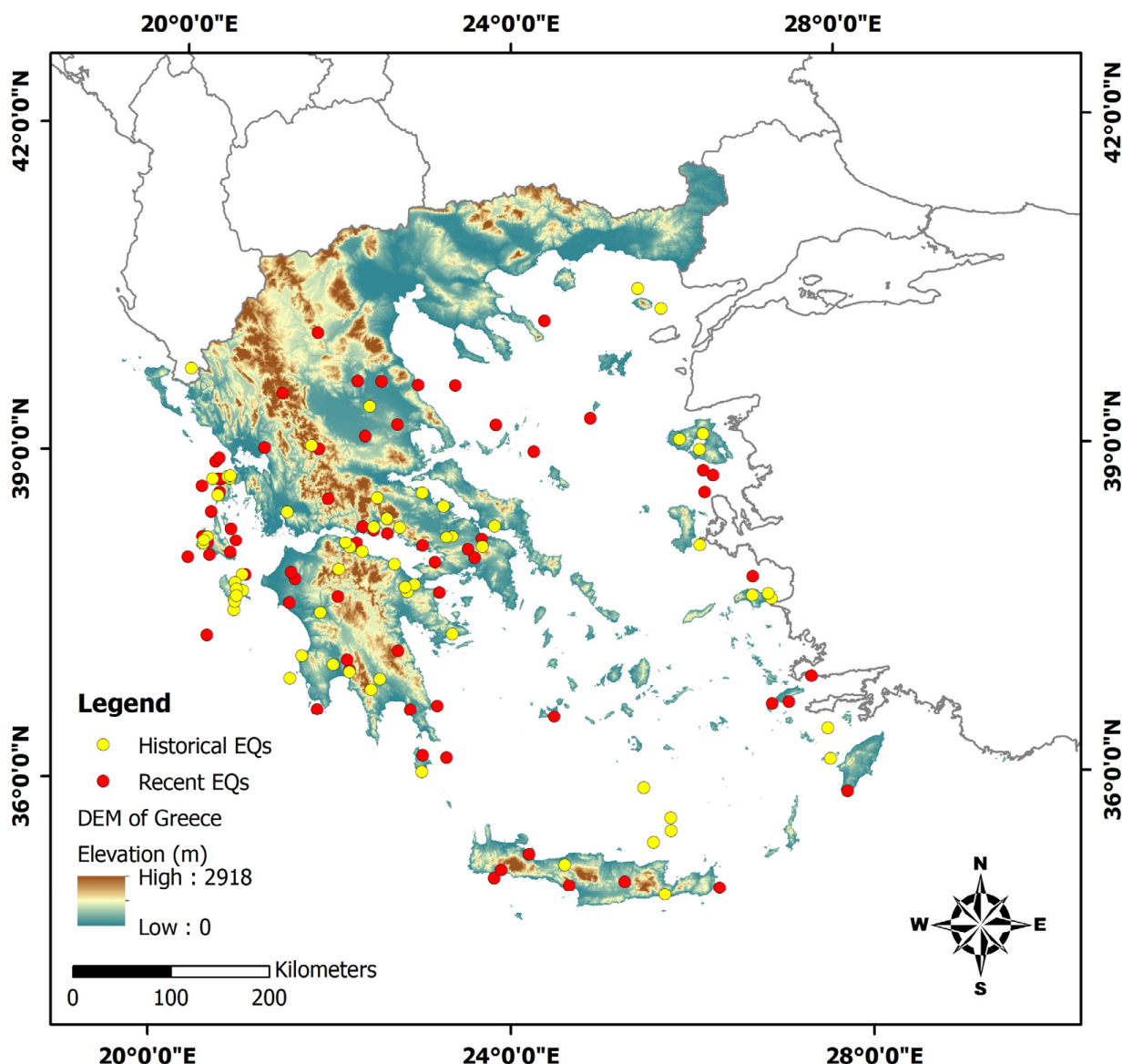


Figure 9. Spatial distribution of earthquakes that triggered landslides in Greece.

Table 3. Numbers of ETLs per historical earthquake.

Landslides per Historical Earthquake	Number of Historical Earthquakes	Percentage of Historical Earthquakes
1	39	51.32
2	11	14.47
3	7	9.21
4	4	5.26
5	3	3.95
6	1	1.32
7	1	1.32
8	1	1.32
9	0	0.00
10	1	1.32
11	2	2.63
not detected	6	7.89

Regarding the triggering period of the studied landslides, there is a slight increase in the number of recorded events towards the end of the 19th century (Figure 10), when double-digit numbers of landslides from various seismic events are observed. This increasing trend becomes even more pronounced after the first half of the 20th century (Figure 10), as

advances in science and technology significantly contribute to the more comprehensive understanding and recording of earthquakes and their effects. Most years with more than 10 ETLs have been recorded after 1980 (Figure 10), when seismic events with significant impacts on the built environment of large cities and towns in Greece occurred. These events underscore the importance of documenting primary and secondary EEEs in the analysis and assessment of seismic hazard and related geohazards, including ETLs.

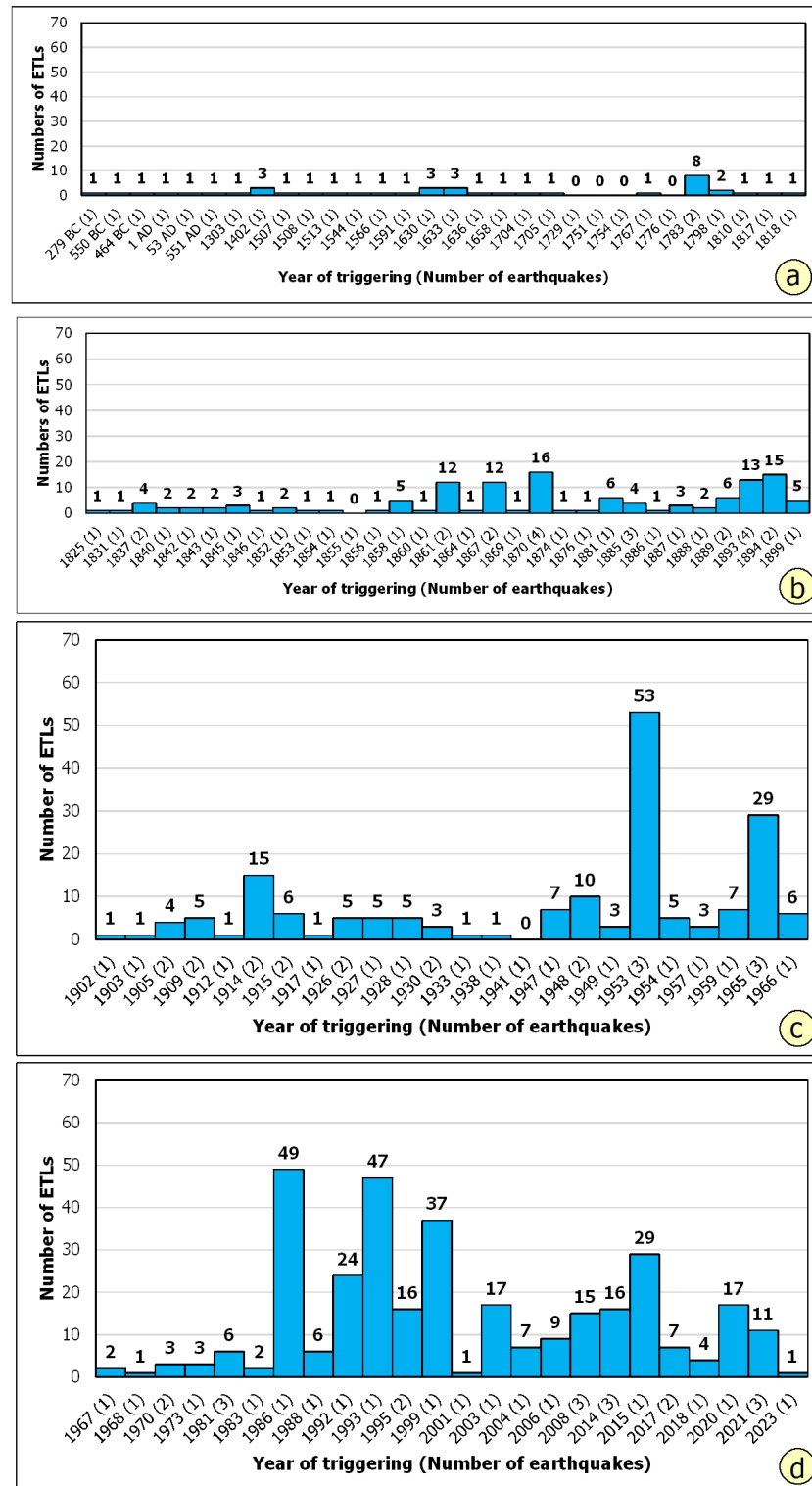


Figure 10. Diagrams of the number of ETLs in Greece by year of triggering: (a) 279 BC to 1818; (b) 1825 to 1899; (c) 1902 to 1966; (d) 1967 to 2023.

Taking into account the numbers of ETLs in Greece presented in Table 3, it is concluded that almost half of the historical earthquakes (39 out of 76, or 51.32%) have caused only one landslide, while the number and the corresponding percentage of historical earthquakes that have caused two landslides (11 earthquakes, 14.47%) is a two-digit number (Table 3). The percentage of earthquakes for which it was not possible to determine the geographic location of the landslides is also notable (6 earthquakes, or 7.89%) (Table 4). The aforementioned do not mean that the properties of the historical earthquakes were such that they did not trigger landslides. This is instead attributed to the limited availability of related information that would make it possible to fully record them. This limited availability is strongly related to various limitations and problems in preparing historical catalogues of landslide events, including historical social, political, scientific factors and accessibility issues, which have already been highlighted in other, similar research on historical landslides [24,165–168]. This situation, in terms of the quantity of recorded ETLs and thus the completeness of the recording of these secondary EEs, is gradually improving during the transition from the historical period to the period of instrumental recordings. While there are only 3 historical earthquakes with double-digit ETLs, recent earthquakes with double-digit ETLs amount to 12, while earthquakes with less than 5 ETLs have been greatly reduced (Table 4).

Table 4. Numbers of ETLs per recent earthquake.

Number of Landslides per Recent Earthquake	Number of Recent Earthquakes	Percentage of Recent Earthquakes
1	19	27.94
2	5	7.35
3	8	11.76
4	7	10.29
5	3	4.41
6	4	5.88
7	5	7.35
8	3	4.41
9	1	1.47
10	0	0.00
11	1	1.47
>11	12	16.18

The historical earthquakes with the most ETLs have occurred in the central–western part of Greece, including the central Ionian Islands (the 4 February 1867, $M_w = 7.4$ earthquake with 11 ETLs) and in the northern Peloponnese, south of the Corinthian Gulf (the 26 December 1861, Valmitika (Achaia), $M_w = 6.7$ earthquake with 11 ETLs). The recent earthquakes with the most landslides have occurred in:

- the central Ionian Islands:
 - Cephalonia Island on 12 August 1953 with 41 landslides and on 26 January 2014 with 11 landslides;
 - Lefkada Island in 2003 with 17 landslides and in 2015 with 29 landslides;
- the Peloponnese:
 - Apiditsa (Arcadia) area in 1965 with 22 landslides;
 - Kalamata (Messinia) area in 1986 with 49 landslides;
 - Pyrgos (Ilia) area in 1993 with 47 landslides;
 - Andavida (Ilia) area in 2008 with 13 landslides;
- Attica (Athens) in 1999 with 37 landslides;
- the Cyclades island complex (Milos Island) in 1992 with 24 landslides;
- the eastern Aegean Sea (Samos Island) in 2020 with 17 landslides;

- Western Macedonia (Grevena-Kozani) in 1995 with 12 landslides.

The disparity between the numbers and percentages of historical and recent landslides can be attributed to various factors, including human activity, advancements in science and technology, as well as the geo-environmental conditions and demographic characteristics of areas affected by earthquakes and landslides. In ancient and historical times, the recording of natural phenomena such as earthquakes and their associated landslides was often unsystematic or entirely absent due to (i) the limited understanding and difficult interpretation of natural processes in antiquity, (ii) the lack of data from areas beyond densely populated regions affected by significant primary and secondary EEEs, (iii) the difficulties in accessing affected areas shortly after the generation of earthquakes and landslides, and (iv) the absence of instruments and methods for monitoring and documenting the impacts of earthquakes and ETLs.

The challenges of recording the environmental effects of historical earthquakes are exemplified in the report of Schmidt [121] on the earthquakes of 1867 in Cephalonia (Ionian Sea) and Lesbos (northeastern Aegean Sea). Schmidt noted that he visited the earthquake-affected island of Cephalonia two months after the destructive earthquake on 4 February 1867. He emphasized that the delay in conducting direct scientific observations resulted in significant loss of both quantitative and qualitative information, which could have served as a foundation for further analysis, interpretations, and lessons learned [121]. This highlights the critical importance of conducting field surveys shortly after an earthquake in historical times.

Over time, particularly during the transition from historical documentation to the era of instrumental recordings, the ability to systematically observe and document earthquake environmental effects has improved. In recent decades, interdisciplinary and multiparametric approaches, combined with the application of modern and innovative methodologies, have enabled accurate and comprehensive mapping of earthquake impacts, the creation of detailed records of seismic phenomena, and the identification of factors contributing to their occurrence [169].

Another key factor contributing to the observed differences in the numbers and percentages of historical versus recent landslides is population density and human activity. In ancient and historical times, both population density and human activity were significantly lower in landslide-prone areas than they are today. In contrast, modern societies, characterized by extensive urbanization and the development of infrastructure in such areas, have increased the likelihood of interactions between the built environment and the secondary EEEs. Among these, ETLs stand out due to their high potential to cause substantial losses, both economic and human.

4.1.2. Location Reliability of the Recorded ETLs in Greece

Regarding the location reliability of ETLs in Greece based on the available quantitative, qualitative and geographical landslide data, the majority of ETLs are classified in the very high and high location reliability class with a percentage of 96.41% (Figures 11 and 12). In particular, the location of 529 out of 669 ETLs (79.07%) was determined with very high reliability, while the location of 116 ETLs (17.34%) was mapped with high reliability. Only 24 events were mapped with moderate reliability (3.59%) and 4 of them with low (0.60%).

ETLs with a very high location reliability index have been identified not only in recent times but also during the historical period. A total of 58 historical ETLs, representing 10.96% of the 529 ETLs in LRI class 1, were recorded between 1513 and 1899. Additionally, 85 historical ETLs, accounting for 73.27% of the 116 ETLs in LRI class 2, were recorded between 279 BC and 1889. These percentages remain relatively stable or are even higher in LRI classes 3 and 4, with 70.83% (17 out of 24 ETLs) and 100%, respectively.

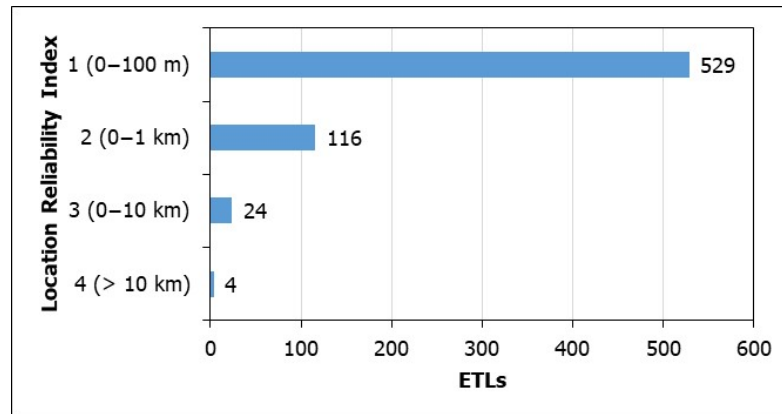


Figure 11. The frequency of ETLs in Greece by LRI classes.

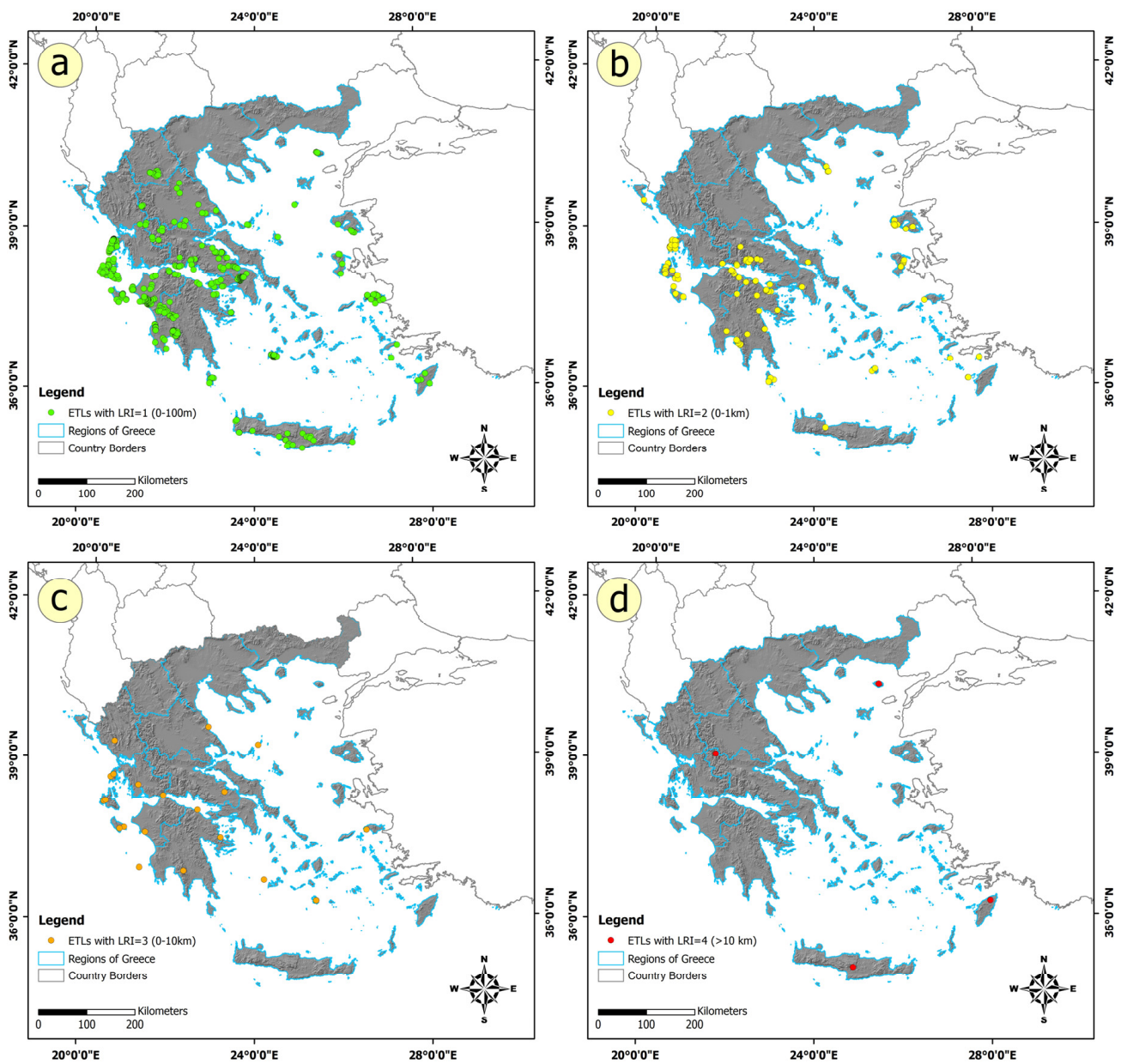


Figure 12. The spatial distribution of ETLs in Greece in different maps based on their LRI. (a) LRI = 1 (0–100 m), (b) LRI = 2 (0–1 km), (c) LRI = 3 (0–10 km) and (d) LRI = 4 (>10 km).

4.1.3. Minimum and Maximum Magnitudes of Causative Earthquakes—Distribution of ETLs in Earthquake Magnitude Classes

The largest earthquake that has occurred in Greece and triggered landslides is the 3 August 1303, $M_w = 8.3$ earthquake. However, the triggered landslide was triggered outside Greece, in Egypt, and is considered in this research to be a far-field effect. The second largest earthquake in Greece that has triggered landslides within the Greek territory is the 12 October 1956, $M_w = 7.7$ earthquake, in the eastern part of the Hellenic Arc. Of the recent earthquakes, the largest one that has triggered landslides was of $M_w = 7.6$ and generated in Kythira on 11 August 1903.

The smallest earthquake found to have triggered landslides in Greece is the 30 June 1970, $M_w = 4.0$ Lefkada (Ionian Islands) earthquake. Regarding the distribution of earthquakes that have caused landslides in Greece in magnitude classes, the following was found (Figure 13a): the largest percentage of earthquakes with ETLs is distributed in class 4 ($6.0 < M_w \leq 6.5$; 46 earthquakes, 31.94%). Double-digit numbers and percentages are also observed in class 5 ($6.5 < M \leq 7.0$; 37 earthquakes, 25.69%) and in class 3 ($5.5 < M \leq 6.0$; 30 earthquakes, 20.83%) (Figure 13a). The numbers and percentages of earthquakes are of a single digit in all other earthquake magnitude classes. The percentage of earthquakes whose magnitude has not been determined in the sources used in this study is 9.03% (13 earthquakes) (Figure 13a). All of them are historical events.

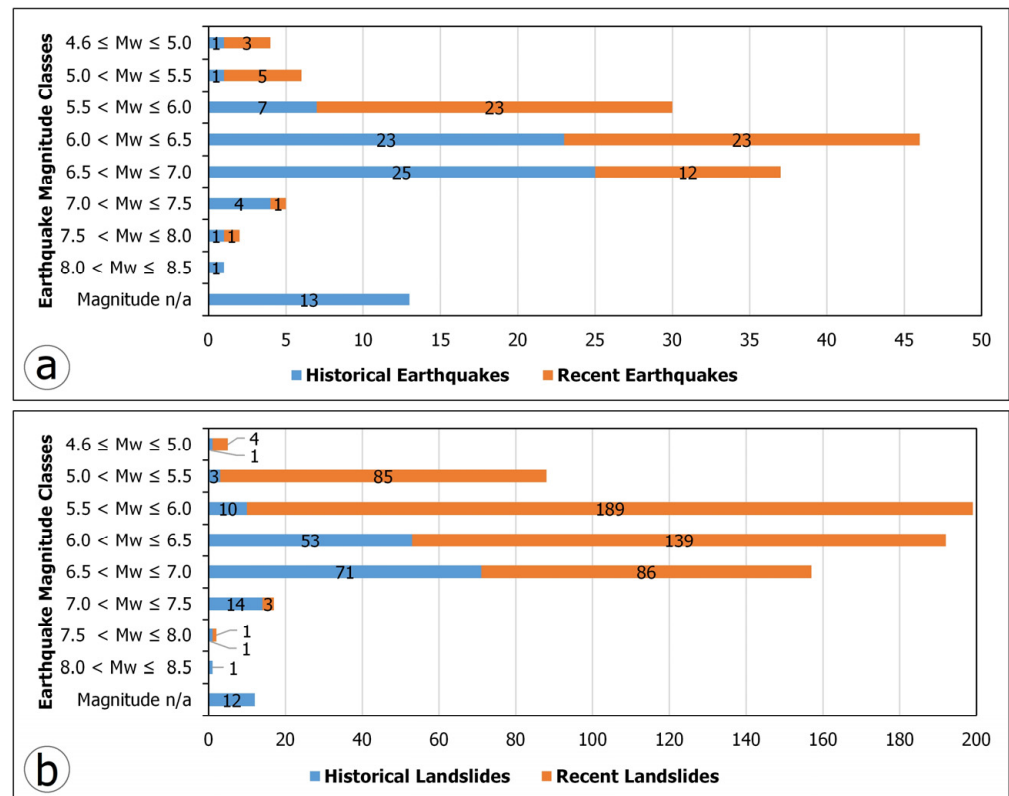


Figure 13. Diagrams showing (a) the frequency of historical and recent earthquakes that have triggered landslides by earthquake magnitude class and (b) the frequency of historical and recent ETLs by earthquake magnitude class.

Most ETLs in Greece are associated with earthquakes in magnitude class 3 ($5.5 < M \leq 6.0$; 199 landslides, 29.57%) (Figure 13b). Double-digit percentages of ETLs are also observed in earthquakes within class 4 ($6.0 < M \leq 6.5$; 192 landslides, 28.53%), class 5 ($6.5 < M \leq 7.0$; 157 landslides, 23.33%), and class 2 ($5.0 < M \leq 5.5$; 88 landslides, 13.08%) (Figure 13b). The lowest percentages of landslides (0.30 and 0.15%) are recorded in the magnitude classes of

major ($7.5 < M \leq 8.0$) and great earthquakes ($8.0 < M \leq 8.5$), respectively, both including events generated before and shortly after 1900 (Figure 13b). While one might expect these larger earthquakes to generate the highest numbers and percentages of landslides, this is not the case for these events. This discrepancy is attributed to the fact that these significant earthquakes occurred in 1303, 1856, and 1903 in Crete, Rhodes, and Kythera, respectively, and are characterized by limited historical sources and insufficient documentation of secondary EEs, including ETLs.

4.1.4. Minimum and Maximum Seismic Intensities of Causative Earthquakes—Frequency of ETLs by Seismic Intensities

The maximum earthquake intensity associated with landslides is XI, while the minimum is V. Most landslides have been triggered by earthquakes with an intensity of IX (248 landslides, 37.07%), followed by intensity VIII (176 landslides, 26.31%) (Figure 14). Combined, earthquakes with intensities of VIII and IX account for approximately 70% of all landslides. Earthquakes of other intensities have triggered far fewer landslides, with double-digit counts corresponding to single-digit percentages (Figure 14).

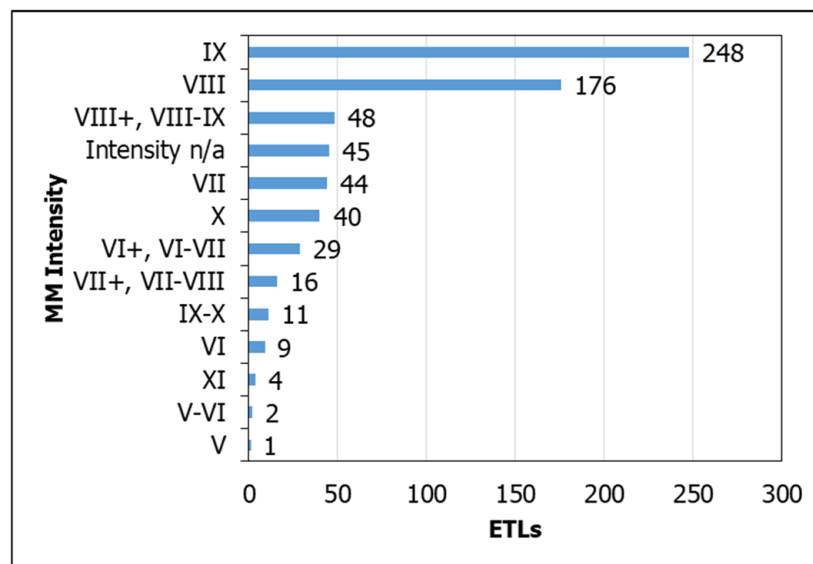


Figure 14. Diagram showing the frequency of ETLs by Modified Mercalli (MM) intensity.

4.1.5. Types of ETLs in Greece

Regarding the type of ETLs in Greece, it was found that the most common are rockfalls (Figure 15). Rockfalls constitute the only type of landslides triggered by 68 earthquakes (47.22%), followed by slides, which are the only type of landslides triggered by 30 earthquakes (20.83%). The percentages of simultaneous triggering of rockfalls and slides are relatively high, with the former predominating in 16 and the latter in 12 earthquakes (11.11% and 8.33%, respectively). Other types of ETLs also included in the respective list are slumps in 5 earthquakes (3.47%), rockslides in 3 earthquakes (2.08%) and other combinations of simultaneous events in the same earthquake. These combinations include slides and slumps in 3 earthquakes (2.08%); slumps and rockfalls in 2 earthquakes (1.39%); slides, rock toppling failures and rockfalls in 1 earthquake (0.69%); slides, rockfalls and rockslides in 1 earthquake (0.69%); and rockfalls and slumps in 1 earthquake (0.69%) (Figure 15a).

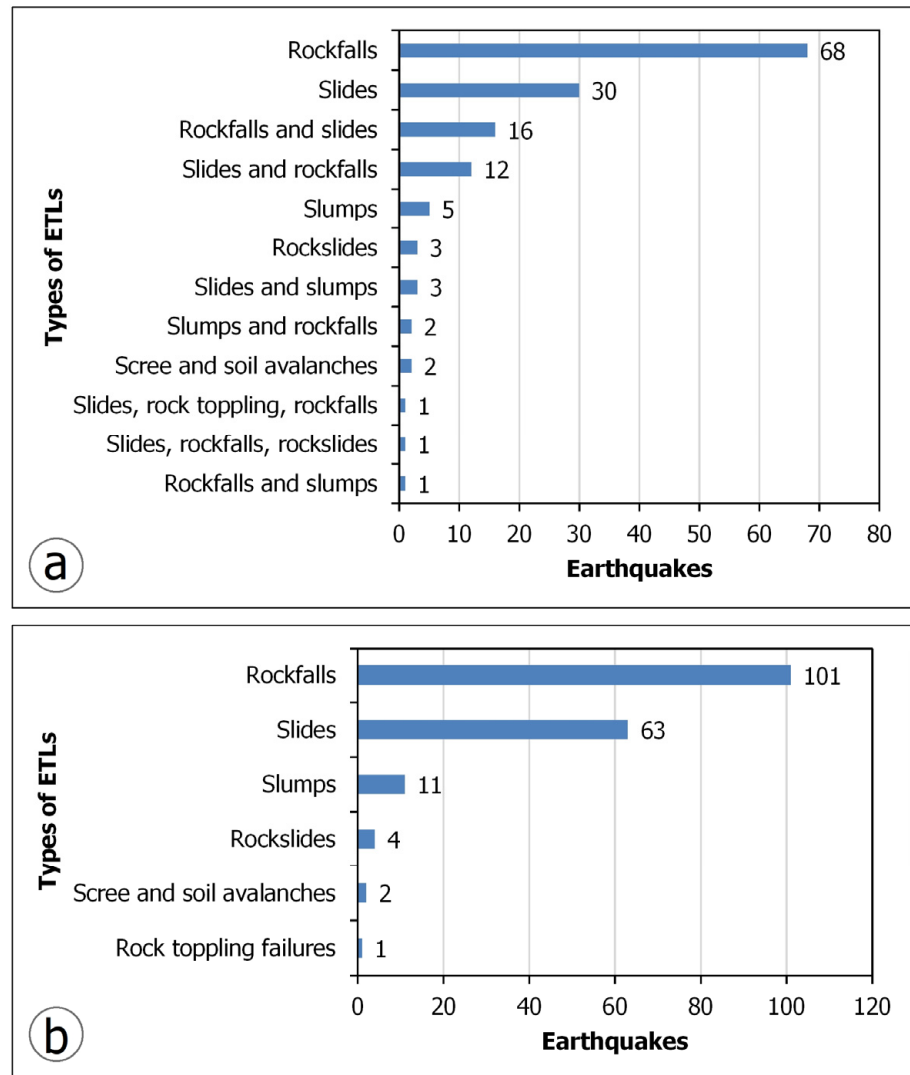


Figure 15. Diagrams showing (a) the number of earthquakes that caused either one or more types of ETLs in the affected area and (b) the number of earthquakes that caused one type of ETLs, regardless of how they occurred (individually or along with others).

If we consider each of the above types of ETLs separately, even if they occur together with other types of ETLs in the same earthquakes, the percentages of rockfalls and slides increase, as follows: for the first type from 47.22% to 70.14% and for the second type from 20.83% to 43.75% (Figure 15b). A similar increase is observed in the occurrence of coastal and submarine slumps from 3.74% to 7.64% (Figure 15b).

4.1.6. ETLs in the Regions of Greece

ETLs have occurred in all of regions of Greece, without exception. However, the percentages vary from region to region, as shown in Figure 16. These differences are attributed to the geotectonic and seismotectonic properties of the regions, as previously mentioned in the respective section. For example, the region of the Ionian Islands in the western part of Greece, with its intense seismicity, has already suffered several destructive earthquakes and ETLs since the historical period, and is at the top of the list in terms of the most ETL-affected regions, while the region of eastern Macedonia and Thrace, which is far from the area of the present Hellenic Arc, is characterized by limited earthquake-triggered landslides (Figures 16 and 17).

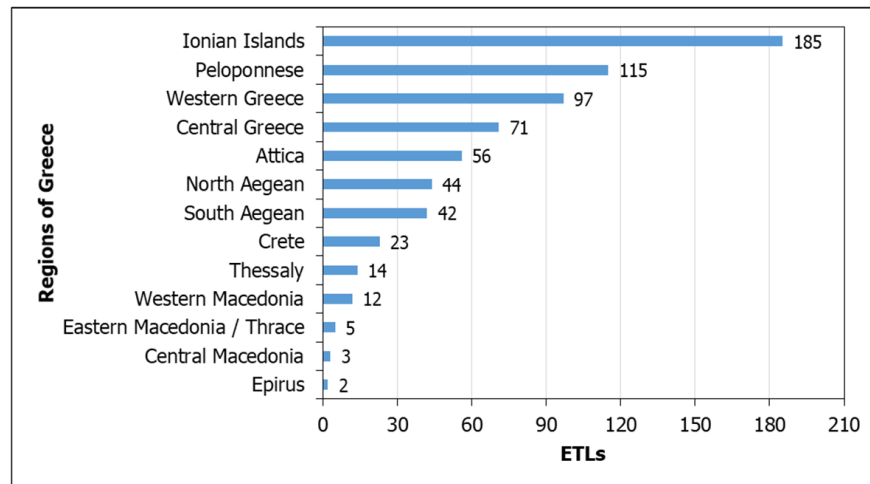


Figure 16. Diagram showing the frequency of ETLs by regions of Greece.

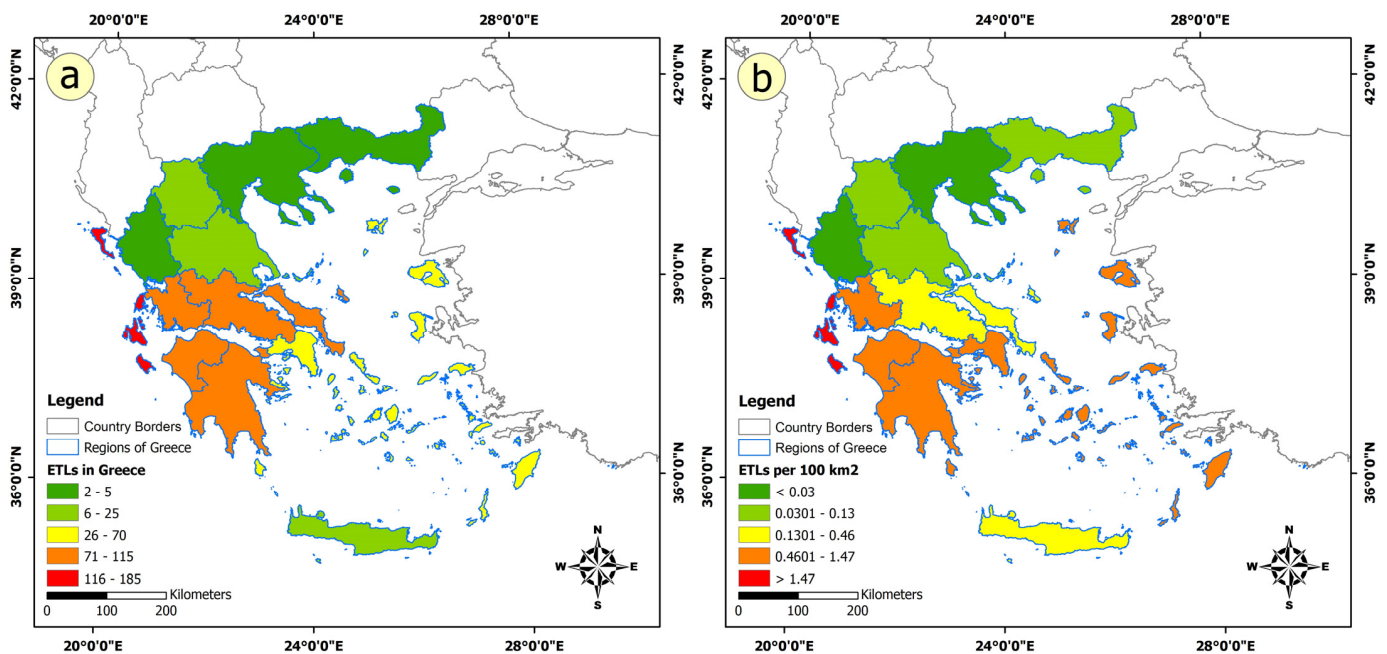


Figure 17. The most ETL-affected regions of Greece based on the contents of Figure 15. (a) Numbers of ETLs in the regions of Greece. (b) ETLs per 100 km² in the regions of Greece. The Ionian Islands (red region) hold first place in both maps.

Another example where the influence of the geodynamic and seismotectonic characteristics of the affected areas on the quantitative characteristics and distribution of landslides is evident is the regional unit of Epirus, which is also at the bottom of the list, although it is located further west than Eastern Macedonia and Thrace and closer to the active part of the Hellenic Arc. However, due to its geotectonic location in the fold and thrust belt located west of the Pindos mountain range, its seismicity is characterized by the occurrence of a large number of earthquakes of low magnitude [170] and a very limited number of earthquakes of high magnitude [171,172]. This results in limited ETLs, and the classification of the region into two seismic hazard zones, with its western part in the Zone II and its eastern part in the Zone I.

4.1.7. ETLs and Morphological Parameters

For the frequency of ETLs by elevation class, the DEM of Greece was reclassified into five elevation classes (Figure 18) following the classification applied by Koukis and Ziourkas [28] in their statistical analysis of slope instability phenomena in Greece. It was found that the highest percentage of ETLs in Greece have occurred in lowlands (<200 m) and hilly (201–600 m) areas with 299 (44.69%) and 252 (37.67%) events, respectively, followed by semi-mountainous (601–1000 m) areas with a remarkable number and relative percentage of landslides (103 events, 15.40%) (Figure 18). Mountainous (1001–1500 m) and very mountainous (>1500 m) areas follow with very low numbers and percentages of ETLs (1.49 and 0.75%, respectively) (Figure 18).

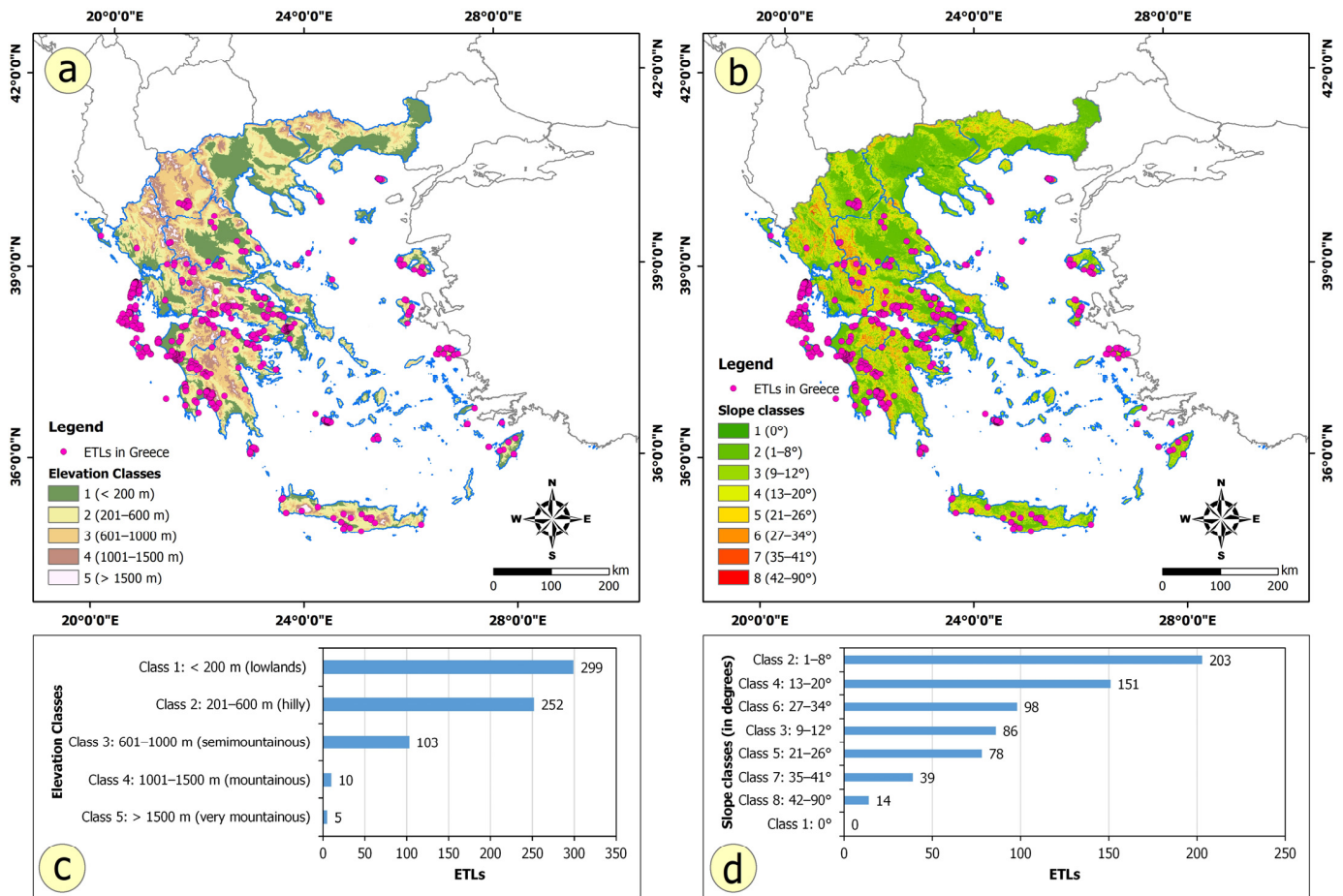


Figure 18. Maps with elevation (a) and slope (b) classes and the spatial distribution of ETLs in Greece. Diagrams of the frequency of ETLs by elevation (c) and slope (d) classes.

Regarding slope, the DEM was converted to slope raster, which was then reclassified into eight slope classes. This classification followed the method applied by Wilde et al. [74] for compiling the European Landslide Susceptibility Map (ELSUS v2).

Most ETLs in Greece have been generated in high percentages on slopes ranging from 1 to 34° (Figure 18). More specifically, 203 ETLs (30.34%) have occurred in slope class 2 (1–8°), 151 ETLs (22.57%) in slope class 4 (13–20°), 98 events (14.65%) in slope class 6 (27–34°), 86 ETLs (12.86%) in slope class 3 (9–12°) and 78 ETLs (11.66%) in slope class 5 (21–26°) (Figure 18). ETLs in the remaining classes, 7 (35–41°) and 8 (42–90°), have occurred in percentages not exceeding 6.0% (39 and 14 events, respectively).

4.1.8. ETLs and Geological Properties of the Affected Formations

For the frequency of ETLs by category of geological formations, we utilized the information contained in the Geological Map of Greece at a scale of 1:500,000 [67]. Taking into account this classification and the dataset of ETLs, it is concluded that most landslides have occurred in alpine formations (375 out of 669 landslides, 56.05%) and in post-alpine deposits (213 out of 669 landslides, 31.84%) (Figure 19a). In all other categories, the percentage of landslides is less than 10%. In particular, 6.43% of ETLs (43 events) have occurred in volcanic formations, 2.39% (16 events) in pre-alpine series, 2.09% (14 events) in metamorphic formations, while the lowest percentage is observed in igneous rocks, amounting to only 1.20% (8 events) (Figure 19a).

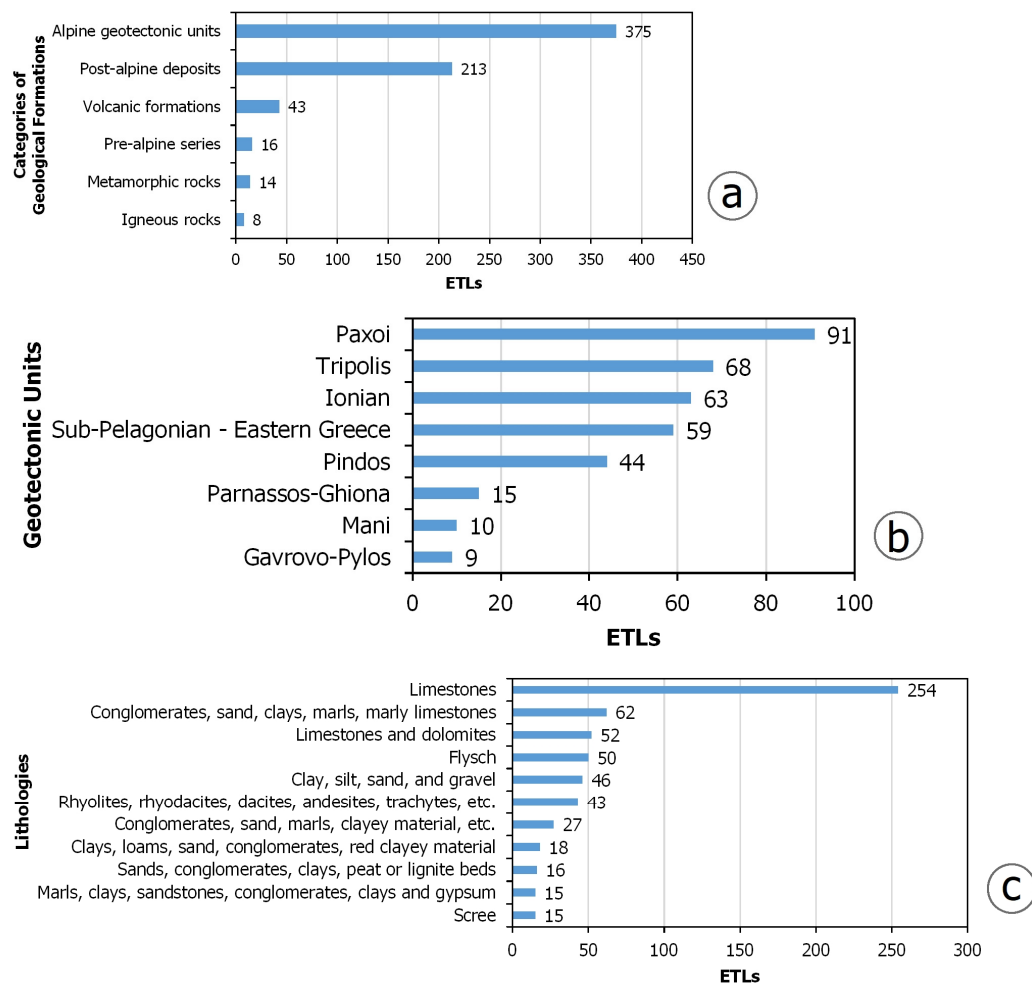


Figure 19. The distribution of ETLs in Greece by category of geological formations. The frequency of ETLs in Greece by categories of (a) geological formations, (b) geotectonic unit and (c) lithology.

For the frequency of ETLs by geotectonic unit and lithology, we used the aforementioned map along with the Geotectonic Map of Greece [80]. It is found that most ETLs have occurred in geotectonic units belonging to the tectonostratigraphic terrane of the External Hellenides (Paxoi, Tripolis, Ionian, Mani and Gavrovo-Pylos units, 241 out of 669 ETLs, 36.02%) (Figure 19b), while most of them have occurred in locations composed of limestone (254 out of 669 ETLs, 37.97%) (Figure 19c).

The limestones are followed by lithologies that are observed mainly in post-alpine deposits and include conglomerates, sand, clays, marls and marly limestones (62 out of 669 ETLs, 9.27%), limestones with dolomites (52 out of 669 ETLs, 7.77%), flysch type lithologies (50 of 669 ETLs, 7.47%), a category of lithologies occurring in post-alpine deposits (clay, silt, sand, and gravel; 46 of 669 ETLs, 6.88%), as well as lithologies of volcanic rocks, including rhyolites, rhyodacites, dacites, andesites, trachyandesites, trachytes, tuffs and ignimbrites (43 of 669 ETLs, 6.43%) (Figure 19c). The remaining lithologies are characterized by even lower percentages, ranging from 0.15% to 4.04% (Figure 19c).

In addition to limestones that have a high percentage of ETLs, lithologies occurring in post-alpine deposits with ages ranging from the Miocene to the Holocene have also been heavily affected by ETLs. By summing the numbers and percentages of ETLs generated in lithologies that mainly include conglomerates, sands, clays, marls, marly limestones, clayey material, and sandstones, it is concluded that the post-alpine lithologies have been significantly impacted by ETLs (190 events, 28.40%).

For the frequency of ETLs by geological period, the Geological Map of Greece [39] was also used. Taking into account the classification of geological formations and the spatial distribution of ETLs, it is found that the most affected geological formations are Triassic–Jurassic and Upper Cretaceous limestones with 90 (13.45%) and 85 (12.71%) events, respectively; the post-alpine deposits of the Pliocene age (62 ETLs, 9.27%); and the Mesozoic–Eocene dolomitic limestones (52 ETLs, 7.77%) (Figure 20). In the first eleven positions of the respective list, post-alpine deposits whose age range from the Miocene to the Holocene are mainly observed (197 ETLs in total, 29.45%). However, if the classification is made on the basis of geological eras, the situation is different, with the Cenozoic formations being the most affected, followed by the Mesozoic formations, while the Paleozoic formations comprise the least affected by ETLs.

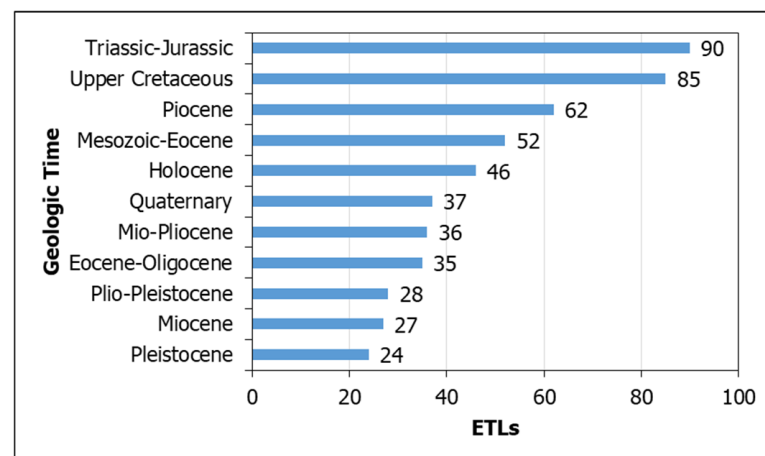


Figure 20. The distribution of ETLs in Greece by formation age.

4.1.9. ETLs and Mechanical Properties of the Affected Formations

For the frequency of ETLs by type of mechanical characteristics and geotechnical behavior of the affected formations, we used the information contained in the Engineering Geological Map of Greece [68]. ETLs in Greece were observed in 23 of these categories. The first four categories of the list, which have either more than 100 or very close to 100 ETLs, with respective percentages above 10%, include the following: (i) limestones—dolomitic limestones—dolomites (136 landslides, 20.33%); (ii) Neogene deposits with mixed phases (115 landslides, 17.19%); (iii) limestones (91 landslides, 13.60%); and (iv) Quaternary loose deposits with mixed phases (90 landslides, 13.45%) (Figure 21). The remaining formation categories follow with numbers of ETLs less than 50 events and corresponding percentages

less than 10% (Figure 21). More information on the parameters of each category is included in Supplementary Table S1.

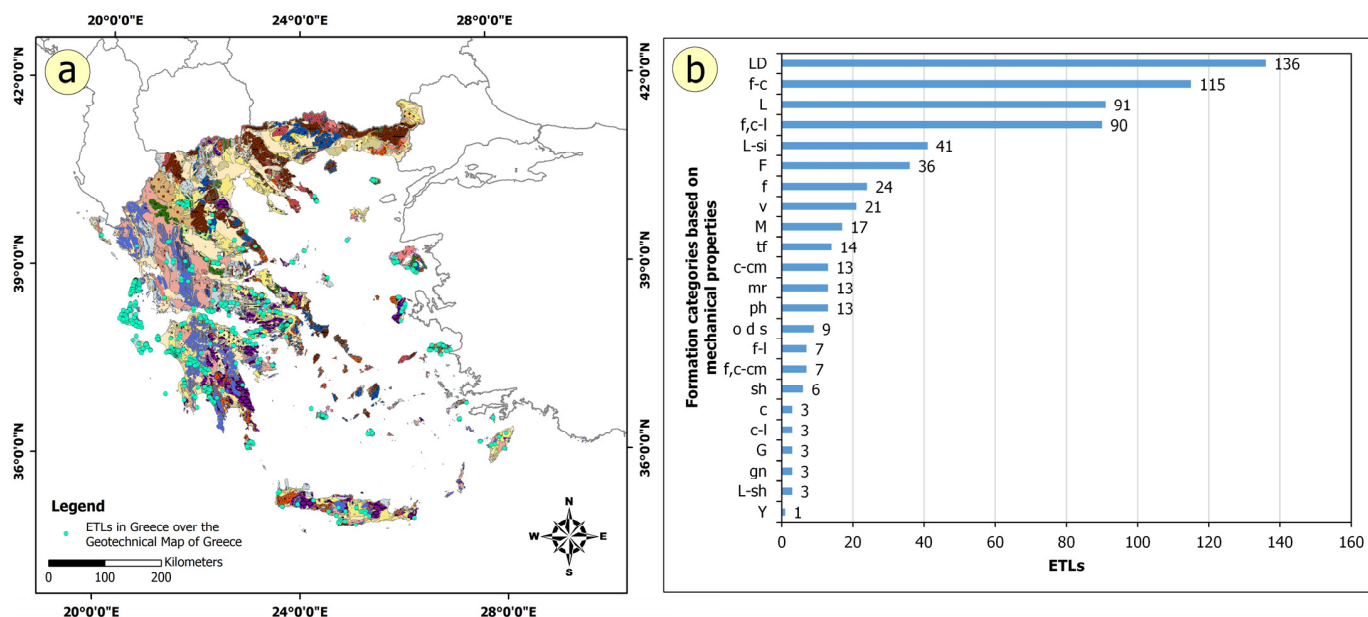


Figure 21. (a) The spatial distribution of the detected ETLs over the engineering geological map of Greece. (b) The frequency of ETLs in Greece by categories of geological formations based on their mechanical characteristics and geotechnical behavior as they are presented in the Engineering Geological Map of Greece [68]. LD: limestones—dolomitic limestones—dolomites; f-c: Neogene deposits with mixed phases; L: limestones; f,c-l: Quaternary loose deposits with mixed phases; L-si: limestones with nodules and lenses of silica; F: undivided flysch; f: Neogene, mainly fine-grained deposits; v: volcanic rocks (lavas); M: molassic sediments; tf: volcanic tuffs; c-cm: Quaternary coherent, coarse-grained deposits; mr: metamorphic carbonate rocks; ph: semi-metamorphic rocks; o d s: basic and ultrabasic igneous rocks; f-l: Quaternary loose, mainly fine-grained deposits; f,c-cm: Quaternary, coherent deposits with mixed phases; sh: shales and cherts; c: Neogene, coarse-grained deposits; c-l: Quaternary loose, mainly coarse-grained deposits; G: Gypsum and calcareous–dolomitic breccia, unbedded; gn: metamorphic rocks; L-sh: limestones, alternating with cherts, schist–chert or schist–marly layers; Y: acid to intermediate plutonic rocks.

4.1.10. ETLs and Land Use

For the frequency of ETLs by land use, CORINE Land Cover (CLC) 2018 [72] was utilized. It is concluded that ETLs have mainly occurred in areas covered by sclerophyllous vegetation (113 out of 669 ETLs, 19.88%) (Figure 22). They are followed by land principally occupied by agriculture, with significant areas of natural vegetation (84 out of 669 ETLs, 12.56%), olive groves (77 out of 669 ETLs, 11.51%) and coniferous forests (61 out of 669 ETLs, 9.12%) (Figure 22). All other land uses follow, with lower percentages of ETLs.

Sclerophyllous vegetation plays a dual role in the context of earthquake-induced landslides. One of the primary functions of sclerophyllous vegetation is its ability to enhance slope stability through root reinforcement. The roots of these plants can bind soil particles together, thereby increasing the shear strength of the slope and reducing the likelihood of landslides during earthquakes. Research indicates that areas with dense vegetation tend to experience fewer and smaller landslides compared with areas with sparse vegetation or bare soil [173]. This is attributed to the root systems of trees, which provide significant mechanical support to the soil, mitigating the effects of ground shaking during an earthquake [174].

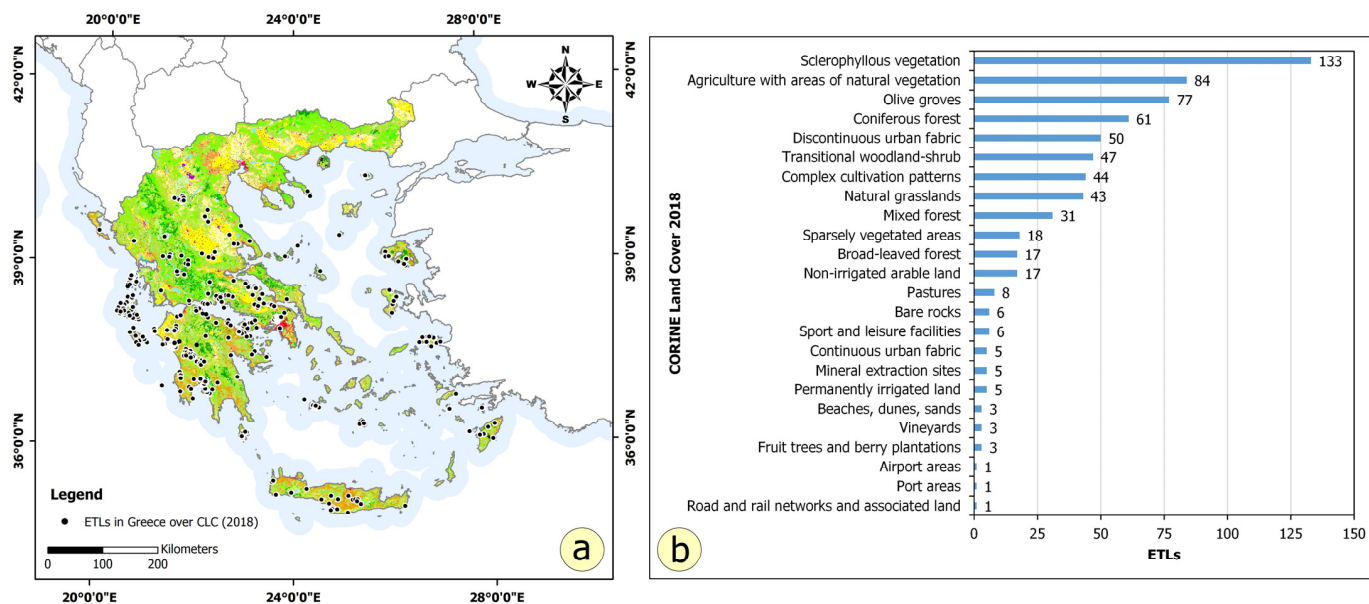


Figure 22. (a) Map with the distribution of the ETLs in Greece over the land use based on CORINE Land Cover (2018) [44] and (b) the frequency of the ETLs by land use.

While sclerophyllous vegetation can enhance slope stability through root reinforcement, it can also contribute to landslide initiation under certain conditions, particularly when vegetation is disturbed or when hydrological factors are unfavorable. In regions where vegetation is sparse or has been disturbed, the landslide hazard can be heightened, as observed in studies of landslides triggered by the 2018 Hokkaido earthquake, where the availability of trees on hillslopes significantly influenced the runout distance of landslides [175].

The role of vegetation in landslide dynamics is further complicated by the interplay of other environmental factors, as seems to be the case for ETLs in Greece. The synergy of several factors, including topography, geology, lithology, active faults affecting the mechanical properties and the geotechnical behavior of geological formations and hydrological conditions, can heavily disturb the vegetation cover and lead to increased landslide susceptibility in the short term when an earthquake occurs, and in the long term if recovery efforts are not effectively implemented [176].

4.1.11. ETLs and Seismic Hazard Zones

From the overlay of the ETLs on the seismic hazard zones, it was found that most landslides have occurred in the second seismic hazard zone (430 out of 669 ETLs, 64.28%) with the third zone following in second place (184 ETLs, 27.50%) and the first zone with the fewest events (55 ETLs, 8.22%) (Figure 23). One would expect the third zone, characterized by the highest expected acceleration, to have the most landslides due to the strong destructive earthquakes that occur as a result of its proximity to active and seismic faults. This difference is not attributed to the seismotectonic setting and seismological properties and the activity of fault structures in the Ionian Islands, but to the much larger area covered by the second zone.

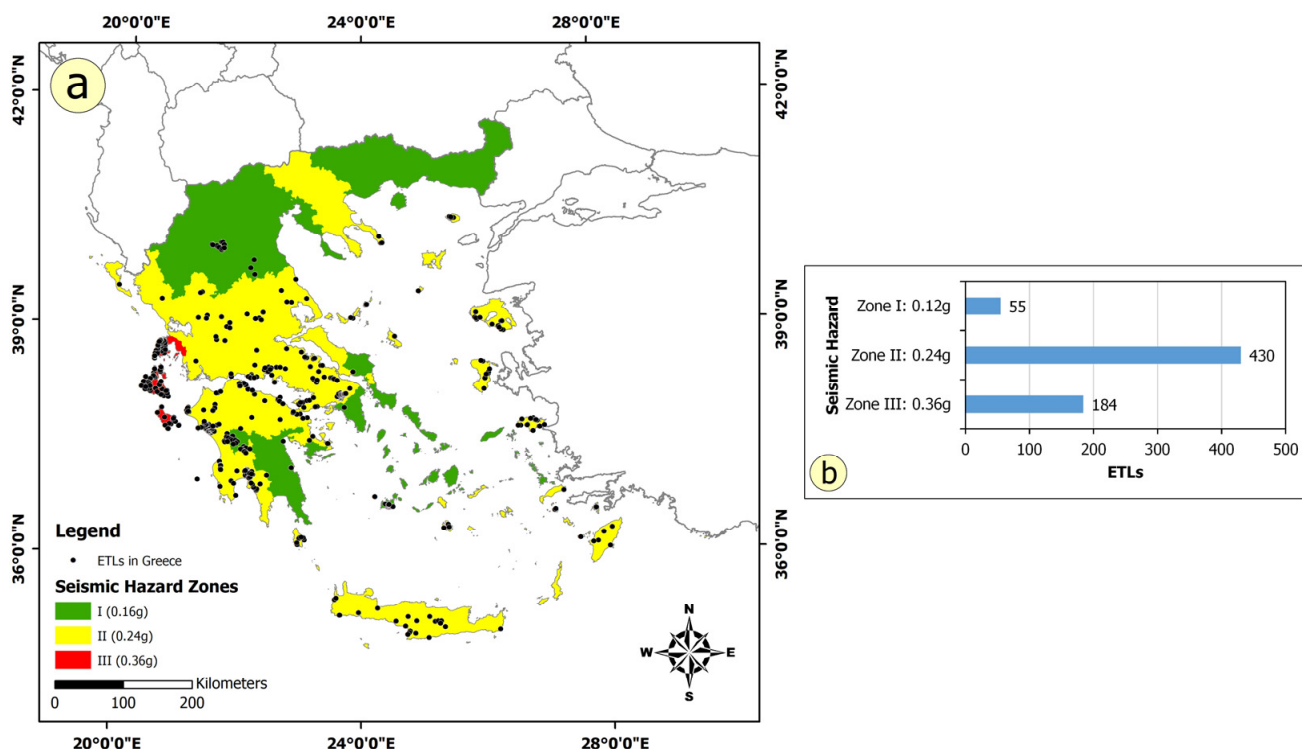


Figure 23. (a) Map with the distribution of ETLs in Greece and (b) the frequency of the detected ETLs by seismic hazard zone according to the relevant map of the EPPO [71].

4.1.12. ETLs and Landslide Susceptibility

For the frequency of ETLs by landslide susceptibility class, the relevant information contained in the European Landslide Susceptibility Map (ELSUS v2) [73] was used. It was found that ETLs in Greece were located in all landslide susceptibility zones, but with different percentages in each of them. More specifically, most ETLs (473, 70.70%) have been observed in the very high and high landslide susceptibility classes (257 and 216 events, respectively, with percentages greater than 30%) (Figure 24). In the areas of moderate landslide susceptibility 124 (18.54%) events occurred, while the zones of low and very low landslide susceptibility host a smaller number of ETLs (49 and 23 events, respectively, with percentages of less than 10%) (Figure 24).

This distribution of ETLs verifies recent research on ETLs in Greece. A prominent example comes from Cephalonia, in the central Ionian Islands. From the research conducted by Mavroulis et al. [36], it is concluded that the spatial distribution of ETLs is not random, but that their majority (82%) were generated within high to critically high susceptible zones, where conditions of instability have already prevailed before the earthquakes. Considering also the results of the study of Sakkas et al. [37] on landslide susceptibility in Greece, it is concluded that several areas with high numbers of ETLs detected in the present study coincide with the high landslide susceptible areas detected in the frame of the aforementioned national-scale study. These areas are western Greece, the northern Peloponnese as well as the north and east Aegean Islands.

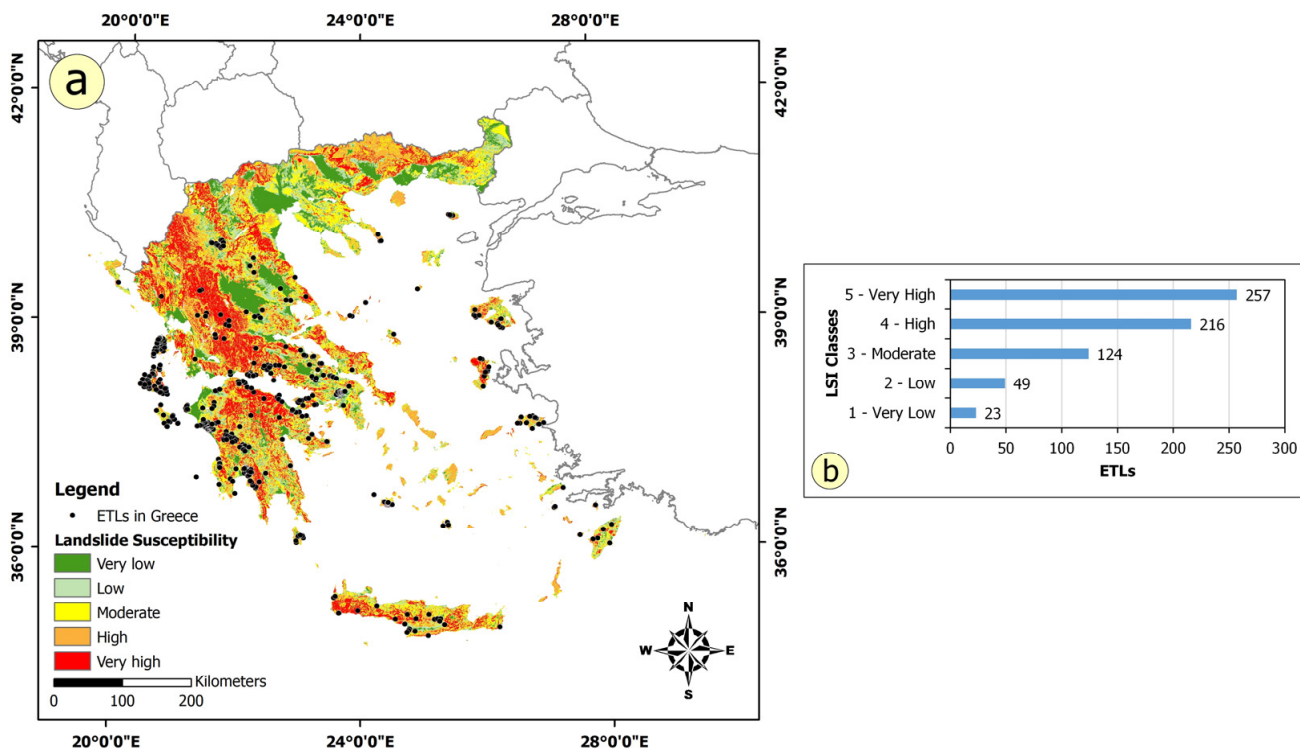


Figure 24. (a) Map with the distribution of ETLs in Greece and (b) their frequency by LSI class according to the European Landslide Susceptibility Map (ELSSUS v2).

4.1.13. ETLs and Tectonic Structure

Regarding the distribution of ETLs by taking into account the tectonic structure, it is found that ETLs in Greece occur mainly near faults and fault zones and within deformation zones. Typical examples come from almost all areas affected by ETLs in Greece: the Ionian Islands, Peloponnese, central Greece, Thessaly, and western Macedonia.

Starting from the central part of the Ionian Islands, it is evident that a large part of the recorded ETLs are distributed in areas where active and seismic faults are developed along the margins of fault blocks, but also along inactive tectonic structures, which, despite their inactivity, have contributed greatly to the intense deformation of geological formations, the deterioration of their mechanical properties and the determination of their geotechnical behavior.

Such areas are found in Lefkada and Cephalonia Islands, located in the central part of the Ionian Sea. Most ETLs in Lefkada have occurred in the western part of the island, which is strongly deformed by active and seismic faults, resulting in almost pulverized carbonate formations [110,163]. Further south, in Cephalonia, ETLs have mainly occurred along transition zones between fault blocks [13,36,77]. As an example, the transition zone (Thinia valley) from the Paliki peninsula (western Cephalonia) to the fault block of central Cephalonia and the transition zone (Pylaros valley) from the central Cephalonia fault block to the Erissos peninsula (northern Cephalonia) are disrupted by oblique-reverse faults, namely the Kontogourata–Agon and the Agia Efimia faults, respectively [161]. These deformations have resulted in the formation of conditions of instability and the subsequent triggering of landslides in case of an earthquake. Tens of landslides have been triggered along the fault-controlled margins of these valleys due to the 1953 [36], 1983 [142] and 2014 [161] Cephalonia earthquakes.

Apart from these cases, ETLs have also occurred along inactive tectonic structures, e.g., the thrust of the Ionian geotectonic unit on the Paxoi unit in the central Ionian Islands. In eastern Cephalonia and southwestern Lefkada, the morphology along the Ionian thrust is rugged, with steep slopes and unstable conditions, which contribute significantly to ETLs [36,163].

Further east, most ETLs occurred within the western part of the morphoneotectonic sectors, which occur in the western Peloponnese, with different neotectonic trends: E–W for the first morphoneotectonic sector and NNW–SSE for the second (Figure 6). These ETLs have occurred along the margins of major fault blocks in the region, such as the southeastern margin of the Pyrgos–Olympia basin and the western margin of the Megalopolis basin affected by the 1965 earthquake [43], the eastern margin of the Kalamata basin affected by the 1986 earthquake [51], and the western margin of the Kyparissia Mountains in the southwestern Peloponnese affected by the 1899 [43,118] and 1947 earthquakes [43,135].

In the western Peloponnese, ETLs have also been recorded in areas with the intense relief that is attributed to the diapiric movements of Triassic evaporites, such as in the Kyllini peninsula (western Peloponnese) during the 1988 earthquake [52] and in the western part of the Pyrgos–Olympia basin during the 1993 earthquake [54,146]. In both cases, landslides occurred largely along morphological discontinuities of tectonic origin.

A similar distribution can be observed in the area of western Attica (the eastern part of mainland Greece) during the 1999 Athens earthquake. Rockfalls occurred along the margins of the Parnitha Mt [123], located at the western edge of the Athens basin. This is similarly to the 1981 earthquake sequence that also struck Athens city, with ETLs occurring along ruptured faults in the eastern onshore part of the Corinth Gulf [99,140].

As for the Corinth Gulf, ETLs are located in the coastal areas north and south of this Quaternary graben, which have been affected by E–W normal faulting, leading to the formation of striking fault-related topography [177,178], which is characterized by not only primary but also secondary EEEs, such as ETLs.

In the Thessalian plain located in central Greece, most ETLs have occurred on its southern margin, where the southern seismogenic zone of Thessaly develops [179]. This seismogenic zone has been associated with earthquakes with magnitudes of up to 7.0, with the most recent major one in the region being the 30 April 1954 Sophades earthquake [180].

Further north, in the area affected by the 1995 Grevena–Kozani earthquake, ETLs are distributed near locations where primary EEEs including coseismic surface ruptures, were observed. These effects, both primary and secondary, are associated with the active Aliakmonas River zone, which has been formed in the area [55,147].

4.2. Maximum Epicentral Distances as a Function of Earthquake Magnitudes

The maximum distance, R_e , from the earthquake epicenter to a triggered landslide is an indirect measure of the threshold level of ground shaking necessary to trigger a landslide. At the same time, it is a valuable parameter for earthquake-induced landslide hazard assessment [10,21].

The epicentral distances of the ETLs in Greece were calculated, taking into account the ETL locations obtained from the present research and the earthquake magnitudes obtained by the aforementioned earthquake catalogues. The maximum epicentral distance of landslides for each earthquake was then selected. The pairs of maximum epicentral distance of ETLs and the magnitude (M_w) of the causative earthquakes were plotted on a graph (Figure 24). The distribution of these points was also compared with the upper bound limit/curve for the maximum observed epicentral distances of disrupted slides and falls proposed by Keefer [10,15], which was based on a dataset of 40 earthquakes worldwide. This curve represents the maximum distances at which ETLs can be expected

to be generated for specific M_w values. The projection of the data for ETLs in Greece together with Keefe's curve enables the Greek data to be placed in a global context and for any deviations from the current international standards for ETLs to be identified.

The graph of Figure 25 shows how the distribution of ETLs in Greece data generally fit the Keefe relationships well. It is concluded that the vast majority of the events are consistent with Keefe's curve, with the exception of four cases, three of which are landslides induced by historical earthquakes. A significant number of points lie between magnitudes M_w 5.5 and 7.0. The outliers represent the historical earthquakes of 8 August 1303 in Crete, 22 March 1783 in Lefkada, 15 August 1837 in Pyrgos and the recent earthquake of 30 June 1970 in Lefkada. The point that can be found significantly above the curve corresponds to the landslide triggered in Egypt by the 1303 earthquake in Crete. The induced phenomenon is numbered among the far-field effects and therefore is observed at a greater distance than average. Two outliers in the dataset are associated with Lefkada Island and reflect the island's unique geological and tectonic conditions. These events highlight the region's high susceptibility to ETLs, possibly due to its steep slopes, loose sediments, and the proximity to active faults and fault zones. While these data points deviate from the general trend, they underscore the importance of accounting for regional variations.

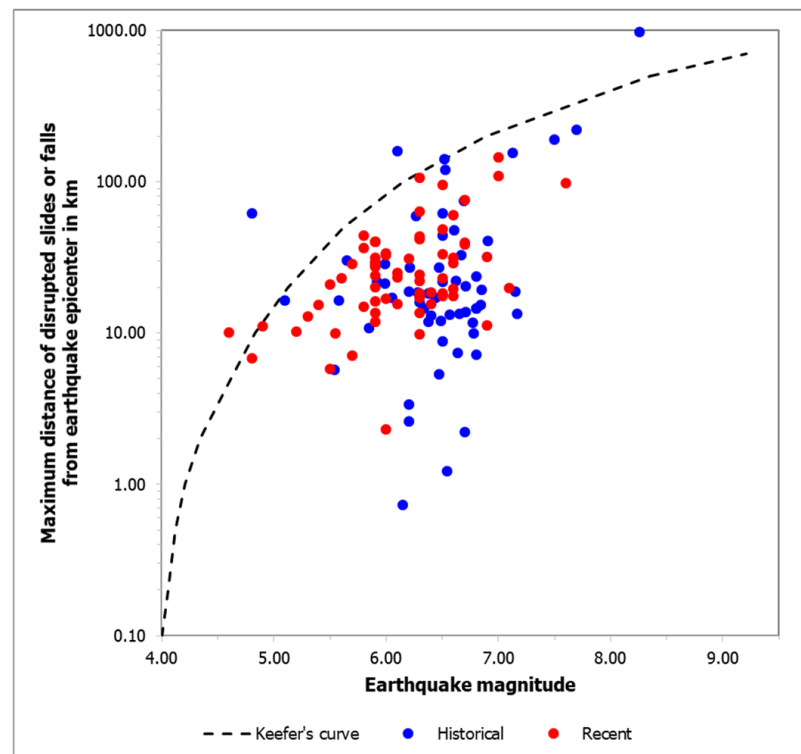


Figure 25. Maximum distance from the earthquake epicenter of disrupted slides and falls induced by historical (blue) and recent (red) earthquakes generated in Greece versus earthquake magnitude. The dashed line is the upper bound for disrupted slides or falls by Keefe [10].

5. Impact of ETLs in Greece on the Natural and Built Environment and the Population

5.1. Impact of ETLs on the Natural and Built Environment

ETLs in Greece have caused significant impacts on the natural and built environment of the affected areas. Starting from the natural environment, the impacts have been recorded not only onshore but also offshore. The onshore impacts of ETLs include geomorphological changes, such as the formation of small hills from the accumulation of mobilized materials

and the creation of dams as a result of unstable geomaterials ending up in riverbeds and streams, resulting in the interruption of their flow and subsequent overflow. A typical example of the first impact was triggered by the 18 March 1874 earthquake in Eretria area (Evia Island, eastern part of mainland Greece), where landslides occurred on Olympus Mt and a small hill was formed by the accumulation of unstable materials [40]. Typical examples of the second impact were recorded after the earthquakes of 24 April 1504 in Pyli, when unstable materials accumulated in the Acheloos riverbed and temporarily interrupted its flow. During the 29 June 1861 earthquake, the collapse of a mountainside in Nisyros Island (Dodecanese island complex) blocked a torrent valley [41].

Offshore impacts come mainly from offshore and coastal ETLs. They include (i) sea disturbance and subsequent tsunamis; (ii) increased sea turbidity from coastal rockfalls and slides; (iii) destruction of telecommunication network offshore components, such as telegraph cables; (iv) structural damage to coastal infrastructure and facilities, such as the destruction of jetties. Sea disturbance and subsequent tsunamis following offshore and coastal landslides have been recorded during the earthquakes of 5 November 1633 in Zakynthos, where coastal landslides at a cape on the southern coast of the island caused a sea level rise that resulted in inundation of the coastal zone and damage to structures along the coastal front [33]. Another example of such impact comes from Messinia (SW Peloponnese) and the earthquake of 6 October 1947, where the beach of Methoni was inundated for a short period of time and at a depth of 15 m by a sea wave. Its origin is attributed to an ETL off the above coast [42,45].

The increase of sea water turbidity from ETLs is a common phenomenon, especially in island regions affected by strong earthquakes. The most typical examples come mainly from the central Ionian Islands. In the bay of Myrtos, famous for its natural beauty in northwestern Cephalonia, the sea has been affected by turbidity many times during historical and recent times, with examples as follows: (i) during the August 1953 seismic sequence, where coastal subsidence and ETLs on the slopes on either side of Myrtos beach disturbed the sea for days [13]; (ii) during the great offshore earthquake of Cephalonia on 17 January 1983, when slides of fine-grained materials and rockfalls increased the turbidity in the bay of Myrtos, downstream of the coastal slope of Harakas, located at the northern end of Myrtos beach [36,142]; (iii) during the earthquake on 26 January 2014 when landslides and rockfalls changed the color of Myrtos bay for days [161].

Destruction of telegraph cables due to offshore landslides has been identified after earthquakes on 27 August 1886 at Filiatra, when the telegraph cable between Crete and Zakynthos was cut [40]; on 9 September 1889 in Achaia when the submarine telegraph cable at a distance of 3 km from the town of Aigio was washed away by a landslide at a depth of 360 m [40,41]; and after the earthquake of 30 May 1909 in Phocis (mainland Greece), where the Corinth Gulf telegraph cable was cut by a submarine landslide near the town of Akrata [44].

Destruction of coastal infrastructure and port facilities by ETLs occurred on 27 November 1914 in Lefkada, where a large slide of coastal deposits increased the depth of the seabed, caused the subsidence of the breakwater in the village of Nydri (eastern Lefkada) and triggered a tsunami [40,42]. From the same earthquake, a coastal area of 3 km² in the area of Kalamitsi (southwestern Lefkada) retreated and was subsequently inundated by the sea [40].

The effects of ETLs on the natural environment also comprise impacts on vegetation and livestock. The most common impact on vegetation is uprooting of trees and vegetation dragging by landslides. This phenomenon has in many cases affected not only crops, such as olive groves and vineyards, but also forests. Typical examples of this have already been reported from the historical period, starting with the 1636 earthquake in Cephalonia,

where rockfalls and slides on the steep slopes of Aenos Mt located in the southern part of the island resulted in many trees being uprooted. Similar phenomena affecting olive groves on the steep southern slopes of Aenos Mt occurred during the main shock of the August 1953 sequence, as well as in the eastern part of the Paliki peninsula in western Cephalonia, where rockfalls along the slopes of Douri hill (Paliokastro, eastern Paliki peninsula) destroyed olive trees [13]. In the western coastal part of central Cephalonia, the generated phenomena destroyed olive trees and vineyards [13]. Similar effects occurred during the Chios earthquake of 3 April 1881, where rockfalls at Gouves uprooted olive trees and many other types of vegetation [119].

There are also many examples of the impact on livestock in areas affected by ETLs caused by earthquakes. The earthquakes of 1636 and 1953 in Cephalonia [13,40], of 1852 in Gravia [44], and of 1881 in Chios Island [124] triggered ETLs, resulting in entire herds of livestock being swept away by the mobilized materials and others disappearing under debris.

Apart from the natural environment, the effects of ETLs in Greece on the built environment of the affected areas are significant. Many examples come from many regions and include non-structural and structural damage to buildings and infrastructure from impact with mobilized landslide materials, dragging of structures and infrastructure by unstable geomaterials, as well as displacement and destruction of buildings and infrastructure located within the landslide zone. Since 1402, many earthquakes have been recorded to have caused landslides with significant impacts on settlements and towns. These landslides have increased damage, economic losses and human losses. Typical examples are as follows:

- The Zakynthos earthquake of 16 April 1513, when slides and rockfalls resulted in the burial of a large part of the ancient city of Psosis and the entrapment of many people [91,108];
- The earthquakes of 1636, 1867 and 1953 in Cephalonia, where many settlements were flattened by landslides that occurred upstream, with dozens of human losses, especially from the main shock on 12 August 1953 [13,36,40,42]. Typical examples of the earthquake-triggered landslide-affected residential areas in Cephalonia include Tzanata village with 14 fatalities and Plateies village with 1 fatality attributed to slope failures generated during the August 1953 earthquake sequence;
- The earthquakes of 22 and 23 March 1783 in Lefkada that caused five fatalities in the area of Agios Petros [41,42] in the southwestern part of the island. The population of this area was also affected after the recent 2015 Lefkada earthquake when rockfalls in the same settlement caused a woman, who had taken refuge in her house for protection, to be fatally injured when a rockfall struck the house and destroyed a large part of it [163];
- The earthquake on 3 April 1831 in Samos (east Aegean), when rockfalls on Kerketeas Mt in the western part of the island caused seven fatalities [40,42].
- The earthquake on 11 October 1845 in Lesvos (northeastern Aegean), when the village of Vrysa experienced rockfalls that affected 60 houses resulting in a fatality [40,41,124];
- The earthquakes in mainland Greece on 14 July 1852 and 1 August 1870 destroyed many settlements, resulting in fatalities which among others included four shepherds in Arachova area when rockfalls were triggered by the second earthquake [40,41,44];
- The Chios earthquake on 3 April 1881, with two fatalities resulting from landslides at the Akrotiri area [117].

The infrastructures that have been affected by ETLs in Greece so far are mainly the road network, the telecommunications network and port facilities. The latter two were mentioned earlier. The impacts on the road network include accumulation of materials on the road surface, resulting in temporary disruption of vehicular and pedestrian traffic; partial or total destruction of the road surface, with cracks and craters from the impact of mainly rocky debris from rockfalls; deformation of road protection barriers as boulders are bounced across the roads; damage to road facilities and usually temporary traffic disruption until recovery and the restoration of damaged areas.

The majority of ETLs in Greece have caused the aforementioned impacts on the road network. ETLs sometimes also affect vehicles that are either parked or moving. Typical examples are the earthquake of 26 July 2001 in Skyros (the Sporades island complex), when landslides triggered on the western side of the castle of Chora crushed 30 cars, and the earthquake of 13 August 2003 in Lefkada, when several cars parked near beaches in the western part of the island were crushed by landslides [156]. A more recent example is the earthquake in Arkalochori (Crete) on 27 September 2021, where moving cars were damaged by rock fragments detached from slopes in the area of Profitis Ilias [66].

5.2. Direct and Indirect Impact of ETLs on Public Health

The health impacts of ETLs on the population are divided into direct and indirect [8]. In the case of Greece, direct impacts include human losses from dragging by unstable materials; from entrapment in buried, displaced or destroyed houses; and from drowning, which has occurred secondarily after a landslide in a coastal area and its subsequent inundation. The first two cases were presented earlier. The rare third case was recorded during the earthquake of 6 July 1965 and was the result of a landslide off the coast of Eratini and the subsequent submergence of part of the coastal zone of the Gulf of Corinth [43].

The indirect public health impacts of landslides include mainly sporadic cases, outbreaks and epidemics of infectious diseases from the stirring of geomaterials and the process of their removal [181]. A typical example of the public health impact of ETLs is the epidemic of coccidioidomycosis that broke out in the San Fernando Valley of the city of Los Angeles (USA) after the $M_w = 6.7$ earthquake on 17 January 1994. Dust clouds were formed as a result of the mainshock and its strongest aftershocks, causing landslides in the Santa Susana Mountains north of Simi Valley [182]. Following landslides, the affected areas presented a sharp rise in coccidioidomycosis cases, which peaked 2 weeks after the earthquake, with 203 cases of coccidioidomycosis or valley fever identified. Fifty-six percent of these were recorded in the town of Simi Valley. Inhalation of airborne spores of the dimorphic fungus *Coccidioides immitis* was identified as the cause of this respiratory disease [183]. Three times as many people as those who did not recall being physically present in dust clouds during the Northridge seismic sequence were more likely to be diagnosed with acute coccidioidomycosis. The risk increased with increasing duration of stay and exposure to dust clouds [184]. In Greece, no such indirect public health effects from ETLs have been recorded.

6. Discussion

The present research includes the identification and evaluation of information on earthquake-triggered landslides in Greece from antiquity to the present based exclusively on the already published scientific literature. The scientific sources that were utilized include articles in scientific journals, conference publications, scientific books, official deliverables of applied research projects, official reports from field and reconnaissance surveys as well as doctoral and master dissertations. This approach enabled the identification of 144 earthquakes that have triggered 673 landslides in total, resulting in a detailed analysis

based on the available scientific literature and revealing the extent of the patterns and behaviors of ground effects caused by past earthquakes in Greece.

Many of these studies have used sources of various types, such as reports of local non-experts, archive material, ancient and Byzantine writers, press of local and national circulation, published sources, historical textbooks, maps and geographic guides, etc. [185]. However, as has emerged from other recent research on the primary and secondary effects of earthquakes on the natural and built environment, the information provided by a particular type of source, which is newspapers of local and national circulation, has not been extensively and widely used. In particular, local newspapers provide important information on destructive events occurring in their area of interest. This has been strikingly demonstrated by recent related research, in which the contribution of such sources to the reconstruction of earthquakes and their primary and secondary EEEs and the extraction of conclusions on the spatial distribution of ETLs and related susceptible zones were valuable.

In more detail, through recent research on the primary and secondary effects of the most destructive earthquakes in the central and southern Ionian Islands, Mavroulis and Lekkas [13] were able to document the effects of the August 1953 earthquake sequence, which included the main earthquake on 12 August and two foreshocks on 9 and 11 of the same month. Using contemporary sources, they reviewed these leveling earthquakes and reconstructed their impact. They managed not only to record the primary and secondary EEEs, including ETLs, but also to distinguish the effects of each earthquake separately.

The same approach was applied to the most destructive historical earthquake of the Ionian Islands, the 4 February 1867 earthquake, with important results. In both cases, dozens of landslides were found, caused by earthquakes that had not been officially recorded before: 53 landslides for the 1953 earthquake sequence, 41 for the main shock, 4 for the first foreshock and 8 for the second foreshock, as determined by Mavroulis and Lekkas [13], and 11 landslides for the 1867 earthquake, determined by Mavroulis et al. [77]. The majority of these landslides were also verified in the field and through multicriteria analysis of landslide susceptibility it was concluded that they are distributed not randomly, but in specific zones characterized by high to critically high susceptibility [13,47].

As is also evident from relevant surveys in other countries around the world, newspapers represent the most important source of landslide information before 1990, in the absence of specific technical reports. The use of such sources will not only increase the recorded events in the earthquake-triggered landslide dataset but may also contribute to either verification or rejection of events that are already included but which are characterized by low location or information reliability.

The significance of historical data in assessing landslide hazard has been widely acknowledged [186]. In recent years, there has been a growing number of studies utilizing historical data to enhance the reliability of landslide hazard assessments and reduce the associated risks [186,187]. Such data contribute to a better understanding of landslide processes, including their timing, location, and magnitude, while also providing valuable social, economic, and ecological insights. However, it is essential to account for the limitations and potential errors inherent in data collection, source evaluation, and data interpretation [165]. While some European countries have a well-established tradition of collecting historical landslide data [166], their use remains limited in others. Taking into account the aforementioned, it is suggested that further information from such sources should be identified and evaluated in the context of future similar research.

The importance of these studies is that any comprehensive assessment of seismic risk and seismic hazard must include the related geohazards, including ETLs [17]. The mapping of ETLs, the recording of their qualitative and quantitative parameters, the identification of areas susceptible to such events and the identification of vulnerable structures and infrastructures contribute to the prevention and mitigation of impacts and the protection of human presence and activity through several structural and non-structural measures.

Information on earthquake-triggered landslides (ETLs) is also crucial for disaster management as it enhances the understanding of seismic risks and informs preparedness, response, and recovery strategies. Earthquakes often trigger landslides, compounding the damage caused by the seismic event itself. Comprehensive landslide studies are essential for assessing the spatial distribution of ETLs and understanding their relationship with several geospatial information [188].

The temporal, spatial and statistical analysis of ETLs provides valuable insights into the studies identifying landslide controlling factors and assessing landslide susceptibility. By employing geospatial statistics, researchers can compile susceptibility maps that illustrate areas at high potential for future landslides, thereby aiding in disaster preparedness and risk mitigation [189]. This predictive capability is vital for effective resource allocation and planning in disaster management.

Furthermore, understanding the temporal dynamics of landslides is critical for disaster response. Research indicates that landslide activity can remain elevated for years following an earthquake, with extensive environmental effects, including ETLs, complicating recovery efforts [190]. For instance, the 2015 Gorkha earthquake in Nepal saw a tenfold increase in landslide activity immediately following the event, which then gradually decreased over subsequent years [191]. This information is essential for emergency responders, as it allows them to prioritize areas for immediate intervention and to plan for long-term recovery efforts.

In addition to immediate response, the information gathered from such ETL studies can inform future land-use planning and infrastructure development. By recognizing the patterns of ETL occurrence and the geological conditions that predispose certain areas to landslides, planners can make more informed decisions that minimize risk [192]. For example, the integration of satellite imagery and remote sensing technologies has proven effective in rapidly mapping landslide occurrences, providing timely data that can be used to inform disaster response strategies [193].

In conclusion, the information on ETLs is invaluable for disaster management. It not only aids in immediate response and recovery efforts but also contributes to long-term risk assessment and mitigation strategies. By leveraging detailed analysis of ETLs, susceptibility mapping, and advanced remote sensing technologies, disaster management agencies can enhance their preparedness for future seismic events and reduce the overall impact of such disasters on communities.

The most important measures include the adoption and implementation of preventive and protective measures, more effective design and construction of buildings and infrastructure, increasing public awareness, informing and educating the general population and its vulnerable groups, and developing effective emergency response and impact management plans for disasters caused by earthquakes and ETLs [194]. All of these actions should be guided by a multi-hazard approach in which natural phenomena should not be treated as isolated hazards without interactions. This approach has been highlighted through research analyzing the interactions between natural hazards [195,196], but also recently during parallel occurrences of different types of hazards, e.g., natural and biological hazards [197].

7. Conclusions

This study provides a detailed analysis of ETLs in Greece, spanning from antiquity to the present, with an emphasis on their temporal, spatial, and statistical characteristics. Using an extensive dataset of 673 identified ETLs, supported by GIS tools, the research offers significant insights into the interplay between geological, morphological, and seismic properties in the occurrence and distribution of ETLs.

The documentation of ETLs shows a gradual increase towards the end of the 19th century, reflecting early efforts in cataloging disasters induced by natural hazards. However, historical data often lack precision due to limited technology and inconsistent record keeping. The transition to instrumental recordings in the 20th century marked a significant improvement in the accuracy and volume of data. This is particularly evident after the 1980s, with advancements in seismic monitoring and interdisciplinary research methodologies. Despite progress, gaps remain in the historical record, emphasizing the need to integrate archival sources with modern data collection techniques.

The analysis reveals that regions such as the Ionian Islands and the Peloponnese exhibit the highest ETL frequencies, a trend linked to their active seismicity and specific geological formations. Specific areas, such as Cephalonia and Lefkada Islands, exhibit unique vulnerabilities due to steep slopes, loose sediments, and their proximity to active faults.

Limestone-dominated lithologies and alpine units were identified as particularly susceptible to ETLs, highlighting the critical role of underlying geology in landslide dynamics. Most ETLs have occurred in geotectonic units belonging to the tectonostratigraphic terrane of the External Hellenides (Paxoi, Tripolis, Ionian, Mani and Gavrovo-Pylos units). Morphologically, ETLs were most commonly triggered in steep slopes in lowlands.

ETLs are strongly associated with earthquakes in the magnitude range of 5.5–7.0. However, larger historical earthquakes (e.g., the 1303 Crete, $M_w = 8.3$ earthquake) have limited recorded landslides, which is attributed to either limited historical sources or insufficient documentation at that time. Rockfalls are the most frequently observed type of ETLs in Greece, accounting for nearly half of all documented events. Slides, slumps, and combinations of multiple landslide types are also common, often triggered by larger seismic events. Coastal and submarine landslides, though less frequent, pose unique risks, including sea disturbances ranging from increased turbidity to tsunami, with moderate coastal impact and disruption to coastal infrastructure.

Regarding their frequency by land use, most ETLs have occurred in areas covered by Sclerophyllous vegetation, followed by land principally occupied by agriculture.

Regarding the seismic hazard zones of Greece, it was found that most ETLs have occurred in the second seismic hazard zone. ETLs occur mainly near faults and fault zones and within deformation zones. Most of these have been observed in areas of very high and high landslide susceptibility.

The impacts of ETLs on both natural and built environments are profound. Geomorphological changes, such as the formation of new landforms and disruptions to riverbeds and slopes, demonstrate the transformative power of ETLs on the landscape. Similarly, the destruction of infrastructure, including buildings, road networks, and telecommunications systems, exacerbates the socio-economic toll of such events. Historical accounts highlight the devastating effects of ETLs on rural and urban communities, with human casualties and injuries. Indirect health impacts, although rare in modern Greece, remain significant concerns, particularly in densely populated regions or inadequately prepared communities.

This research represents a crucial step toward comprehensive landslide hazard assessment and effective disaster management in one of the world's most seismically active regions. The data, results, and conclusions derived from this research have the potential to be valuable resources for a wide range of stakeholders. This includes researchers such as geologists, engineers, and architects, who may use the findings to advance scientific understanding or inform project designs. Additionally, operational staff, including civil protection authorities operating at local, regional, and central levels, could leverage these insights to enhance disaster preparedness, improve decision-making processes, and develop more effective risk mitigation strategies.

Supplementary Materials: The following supporting information can be downloaded at: <https://www.mdpi.com/article/10.3390/land14020307/s1>, Table S1: Mechanical properties and geotechnical behavior of geological formations affected by ETLs in Greece. The main properties are from the Engineering Geological Map of Greece compiled by Andronopoulos et al. (1993) [68].

Author Contributions: Conceptualization, S.M.; methodology, S.M.; software, S.M. and A.S.; validation, S.M. and A.S.; formal analysis, S.M. and A.S.; investigation, S.M., A.S. and E.L.; resources, E.L.; data curation, S.M. and A.S.; writing—original draft preparation, S.M. and A.S.; writing—review and editing, S.M. and A.S.; visualization, S.M.; supervision, S.M.; project administration, S.M.; funding acquisition, E.L. All authors have read and agreed to the published version of the manuscript.

Funding: This research received no external funding.

Data Availability Statement: The raw data supporting the conclusions of this article will be made available by the authors on request.

Acknowledgments: Four anonymous reviewers are acknowledged for their constructive comments that helped improve the clarity, the scientific soundness, and the overall merit of this work.

Conflicts of Interest: The authors declare no conflicts of interest.

References

1. EM-DAT Documentation. Geophysical Hazards. Available online: <https://doc.emdat.be/docs/data-structure-and-content/glossary/geophysical-hazards/> (accessed on 15 November 2024).
2. United Nations Office for Disaster Risk Reduction (UNDRR). Report of the Open-Ended Intergovernmental Expert Working Group on Indicators and Terminology Relating to Disaster Risk Reduction. Available online: https://www.preventionweb.net/files/50683_oiewgreportenglish.pdf (accessed on 6 January 2025).
3. Michetti, A.M.; Esposito, E.; Guerrieri, L.; Porfido, S.; Serva, L.; Tatevossian, R.; Vittori, E.; Audemard, F.; Azuma, T.; Clague, J.; et al. Environmental Seismic Intensity Scale 2007—ESI. *Mem. Descr. Carta Geol. Ital.* **2007**, *74*, 7–54.
4. Centre for Research on the Epidemiology of Disasters (CRED). EM-DAT—The International Disaster Database. Available online: <https://public.emdat.be/> (accessed on 25 November 2024).
5. Marano, K.D.; Wald, D.J.; Allen, T.I. Global earthquake casualties due to secondary effects: A quantitative analysis for improving rapid loss analyses. *Nat. Hazards* **2010**, *52*, 319–328. [[CrossRef](#)]
6. Petley, D. Global patterns of loss of life from landslides. *Geology* **2012**, *40*, 927–930. [[CrossRef](#)]
7. Petley, D.N. Landslides and Engineered Slopes: Protecting Society through Improved Understanding. In *Landslides and Engineered Slopes*; Eberhardt, E., Froese, C., Turner, K., Leroueil, S., Eds.; CRC Press: Mississauga, ON, Canada, 2012.
8. Bird, J.F.; Bommer, J.J. Earthquake losses due to ground failure. *Eng. Geol.* **2014**, *75*, 147–179. [[CrossRef](#)]
9. Kennedy, I.T.R.; Petley, D.N.; Williams, R.; Murray, V. A Systematic Review of the Health Impacts of Mass Earth Movements (Landslides). *PLoS Curr.* **2015**, *30*, 7. [[CrossRef](#)]
10. Keefer, D.K. Landslides caused by earthquakes. *Geol. Soc. Am.* **1984**, *95*, 406–421. [[CrossRef](#)]
11. Marui, H.; Nadim, F. Landslides and Multi-Hazards. In *Landslides—Disaster Risk Reduction*; Sassa, K., Canuti, P., Eds.; Springer: Berlin/Heidelberg, Germany, 2009; pp. 435–450.
12. Shieh, C.-L.; Wang, C.-M.; Lai, W.-C.; Tsang, Y.-C.; Lee, S.P. The composite hazard resulted from Typhoon Morakot in Taiwan. *J. JSECE* **2009**, *62*, 61–65.

13. Mavroulis, S.; Lekkas, E. Revisiting the Most Destructive Earthquake Sequence in the Recent History of Greece: Environmental Effects Induced by the 9, 11 and 12 August 1953 Ionian Sea Earthquakes. *Appl. Sci.* **2021**, *11*, 8429. [[CrossRef](#)]
14. Hansen, A.; Franks, C.A.M. Characterization and mapping of earthquake triggered landslides for seismic zonation. State-of-the art Paper. In Proceedings of the Fourth International Conference on Seismic Zonation, Stanford, CA, USA, 26–29 August 1991; Volume 1, pp. 149–195.
15. Keefer, D.K. Investigating Landslides Caused by Earthquakes—A Historical Review. *Surv. Geophys.* **2002**, *23*, 473–510. [[CrossRef](#)]
16. Keefer, D.K. Landslides generated by earthquakes: Immediate and long-term effects. In *Treatise on Geomorphology*; Shroder, J., Owen, L.A., Eds.; Academic Press: San Diego, CA, USA, 2013; Volume 5, pp. 250–266.
17. Rodriguez, C.; Bommer, J.; Chandler, R. Earthquake-induced landslides: 1980–1997. *Soil Dyn. Earthq. Eng.* **1999**, *18*, 325–346. [[CrossRef](#)]
18. Hancox, G.T.; Perrin, N.D.; Dellow, G. Recent studies of historical earthquake-induced landsliding, ground damage, and MM intensity in New Zealand. *Bull. N. Z. Soc. Earthq. Eng.* **2002**, *35*, 59–95. [[CrossRef](#)]
19. Hancox, G.T.; Perrin, N.D.; Dellow, G.D. *Earthquake-Induced Landsliding in New Zealand and Implications for MM Intensity and Seismic Hazard Assessment*; Institute of Geological & Nuclear Sciences Client Report 43601 B; Lower Hutt: Wellington, New Zealand, 1997.
20. Rosser, B.; Dellow, S.; Haubrock, S.; Glassey, P. New Zealand’s National Landslide Database. *Landslides* **2017**, *14*, 1949–1959. [[CrossRef](#)]
21. Papadopoulos, G.A.; Plessa, A. Magnitude–distance relations for earthquake-induced landslides in Greece. *Eng. Geol.* **2000**, *58*, 377–386. [[CrossRef](#)]
22. Bommer, J.J.; Rodríguez, C.E. Earthquake-induced landslides in Central America. *Eng. Geol.* **2002**, *63*, 189–220. [[CrossRef](#)]
23. Rodriguez, C.E. Earthquake-induced Landslides in Colombia. In *Geohazards*; Nadim, F., Pöttler, R., Einstein, H., Klapperich, H., Kramer, S., Eds.; ECI Symposium Series; Engineering Conferences International (ECI): New York, NY, USA, 2006. Available online: <https://dc.engconfintl.org/geohazards/38> (accessed on 20 November 2024).
24. Devoli, G.; Morales, A.; Høeg, K. Historical landslides in Nicaragua—Collection and analysis of data. *Landslides* **2007**, *4*, 5–18. [[CrossRef](#)]
25. Chen, X.L.; Zhou, Q.; Ran, H.; Dong, R. Earthquake-triggered landslides in southwest China. *Nat. Hazards Earth Syst. Sci.* **2012**, *12*, 351–363. [[CrossRef](#)]
26. Prestininzi, A.; Romeo, R. Earthquake-induced ground failures in Italy. *Eng. Geol.* **2000**, *58*, 387–397. [[CrossRef](#)]
27. Martino, S.; Prestininzi, A.; Romeo, R.W. Earthquake-induced ground failures in Italy from a reviewed database. *Nat. Hazards Earth Syst. Sci.* **2014**, *14*, 799–814. [[CrossRef](#)]
28. Koukis, G.; Ziourkas, C. Slope instability phenomena in Greece: A statistical analysis. *Bull. Int. Assoc. Eng. Geol.* **1991**, *43*, 47–60. [[CrossRef](#)]
29. Koukis, G.; Tsiambaos, G.; Sabatakakis, N. Slope movements in Greek territory: A statistical approach. In Proceedings of the 7th International Congress of IAEG, Lisboa, Portugal, 5–9 September 1994; Oliveira, R., Rodrigues, L.F., Coelho, A.G., Cunha, A.P., Eds.; A. A. Balkema: Rotterdam, The Netherlands, 1994; pp. 4621–4628.
30. Koukis, G.; Tsiambaos, G.; Sabatakakis, N. Landslides movements in Greece: Engineering geological characteristics and environmental consequences. In Proceedings of the International Symposium of Engineering Geology and Environment, Athens, Greece, 23–27 June 1997; A. A. Balkema: Rotterdam, The Netherlands, 1997; Volume 1, pp. 789–792.
31. Koukis, G.; Sabatakakis, N.; Nikolau, N.; Loupasakis, C. Landslide Hazard Zonation in Greece. In *Landslides*; Sassa, K., Fukuoka, H., Wang, F., Wang, G., Eds.; Springer: Berlin/Heidelberg, Germany, 2005.
32. Eleftheriou, A. *Map of Landsliding Urban Areas of the Greek Territory*; Institute of Geology and Mineral Exploration: Athens, Greece, 1993.
33. Sabatakakis, N.; Koukis, G.; Vassiliades, E.; Lainas, S. Landslide susceptibility zonation in Greece. *Nat. Hazards* **2013**, *65*, 523–543. [[CrossRef](#)]
34. Papathanassiou, G.; Valkaniotis, S.; Ganas, A.; Pavlides, S. GIS-based statistical analysis of the spatial distribution of earthquake-induced landslides in the island of Lefkada, Ionian Islands, Greece. *Landslides* **2013**, *10*, 771–783. [[CrossRef](#)]
35. Polykretis, C.; Kalogeropoulos, K.; Andreopoulos, P.; Faka, A.; Tsatsaris, A.; Chalkias, C. Comparison of Statistical Analysis Models for Susceptibility Assessment of Earthquake-Triggered Landslides: A Case Study from 2015 Earthquake in Lefkada Island. *Geosciences* **2019**, *9*, 350. [[CrossRef](#)]
36. Mavroulis, S.; Diakakis, M.; Kranis, H.; Vassilakis, E.; Kapetanidis, V.; Spingos, I.; Kaviris, G.; Skourtsos, E.; Voulgaris, N.; Lekkas, E. Inventory of Historical and Recent Earthquake-Triggered Landslides and Assessment of Related Susceptibility by GIS-Based Analytic Hierarchy Process: The Case of Cephalonia (Ionian Islands, Western Greece). *Appl. Sci.* **2022**, *12*, 2895. [[CrossRef](#)]
37. Sakkas, G.; Misailidis, I.; Sakelliariou, N.; Kouskouna, V.; Kaviris, G. Modeling landslide susceptibility in Greece: A weighted linear combination approach using analytic hierarchical process, validated with spatial and statistical analysis. *Nat. Hazards* **2016**, *84*, 1873–1904. [[CrossRef](#)]

38. Mavroulis, S. Environmental Effects and Evaluation of Environmental Intensities of Historic and Recent Earthquakes in Western Greece (Western Peloponnese and Central Ionian Islands) and Correlation with Active Tectonics and Seismological Parameters. Ph.D. Thesis, National and Kapodistrian University of Athens, Athens, Greece, 2020; 876p.
39. Sarantopoulou, A. Distribution and Properties of Landslides Induced by Historical and Recent Earthquakes in the Hellenic Island Arc. Master's Thesis, National and Kapodistrian University of Athens, Athens, Greece, 2023; 269p.
40. Papazachos, B.; Papazachou, K. *The Earthquakes of Greece*; Ziti Publications: Thessaloniki, Greece, 2003; 286p.
41. Ambraseys, N. *Earthquakes in the Mediterranean and Middle East, a Multidisciplinary Study of Seismicity up to 1900*; Cambridge University Press: Cambridge, UK, 2009; 970p.
42. Spyropoulos, P. *Chronicle of the Earthquakes of Greece, from Antiquity to Present*; Dodoni Publications: Athens, Greece, 1997; 456p.
43. Ambraseys, N.N.; Jackson, J. Seismicity and associated strain of central Greece between 1890 and 1988. *Geoph. J. Int.* **1990**, *101*, 663–708. [[CrossRef](#)]
44. Ambraseys, N.N.; Jackson, J.A. Seismicity and Strain in the Gulf of Corinth (Greece) since 1694. *J. Earth. Eng.* **1997**, *1*, 433–474. [[CrossRef](#)]
45. Soloviev, S.L.; Solovieva, O.N.; Go, C.N.; Kim, K.S.; Shchetnikov, N.A. *Tsunamis in the Mediterranean Sea 2000 B.C.–2000 A.D.*; Springer Science & Business Media: Dordrecht, The Netherlands, 2000; 256p.
46. Makropoulos, K.; Kaviris, G.; Kouskouna, V. An updated and extended earthquake catalogue for Greece and adjacent areas since 1900. *Nat. Hazards Earth Syst. Sci.* **2012**, *12*, 1425–1430. [[CrossRef](#)]
47. Stucchi, M.; Rovida, A.; Gomez Capera, A.A.; Alexandre, P.; Camelbeeck, T.; Demircioglu, M.B.; Gasperini, P.; Kouskouna, V.; Musson, R.M.W.; Radulian, M.; et al. The SHARE European earthquake catalogue (SHEEC) 1000–1899. *J. Seismol.* **2013**, *17*, 523–544. [[CrossRef](#)]
48. Istituto Nazionale di Geofisica e Vulcanologia (INGV). *EPICA—European PreInstrumental Earthquake Catalogue, Version 1.1*; Istituto Nazionale di Geofisica e Vulcanologia (INGV): Rome, Italy, 2021. Available online: https://www.emidius.eu/epica/data/EPICA_v1.1.xlsx (accessed on 6 January 2024).
49. Rovida, A.; Antonucci, A.; Locati, M. The European Preinstrumental Earthquake Catalogue EPICA, the 1000–1899 catalogue for the European Seismic Hazard Model 2020. *Earth Syst. Sci. Data* **2022**, *14*, 5213–5231. [[CrossRef](#)]
50. Mariolakos, I.; Sabot, V.; Alexopoulos, A.; Danamos, G.; Lekkas, E.; Logos, E.; Lozios, S.; Mertzanis, A.; Fountoulis, I. *Microzonical study of Kalamata, (Geomorphology, Geology, Neotectonics)*; Report; Earth Planning Protection Organization: Athens, Greece, 1986; 110p.
51. Fountoulis, I.G.; Mavroulis, S.D. Application of the Environmental Seismic Intensity scale (ESI 2007) and the European Macroseismic Scale (EMS-98) to the Kalamata (SW Peloponnese, Greece) earthquake ($M_s = 6.2$, September 13, 1986) and correlation with neotectonic structures and active faults. *Ann. Geophys.* **2013**, *56*, S0675. [[CrossRef](#)]
52. Lekkas, E.; Logos, E.; Danamos, G.; Fountoulis, I.; Adamopoulou, E. Macroseismic observations after the earthquake of October 16th, 1988 in Kyllini peninsula (NW Peloponnese, Greece). In Proceedings of the Geological Congress of the Geological Society of Greece, Thessaloniki, Greece, 25–27 May 1990.
53. Papanikolaou, D.; Lekkas, E.; Syskakis, D.; Adamopoulou, E. Correlation on neotectonic structures with the geodynamic activity in Milos during the earthquakes of March 1992. *Bull. Geol. Soc. Greece* **1993**, *28*, 413–428.
54. Lekkas, E.; Fountoulis, I.; Papanikolaou, D. Intensity Distribution and Neotectonic Macrostructure Pyrgos Earthquake Data (26 March 1993, Greece). *Nat. Hazards* **2000**, *21*, 19–33. [[CrossRef](#)]
55. Lekkas, E.; Fountoulis, I.; Lozios, S.; Kranis, C.H.; Adamopoulou, E. Neotectonic implications of the Grevena-Kozani earthquake (May 13, 1995, W. Macedonia, Greece). In Proceedings of the Intern. Meeting on results of the May 13, 1995 earthquake of W. Macedonia: One Year after, Kozani, Greece, 24–27 May 1996.
56. Lekkas, E.; Lozios, S.; Kranis, H.; Skourtsos, M. Concomitant geodynamic catastrophic phenomena of the Aigio earthquake (15 June 1995). Determination of their occurrence by applying the fuzzy method and using G.I.S. In Proceedings of the International Scientific Symposium “Earthquake 6.1R Egio—Fokida, 1995”, Aegion, Greece, 22–23 November 1996.
57. Lekkas, E. The Athens earthquake (7 September 1999): Intensity distribution and controlling factors. *Eng. Geol.* **2001**, *59*, 297–311. [[CrossRef](#)]
58. Lekkas, E.; Papanikolaou, I.; Papanikolaou, D.; Danamos, G. Correlating the damage pattern and the geological structure. Local site effects from the 2006 $M_w=6.7$ Kythira island intermediate depth event, SW Greece. In Proceedings of the 14th World Conference on Earthquake Engineering, International Association for Earthquake Engineering (IAEE), Beijing, China, 12–17 October 2008; Chinese Association of Earthquake Engineering (CAEE): Beijing, China, 2008.
59. Lekkas, E.; Danamos, G. Preliminary Observations of the January 8, 2006 Kythira Island (South Western Greece) Earthquake ($M_w 6.9$). Newsletter EERI (Earthquake Engineering Research Institute). 2006. Available online: http://www.eeri.org/lfe/greece_kythira_island.html (accessed on 20 November 2024).

60. Mavroulis, S.; Fountoulis, I.; Lekkas, E. Environmental effects caused by the Andravida (08-06-2008, ML = 6.5, NW Peloponnese, Greece) earthquake. In Proceedings of the Geologically Active: 11th IAEG Congress, Auckland, New Zealand, 5–10 September 2010.
61. Mavroulis, S.D.; Fountoulis, I.G.; Skourtsos, E.N.; Lekkas, E.L.; Papanikolaou, I.D. Seismic intensity assignments for the 2008 Andravida (NW Peloponnese, Greece) strike-slip event (June 8, Mw = 6.4) based on the application of the Environmental Seismic Intensity scale (ESI 2007) and the European Macroseismic scale (EMS-98). Geological structure, active tectonics, earthquake environmental effects and damage pattern. *Ann. Geophys.* **2013**, *56*, S0681. [CrossRef]
62. Lekkas, E.; Mavroulis, S.; Skourtsos, E.; Andreadakis, E.; Antoniou, V.; Kranis, C.; Soukis, K.; Lozios, S.; Alexoudi, V. Earthquake environmental effects induced by the 2017 June 12, Mw 6.3 Lesvos (North Aegean Sea, Greece) earthquake. In Proceedings of the 8th International INQUA Meeting on Paleoseismology, Active Tectonics and Archeoseismology (PATA), New Zealand, 13–16 November 2017.
63. Lekkas, E.; Carydis, P.; Mavroulis, S.; Gogou, M.; Andreadakis, E.; Katsetsiadou, K.-N.; Skourtsos, E.; Minos-Minopoulos, D.; Bardouli, P.; Voulgaris, N.; et al. The Mw 6.6, July 21, 2017 Kos Earthquake, Scientific Report (Version 2.0). *Newsl. Environ. Disaster Cris. Manag. Strateg.* **2017**, *1*, 1–56.
64. Mavroulis, S.; Triantafyllou, I.; Karavias, A.; Gogou, M.; Katsetsiadou, K.-N.; Lekkas, E.; Papadopoulos, G.A.; Parcharidis, I. Primary and Secondary Environmental Effects Triggered by the 30 October 2020, Mw = 7.0, Samos (Eastern Aegean Sea, Greece) Earthquake Based on Post-Event Field Surveys and InSAR Analysis. *Appl. Sci.* **2021**, *11*, 3281. [CrossRef]
65. Lekkas, E.; Agorastos, K.; Mavroulis, S.; Kranis, C.; Skourtsos, E.; Carydis, P.; Gogou, M.; Katsetsiadou, K.-N.; Papadopoulos, G.; Triantafyllou, I.; et al. The early March 2021 Thessaly earthquake sequence. *Newsl. Environ. Disaster Cris. Manag. Strateg.* **2021**, *22*, 1–195.
66. Mavroulis, S.; Kranis, H.; Lozios, S.; Argyropoulos, I.; Vassilakis, E.; Soukis, K.; Skourtsos, E.; Lekkas, E.; Carydis, P. The impact of the September 27, 2021, Mw = 6.0 Arkalochori (Central Crete, Greece) earthquake on the natural environment and the building stock. In Proceedings of the EGU General Assembly 2022, Vienna, Austria, 23–27 May 2022. [CrossRef]
67. Bornovas, I.; Rondogianni-Tsiambaou, T. *The Geological Map of Greece, Scale 1:500,000*, 2nd ed.; Institute of Geology and Mineral Exploration: Athens, Greece, 1983.
68. Andronopoulos, V.; Rozos, D.; Kynigalaki, M.; Koukis, G.; Tzitziras, A.; Pogiatzi, E.; Apostolidis, E. *Engineering Geological Map of Greece, Scale 1:500,000*; Geological Map Publication Office, Directorate of Geology and Geological Mapping, Institute of Geology and Mineral Exploration: Athens, Greece, 1993.
69. Mouyiaris, N.; Andronopoulos, V.; Eleftheriou, A.; Kynigalaki, M.; Koukis, G.; Rontogianni, T.; Mettos, A.; Katsikatsos, G.; Perisoratis, K.; Drakopoulos, I.; et al. *Seismotectonic Map of Greece with Seismogeological Data, Scale 1:500,000*; Geological Map Publication Office, Directorate of General Services, Institute of Geology and Mineral Research: Athens, Greece, 1989.
70. Papanikolaou, D. *Geology of Greece (with Attached Geotectonic Map of Greece and the Mediterranean)*; Patakis Publications: Athens, Greece, 2015; 448p.
71. EAK. *Modification of the Provisions of the Greek Seismic Code EAK 2000*; Earthquake Planning and Protection Organization: Neo Psychiko, Greece, 2003.
72. Copernicus Land Monitoring Service. CORINE Land Cover 2018. Available online: <https://sdi.eea.europa.eu/catalogue/copernicus/api/records/71c95a07-e296-44fc-b22b-415f42acfd0?language=all> (accessed on 15 November 2024).
73. European Commission, Joint Research Centre, European Soil Data Centre (ESDAC). European Landslide Susceptibility Map Version 2 (ELSUS v2). Available online: <https://esdac.jrc.ec.europa.eu/content/european-landslide-susceptibility-map-elsus-v2> (accessed on 25 November 2024).
74. Wilde, M.; Günther, A.; Reichenbach, P.; Malet, J.-P.; Hervás, J. Pan-European landslide susceptibility mapping: ELSUS Version 2. *J. Maps* **2018**, *14*, 97–104. [CrossRef]
75. ESRI. ArcGIS 10.8.2. Available online: <https://desktop.arcgis.com/en/arcmap/latest/get-started/setup/arcgis-desktop-quick-start-guide.htm> (accessed on 17 December 2024).
76. Comerci, V.; Vittori, E.; Blumetti, A.M.; Brustia, E.; Di Manna, P.; Guerrieri, L.; Lucarini, M.; Serva, L. Environmental effects of the December 28, 1908, Southern Calabria–Messina (Southern Italy) earthquake. *Nat. Hazards* **2015**, *76*, 1849–1891. [CrossRef]
77. Mavroulis, S.; Mavrouli, M.; Lekkas, E.; Carydis, P. Reconstructing Impact of the 1867 Ionian Sea (Western Greece) Earthquake by Focusing on New Contemporary and Modern Sources for Building Damage, Environmental and Health Effects. *Geosciences* **2024**, *14*, 214. [CrossRef]
78. Caputo, R.; Chatzipetros, A.; Pavlides, S.; Sboras, S. The Greek Database of Seismogenic Sources (GreDaSS): State-of-the-art for northern Greece. *Ann. Geophys.* **2012**, *55*, 859–894.
79. Styron, R.; Pagani, M. The GEM Global Active Faults Database. *Earthq. Spectra* **2020**, *36*, 160–180. [CrossRef]

80. Papanikolaou, D.I. The Geology of Greece. In *Regional Geology Reviews*; Springer International Publishing: Cham, Switzerland, 2021; 345p.
81. Monod, O. La «courbure d’Isparta»: Une mosaïque de blocs autochtones surmontés de nappes composites à la jonction de l’arc hellénique et de l’arc taurique. *Bull. Soc. Geol. France* **1976**, *18*, 521–531. [[CrossRef](#)]
82. Le Pichon, X.; Angelier, J. The Hellenic Arc and Trench system: A key to the neotectonic evolution of the Eastern Mediterranean area. *Tectonophysics* **1979**, *60*, 1–42. [[CrossRef](#)]
83. Mariolakos, I.; Zagorchev, I.; Fountoulis, I.; Ivanov, M. Neotectonic Transect Moesia Apulia Field Trip Guide Book. In Proceedings of the 32nd International Geological Congress—Pre-Congress Field Trip, Firenze, Italy, 20–28 August 2004.
84. Le Pichon, X.; Angelier, J. The Aegean Sea. *Phil. Trans. R. Soc. Lond.* **1981**, *A300*, 357–372.
85. Huguen, C.; Mascle, J.; Chaumillon, E.; Woodside, J.M.; Benkhelil, J.; Kopf, A.; Volkonskaia, A. Deformational styles of the Eastern Mediterranean Ridge and surroundings from combined swath mapping and seismic reflection profiling. *Tectonophysics* **2001**, *343*, 21–47. [[CrossRef](#)]
86. Finetti, I. Structure, stratigraphy and evolution of Central Mediterranean. *Bol. Geol. Teor. Appl. Trieste* **1982**, *34*, 296–298.
87. Finetti, I.; Papanikolaou, D.; Del Ben, A.; Karvelis, P. Preliminary geotectonic interpretation of the East Mediterranean chain and the Hellenic Arc. *Bull. Geol. Soc. Greece* **1990**, *25*, 509–526.
88. Le Pichon, X.; Huchon, P.; Angelier, J.; Lyberis, N.; Boulin, J.; Bureau, D.; Cadet, J.P.; Dercourt, J.; Glacon, G.; Got, H.; et al. Active tectonics in the Hellenic trench. In Proceedings of the 26th International Geological Congress, Geology of Continental Margins Symposium, Paris, France, 7–17 July 1980.
89. Freyberg, B.V. Geologie des Isthmus von Korinth. *Erlanger Geol. Abh.* **1973**, *95*, 183.
90. Hollenstein, C.; Müller, M.D.; Geiger, A.; Kahle, H.-G. Crustal motion and deformation in Greece from a decade of GPS measurements, 1993–2003. *Tectonophysics* **2008**, *449*, 17–40. [[CrossRef](#)]
91. Mavroulis, S.; Stanota, E.-S.; Lekkas, E. Evaluation of environmental seismic intensities of all known historical and recent earthquakes felt in Zakynthos Island, Greece using the Environmental Seismic Intensity (ESI 2007) scale. *Quat. Int.* **2019**, *532*, 1–22. [[CrossRef](#)]
92. Sakkas, V.; Kapetanidis, V.; Kaviris, G.; Spingos, I.; Mavroulis, S.; Diakakis, M.; Alexopoulos, J.D.; Kazantzidou-Firtinidou, D.; Kassaras, I.; Dilalos, S.; et al. Seismological and Ground Deformation Study of the Ionian Islands (W. Greece) during 2014–2018, a Period of Intense Seismic Activity. *Appl. Sci.* **2022**, *12*, 2331. [[CrossRef](#)]
93. Kaviris, G.; Zymvragakis, A.; Bonatis, P.; Kapetanidis, V.; Spingos, I.; Mavroulis, S.; Kotsi, E.; Lekkas, E.; Voulgaris, N. A Logic-Tree Approach for Probabilistic Seismic Hazard Assessment in the Administrative Region of Attica (Greece). *Appl. Sci.* **2023**, *13*, 7553. [[CrossRef](#)]
94. Kaviris, G.; Zymvragakis, A.; Kapetanidis, V.; Kouskouna, V.; Spingos, I.; Sakellariou, N.; Voulgaris, N. A logic-tree based probabilistic seismic hazard assessment for the central ionian islands of cephalonia and ithaca (Western Greece). *J. Seismol.* **2024**, *28*, 1087–1103. [[CrossRef](#)]
95. Petseti, A.; Nektarios, M. Earthquake insurance for Greece: Comparative analysis and pricing issues. *J. Risk Financ.* **2013**, *14*, 251–265. [[CrossRef](#)]
96. Psycharis, I. *The Salonica (Thessaloniki) Earthquake of June 20, 1978*; California Institute of Technology, Earthquake Engineering Research Laboratory: Pasadena, CA, USA, 1978; 32p.
97. Soufleris, C.; Jackson, J.A.; King, G.C.P.; Spencer, C.P.; Scholz, C.H. The 1978 earthquake sequence near Thessaloniki (northern Greece). *Geophys. J. R. Astron. Soc.* **1982**, *68*, 429–458. [[CrossRef](#)]
98. Tranos, M.D.; Papadimitriou, E.E.; Kiliass, A.A. Thessaloniki–Gerakarou Fault Zone (TGFZ): The western extension of the 1978 1181 Thessaloniki earthquake fault (Northern Greece) and seismic hazard assessment. *J. Struct. Geol.* **2003**, *25*, 2109–2123. [[CrossRef](#)]
99. Mariolakos, I.; Papanikolaou, D.; Symeonidis, N.; Lekkas, S.; Karotsieris, Z.; Sideris, C.H. The deformation of the area around the Eastern Corinthian Gulf, affected by the earthquakes of February–March 1981. In Proceedings of the HEAT Symposium, Athens, Greece, 8–10 April 1981; Volume 1, pp. 400–420.
100. Christoulas, S.G.; Tsiambaos, G.K.; Sabatakakis, N.S. Engineering Geological Conditions and the Effects of the 1981 Earthquake in Athens, Greece. *Eng. Geol.* **1985**, *22*, 141–155. [[CrossRef](#)]
101. Hubert, A.; King, G.; Armijo, R.; Meyer, B.; Papanastasiou, D. Fault reactivation, stress interaction and rupture propagation of 1190 the 1981 Corinth earthquake sequence. *Earth Planet. Sci. Lett.* **1996**, *142*, 573–585. [[CrossRef](#)]
102. Lekkas, E.L.; Lozios, S.G.; Skourtsos, E.N.; Kranis, H.D. Egio earthquake (15 June 1995): An episode in the neotectonic evolution of Corinthiakos Gulf. *J. Geodyn.* **1998**, *26*, 487–499. [[CrossRef](#)]
103. SL NKUA. Seismological Laboratory of the National and Kapodistrian University of Athens. Earthquake Catalogue Search. Available online: http://www.geophysics.geol.uoa.gr/stations/gmapv3_db/index.php (accessed on 10 January 2024).

104. Guidoboni, E.; Comastri, A.; Traina, G. *Catalogue of Ancient Earthquakes in the Mediterranean Area up to the 10th Century*; INGV-SGA: Bologna, Italy, 1994.
105. Guidoboni, E.; Comastri, A. The large earthquake of 8 August 1303 in Crete: Seismic scenario and tsunami in the Mediterranean area. *J. Seismol.* **1997**, *1*, 55–72. [[CrossRef](#)]
106. Guidoboni, E.; Comastri, A. *Catalogue of Earthquakes and Tsunamis in the Mediterranean Area from the 11th to the 15th Century*; INGV-SGA: Bologna, Italy, 2005; 1037p.
107. Papadopoulos, G.A. *The Earthquake Log of Creta by Pavlos Vlastos. 464 BC–1926 A.D.*; Oselotos Publications: Athens, Greece, 2013; 204p. (In Greek)
108. Lekkas, E.; Kolyva, M.; Antonopoulos, G.; Kopanas, I. The earthquakes of Zakynthos. An interpretation of the descriptions of earthquakes and correlation with the existing geological structure. *Ann. Geol. Pays Hell.* **1997**, *1*, 1033–1073.
109. Konomos, N. *Chronicles of Zakynthos (1485–1953)*; Konstantinidis and Michala Publications: Athens, Greece, 1970; 191p.
110. Rondoyanni, T.; Sakellariou, M.; Baskoutas, J.; Christodoulou, N. Evaluation of active faulting and earthquake secondary effects in Lefkada Island, Ionian Sea, Greece: An overview. *Nat. Hazards* **2012**, *61*, 843–860. [[CrossRef](#)]
111. Tsitselis, H.A. *Kefalliniaka Symmikta*; Argostoli: Cephalonia, Greece, 1904.
112. Barbiani, D.; Barbiani, B. Tremblements de terre dans l'île de Zante. *Mémoires L'acad. Dijon Sci.* **1863**, *11*, 1–112.
113. Taxeidis, K. Study of Historical Seismicity of the Eastern Aegean Islands. Ph.D. Thesis, National and Kapodistrian University of Athens, Athens, Greece, 2003. Available online: <http://macroseismology.geol.uoa.gr/studies/TAXE003.pdf> (accessed on 20 August 2024).
114. Albini, P.; Ambraseys, N.N.; Monachesi, G. Materials for the investigation of the seismicity of the Ionian Islands between 1704 and 1766. In *Materials of the CEC Project "Review of Historical Seismicity in Europe"*; Albini, P., Moroni, A., Eds.; CNR: Milano, Italy, 1994; Volume 2, pp. 11–26.
115. Papathanassiou, G.; Valkaniotis, S.; Ganas, A. Evaluation of the macroseismic intensities triggered by the January/February 2014 Cephalonia, (Greece) earthquakes based on ESI-07 scale and their comparison to 1867 historical event. *Quat. Int.* **2017**, *451*, 234–247. [[CrossRef](#)]
116. Papadopoulos, G. *Rhodes—The Earthquake and Tsunamis from Antiquity to Present*; Oselotos Publications: Athens, Greece, 2014; 224p. (In Greek)
117. Papadopoulos, G. *Kythera—The Earthquake and Tsunamis from Antiquity to Present*; Oselotos Publications: Athens, Greece, 2013; 106p. (In Greek)
118. Mavroulis, S.; Lekkas, E. Evaluation of seismic intensities of historical earthquakes in the southern and southwestern Peloponnese (Greece) based on the Environmental Seismic Intensity (ESI 2007) scale. In *Proceedings of the 9th International INQUA Meeting on Paleoseismology, Active Tectonics and Archeoseismology (PATA)*, Possidi, Greece, 25–27 June 2018.
119. Papadopoulos, G. *Lesvos—Chios—Psara. The Earthquake and Tsunamis from Antiquity to Present*; Oselotos Publications: Athens, Greece, 2015; 244p. (In Greek)
120. Schmidt, J. *Studien über Erdbeben*; Alwin Georgi: Leipzig, Germany, 1879; 393p.
121. Schmidt, J. *Study About the Kefalonia Earthquake of 23 January 1867*; Ethniko Typografeio: Athens, Greece, 1867; 30p.
122. Partsch, J. *Cephalonia and Ithaki: Geographic Monograph*; UNESCO: Athens, Greece, 1892; pp. 69–77.
123. Tsitselis, E. *Cephalonian Miscellaneous—A Contribution to the History and Laography of the Island of Cephalonia*; Minas Mirtidis Publications: Athens, Greece, 1960.
124. Choutzaivos, G.M. *Contribution to the Study of the Seismicity of the Island of Lesvos and the Surrounding Area (Chios-Lemnos-Agios Efstratios-Psara-Antipsara-Oinuses)*; Publications of the Prefectural Government of Lesvos: Mytilini, Greece, 1998. (In Greek)
125. Fouqué, F. *Rapport sur les Tremblements de Terre de Céphalonie et de Mételin en 1867*; Imprimerie Impériale: Paris, France, 1868; 40p.
126. Kolaxizellis, S. *Legend and History of Agiasos of the Island of Lesvos*; Phoenix Printing House: Mytilini, 1948; Photomechanical Reprint; Philoproodos Association of Agiasotes: Athens, Greece, 1948; Volume 3. (In Greek)
127. Ambraseys, N.N.; Pantelopoulos, P. The Fokis (Greece) earthquake of 1 August 1870.1. *Euro. Earthq. Eng.* **1989**, *3*, 10–18.
128. Papadopoulos, G.A. *A Seismic History of Crete—The Hellenic Arc and Trench—Earthquakes and Tsunamis: 2000 BC–2011 AD*; Oselotos Publications: Athens, Greece, 2011; 416p. (In Greek)
129. Christomanos, A.K. *The Island of Samothraki and the Earthquake of January 28 (February 9) 1893*; Printing Office of Hestia, K. Meissner and N. Cargadouri: Athens, Greece, 1899; 51p. (In Greek)
130. Albini, P.; Pantosti, D. The 20 and 27 April 1894 (Locris, Central Greece) Earthquake Sources through Coeval Records on Macroseismic Effects. *Bull. Seismol. Soc. Am.* **2004**, *94*, 1305–1326. [[CrossRef](#)]
131. Triantafyllou, I.; Koukouvelas, I.; Papadopoulos, G.A.; Lekkas, E. A Reappraisal of the Destructive Earthquake (Mw5.9) of 15 July 1909 in Western Greece. *Geosciences* **2022**, *12*, 374. [[CrossRef](#)]
132. Ambraseys, N.N.; Adams, R.D. *The Seismicity of Saudi Arabia and Adjacent Areas, Part B*; Engineering Seismology and Earthquake Engineering (ESEE) Publication no 88/11; Imperial College: London, UK, 1988.

133. Drakopoulos, J.; Leventakis, G.; Roussopoulos, A. Microzonation in the seismic area of Corinth-Loutraki. *Ann. Geophys.* **1978**, *31*, 51–95. [[CrossRef](#)]
134. Triantafyllou, I.; Papadopoulos, G.A.; Lekkas, E. Impact on built and natural environment of the strong earthquakes of 23 April 1933, and 20 July 2017, in the southeast Aegean Sea, eastern Mediterranean. *Nat. Hazards* **2020**, *100*, 671–695. [[CrossRef](#)]
135. Galanopoulos, A.G. The Koroni (Messinia) earthquake of October 6, 1947. *Bull. Seismol. Soc. Am.* **1949**, *39*, 33–39. [[CrossRef](#)]
136. Papathanassiou, G.; Pavlides, S. Using the INQUA scale for the assessment of intensity: Case study of the 2003 Lefkada (Ionian Islands), Greece earthquake. *Quat. Int.* **2007**, *173–174*, 4–14. [[CrossRef](#)]
137. Papastamatiou, D.; Mouyaris, N. The earthquake of April 30, 1954, in Sophades (Central Greece). *Geoph. J. Int.* **1986**, *87*, 885–895. [[CrossRef](#)]
138. Pavlides, S.B.; Tranos, M.D. Structural characteristics of two strong earthquakes in the North Aegean: Ierissos (1932) and Agios Efstratios (1968). *J. Str. Geol.* **1991**, *13*, 205–214. [[CrossRef](#)]
139. Vetoulis, D. *Geological and Seismological Report of Lefkada Island and the Seismic Tremors of June 30, 1970*; Institute of Geology and Subsoil Research (IGEY): Athens, Greece, 1970.
140. Andronopoulos, B.; Eleftheriou, A.; Koukis, G.; Rozos, D.; Angelidis, C. Macroseismic, geological and tectonic observations in the area affected by the earthquakes of the Corinthian Gulf (February–March 1981). In Proceedings of the International Symposium on the Hellenic Arc and Trench (H.E.A.T.), Athens, Greece, 8–11 April 1981.
141. Papanikolaou, I.D.; Papanikolaou, D.I.; Lekkas, E.L. Advances and limitations of the Environmental Seismic Intensity scale (ESI 2007) regarding near-field and far-field effects from recent earthquakes in Greece: Implications for the seismic hazard assessment. *Geol. Soc. Lond. Spec. Publ.* **2009**, *316*, 11–30. [[CrossRef](#)]
142. Eleftheriou, A.; Mouyiaris, N. *Macroseismic Reconnaissance in the Area of Cephalonia-Zakynthos (Earthquakes 17 & 19-1-83)*; Monograph; Institute of Geological and Mineral Research: Athens, Greece, 1983.
143. Fountoulis, I. The neotectonic macrostructures and the geological basement, the main factors controlling the spatial distribution of the damage and geodynamic phenomena resulting from the Kalamata (13 September 1986) and Athens (7 September 1999) earthquakes. In *Earthquake Geodynamics: Seismic Case Studies*; Lekkas, E.L., Ed.; Advances in Earthquake Engineering, Earthquake Geodynamics—Seismic Case Studies; WIT Press: Southampton, UK, 2004; Volume 12, pp. 45–63.
144. Delibasis, N.D.; Darkopoulos, J.C. The Milos island earthquake of March 20, 1992 and its tectonic significance. *PAGEOPH* **1993**, *141*, 43–58. [[CrossRef](#)]
145. Papadopoulos, G.A. The 20 March 1992 South Aegean, Greece, earthquake (Ms= 5.3): Possible anomalous effects. *Terra Nova* **1993**, *5*, 399–404. [[CrossRef](#)]
146. Koukouvelas, I.; Mpresiakas, A.; Sokos, E.; Doutsos, T. The tectonic setting and earthquake ground hazards of the 1993 Pyrgos earthquake, Peloponnese, Greece. *J. Geol. Soc.* **1996**, *153*, 39–49. [[CrossRef](#)]
147. Pavlides, S.B.; Zouros, N.C.; Chatzipetros, A.A.; Kostopoulos, D.S.; Mountrakis, D.M. The 13 May 1995 western Macedonia, Greece (Kozani Grevena) earthquake; preliminary results. *Terra Nova* **1995**, *7*, 544–549. [[CrossRef](#)]
148. Papanastasiou, D.; Gaki-Papanastasiou, K. The Aegean earthquake (15-6-1995), seismotectonic observations and geo-morphic effects on the natural environment. In Proceedings of the 4th Panhellenic Geographical Conference, Athens, Greece, 12–14 October 1995.
149. Papanikolaou, D.; Chronis, G.; Lykousis, B.; Sakellariou, D.; Papoulia, I. Neotectonic Structure of W. Gulf of Corinth and Geodynamic Phenomena of the Aegion Earthquake. In Proceedings of the 5th Hellenic Oceanography & Fish. Symposium, Kavala, Greece, 15–18 April 1997.
150. Bernard, P.; Briole, P.; Meyer, B.; Lyon-Caen, H.; Gomez, J.M.; Tiberi, C.; Berge, C.; Cattin, R.; Hatzfeld, D.; Lachet, C.; et al. The Ms = 6.2, June 15, 1995 Aigion earthquake (Greece): Evidence for low angle normal faulting in the Corinth rift. *J. Seismol.* **1997**, *1*, 131–150. [[CrossRef](#)]
151. Mariolakos, I.; Fountoulis, I.; Mariolakos, D. Deformation structures at the Gulf of Corinth, Greece, induced by the Egean Earthquake of 15-6-1995. In Proceedings of the 8th IAEG Congress, Vancouver, BC, Canada, 21–26 September 1998.
152. Papadopoulos, G.A.; Ganas, A.; Koukouvelas, I. Landsliding phenomena in NW Peloponnese, Greece: A test-site of the EC LEWIS research project. *Geophys. Res. Abstr.* **2006**, *8*, 04402.
153. Mariolakos, I.; Fountoulis, I.; Mariolakos, D.; Andreadakis, M.; Georgakopoulos, A. Geodynamic phenomena observed during the Athens earthquake (Ms=5.9) 7-9-99. *Ann. Geol. Pays Hellen.* **2000**, *38*, 175–186.
154. Margaritis, B.; Papaioannou, C.; Theodulidis, N.; Savvaidis, A.; Anastasiadis, A.; Klimis, N.; Makra, K.; Demosthenous, M.; Karakostas, C.; Lekidis, V.; et al. *Preliminary Observations on the August 14, 2003 Lefkada Island (Western Greece) Earthquake*, EERI Special Earthquake Report, Nov. 2003; Joint report by Institute of Engineering Seismology and Earthquake Engineering, National Technical University of Athens and University of Athens; Institute of Engineering Seismology and Earthquake Engineering: Athens, Greece, 2003; pp. 1–12.

155. Pavlides, S.B.; Papadopoulos, G.A.; Ganas, A.; Papathanassiou, G.; Karastathis, V.; Keramydas, D.; Fokaefs, A. The 14 August 2003 Lefkada (Ionian Sea) Earthquake. In Proceedings of the 5th International Symposium on Eastern Mediterranean Geology, Thessaloniki, Greece, 14–20 April 2004; pp. 14–20.
156. Lekkas, E.; Danamos, G.; Lozios, S.; Skourtsos, E.; Verykiou, E. Geographical distribution of landslides in the Lefkada earthquake (14 August 2003) and factors favoring their occurrence. In Proceedings of the 10th International Congress of the Greek Geological Society, Thessaloniki, Greece, 15–17 April 2004; pp. 130–131.
157. Papathanassiou, G.; Pavlides, S.; Ganas, A. The 2003 Lefkada earthquake: Field observations and preliminary microzonation map based on liquefaction potential index for the town of Lefkada. *Eng. Geol.* **2005**, *82*, 12–31. [[CrossRef](#)]
158. Karfakis, I.; Psonis, K. *Report of Macroscopic Observations of Geological Phenomenon Sessions of the March 1st Earthquake in the City of Kalamata in the Prefecture of Messinia*; Institute of Geological and Mining Research: Athens, Greece, 2004; 47p.
159. Institute of Technical Seismology & Antiseismic Structures. The Leonidio Earthquake, M = 6.5, January 6, 2008. 2008. Available online: https://www.itsak.gr/uploads/news/earthquake_reports/Leonidio_2008.pdf (accessed on 20 August 2024).
160. Earthquake Planning and Protection Organization (EPPO). Rhodes 2008. Available online: <https://oasp.gr/node/7141> (accessed on 15 October 2024).
161. Lekkas, E.L.; Mavroulis, S.D. Earthquake environmental effects and ESI 2007 seismic intensities of the early 2014 Cephalonia (Ionian Sea, Western Greece) earthquakes (January 26 and February 3, Mw 6.0). *Nat. Hazards* **2015**, *78*, 1517–1544. [[CrossRef](#)]
162. Lekkas, E.L.; Mavroulis, S.D. Fault zones ruptured during the early 2014 Cephalonia Island (Ionian Sea, Western Greece) earthquakes (January 26 and February 3, Mw 6.0) based on the associated co-seismic surface ruptures. *J. Seismol.* **2016**, *20*, 63–78. [[CrossRef](#)]
163. Lekkas, E.; Mavroulis, S.; Carydis, P.; Alexoudi, V. The 17 November 2015 Mw 6.4 Lefkas (Ionian Sea, Western Greece) Earthquake: Impact on Environment and Buildings. *Geotech. Geol. Eng.* **2018**, *36*, 2109–2142. [[CrossRef](#)]
164. Lekkas, E.; Mavroulis, S. The Mw 6.8 October 26, 2018 Zakynthos (Ionian Sea, Greece) Earthquake. *Newsl. Environ. Disaster Crisis Manag. Strateg.* **2018**, *10*, 1–63.
165. Ibsen, M.-L.; Brunnsden, D. The nature, use and problems of historical archives for the temporal occurrence of landslides, with specific reference to the south coast of Britain, Ventnor, Isle of Wight. *Geomorphology* **1996**, *15*, 241–258. [[CrossRef](#)]
166. Dominguez Cuesta, M.J.; Jiménez Sánchez, M.; Rodríguez Garcia, A. Press archives as temporal records of landslides in the North of Spain: Relationships between rainfall and instability slope events. *Geomorphology* **1999**, *30*, 125–132. [[CrossRef](#)]
167. Calcaterra, D.; Parise, M. The contribution of historical information in the assessment of the landslide hazards. In *The Use of Historical Data in Natural Hazards Assessment*; Glade, T., Albini, P., Frances, F., Eds.; Kluwer: Norwell, MA, USA, 2001; pp. 201–217.
168. Calcaterra, D.; Parise, M.; Palma, B. Combining historical and geological data for the assessment of the landslide hazard: A case study from Campania, Italy. *Nat. Hazards Earth Syst. Sci.* **2003**, *3*, 3–16. [[CrossRef](#)]
169. Mavroulis, S.; Lekkas, E. Special Issue on Mapping, Monitoring and Assessing Disasters. *Appl. Sci.* **2023**, *13*, 963. [[CrossRef](#)]
170. Hatzfeld, D.; Kassaras, I.; Panagiotopoulos, D.; Amorese, D.; Makropoulos, K.; Karakaisis, K.; Coutant, O. Microseismicity and strain pattern in northwestern Greece. *Tectonics* **1995**, *14*, 773–785. [[CrossRef](#)]
171. Papazachos, B.C.; Comninakis, P.E. Deep structure and tectonics of the Eastern Mediterranean. *Tectonophysics* **1978**, *46*, 285–296. [[CrossRef](#)]
172. Voidomatis, P. Some aspects of seismotectonic synthesis in the North Aegean Sea and surrounding area. *Boll. Geofis. Teor. Appl.* **1989**, *31*, 49–61.
173. Peduzzi, P. Landslides and vegetation cover in the 2005 North Pakistan earthquake: A GIS and statistical quantitative approach. *Nat. Hazards Earth Syst. Sci.* **2010**, *10*, 623–640. [[CrossRef](#)]
174. Sidle, R.C.; Gomi, T.; Usuga, J.C.L.; Jarihani, B. Hydrogeomorphic processes and scaling issues in the continuum from soil pedons to catchments. *Earth-Sci. Rev.* **2017**, *175*, 75–96. [[CrossRef](#)]
175. Ritonga, R.P.; Gomi, T.; Tarigan, S.D.; Kaswanto, R.L.; Kharismalatri, H.S.; Noviandi, R.; Arata, Y.; Ishikawa, Y. Land Cover and Characteristics of Landslides Induced by the 2018 Mw 6.7 Eastern Iburi Earthquake, Hokkaido. *Int. J. Eros. Control. Eng.* **2021**, *13*.
176. Hong, N.M.; Chu, H.J.; Lin, Y.P.; Deng, D.P. Effects of land cover changes induced by large physical disturbances on hydrological responses in Central Taiwan. *Environ. Monit. Assess.* **2010**, *166*, 503–520. [[CrossRef](#)] [[PubMed](#)]
177. Gawthorpe, R.L.; Leeder, M.R.; Kranis, H.; Skourtsos, E.; Andrews, J.E.; Henstra, G.A.; Mack, G.H.; Muravchik, M.; Turner, J.A.; Stamatakis, M. Tectono-sedimentary evolution of the Plio-Pleistocene Corinth rift, Greece. *Basin Res.* **2018**, *30*, 448–479. [[CrossRef](#)]
178. Skourtsos, E.; Kranis, H. Structure and evolution of the western Corinth Rift, through new field data from the Northern Peloponnesus. In *Extending a Continent: Architecture, Rheology and Heat Budget*; Ring, U., Wernicke, B., Eds.; Geological Society of London, Special Publication: London, UK, 2009; Volume 321, pp. 119–138.
179. Lekkas, E.; Kranis, H.; Voulgaris, N. The Sophades (Thessaly) earthquake revisited: Morphotectonic analysis of the Ekkara fault system and seismic risk assessment of SW Thessaly. *Geophys. Res. Abstr.* **2007**, *9*, 07897.

180. Papazachos, G.; Papazachos, C.; Skarlatoudis, A.; Kkallas, H.; Lekkas, E. Modelling macroseismic observations for historical earthquakes: The cases of the M = 7.0, 1954 Sofades and M = 6.8, 1957 Velestino events (central Greece). *J. Seismol.* **2015**, *20*, 151–165. [[CrossRef](#)]
181. Mavroulis, S.; Mavrouli, M.; Lekkas, E.; Tsakris, A. Managing Earthquake Debris: Environmental Issues, Health Impacts, and Risk Reduction Measures. *Environments* **2023**, *10*, 192. [[CrossRef](#)]
182. Jibson, R.W. A Public Health Issue Related to Collateral Seismic Hazards: The Valley Fever Outbreak Triggered by the 1994 Northridge, California Earthquake. *Surv. Geophys.* **2002**, *23*, 511–528. [[CrossRef](#)]
183. Stevens, D.A. Coccidioidomycosis. *N. Engl. J. Med.* **1995**, *332*, 1077–1082. [[CrossRef](#)]
184. Schneider, E.; Hajjeh, R.A.; Spiegel, R.A.; Jibson, R.W.; Harp, E.L.; Marshall, G.A.; Gunn, R.A.; McNeil, M.M.; Pinner, R.W.; Baron, R.C.; et al. A coccidioidomycosis outbreak following the Northridge, Calif, earthquake. *J. Am. Med. Assoc. JAMA* **1997**, *277*, 904–908. [[CrossRef](#)]
185. Kouskouna, V.; Makropoulos, K. Historical earthquake investigations in Greece. *Ann. Geophys.* **2004**, *47*, 723–731. [[CrossRef](#)]
186. Luino, F.; Barriendos, M.; Gizzi, F.T.; Glaser, R.; Gruetzner, C.; Palmieri, W.; Porfido, S.; Sangster, H.; Turconi, L. Historical Data for Natural Hazard Risk Mitigation and Land Use Planning. *Land* **2023**, *12*, 1777. [[CrossRef](#)]
187. Glade, T. Landslide hazard assessment and historical landslide data—An inseparable couple? In *The Use of Historical Data in Natural Hazard Assessments—Advances of Technological and Natural Hazard Research*; Glade, T., Albini, P., Frances, F., Eds.; Kluwer: Norwell, MA, USA, 2001; pp. 153–169.
188. Ferrario, M.F. Landslides triggered by multiple earthquakes: Insights from the 2018 Lombok (Indonesia) events. *Nat. Hazards* **2019**, *98*, 575–592. [[CrossRef](#)]
189. Miao, Z.; Pu, M.; He, Y.; Li, K.; Peng, R.; Chen, S.; Jiang, C.; Deng, B.; He, Z. Evaluation of seismic landslide susceptibility by integrating statistical learning model and newmark model—A case study of the Wenchuan earthquake. *Adv. Trans. Eng.* **2021**, *19*, 223–233. [[CrossRef](#)]
190. Robinson, T.R.; Rosser, N.J.; Densmore, A.L.; Williams, J.G.; Kincey, M.E.; Benjamin, J.; Bell, H.J.A. Rapid post-earthquake modelling of coseismic landslide intensity and distribution for emergency response decision support. *Nat. Hazards Earth Syst. Sci* **2017**, *17*, 1521–1540. [[CrossRef](#)]
191. Dahlquist, M.P.; West, A.J. Initiation and Runout of Post-Seismic Debris Flows: Insights From the 2015 Gorkha Earthquake. *Geophys. Res. Lett.* **2019**, *46*, 9658–9668. [[CrossRef](#)]
192. Zhou, J.; Cui, P.; Yang, X. Dynamic process analysis for the initiation and movement of the donghekou landslide-debris flow triggered by the wenchuan earthquake. *J. Asian Earth Sci* **2013**, *76*, 70–84. [[CrossRef](#)]
193. Williams, J.G.; Rosser, N.J.; Kincey, M.E.; Benjamin, J.; Oven, K.J.; Densmore, A.L.; Milledge, D.G.; Robinson, T.R.; Jordan, C.A.; Dijkstra, T.A. Satellite-based emergency mapping using optical imagery: Experience and reflections from the 2015 Nepal earthquakes. *Nat. Hazards Earth Syst. Sci.* **2018**, *18*, 185–205. [[CrossRef](#)]
194. Lekkas, E.; Mavroulis, S.; Kourou, A.; Manousaki, M.; Thoma, T.; Karveleas, N. *The October 30, 2020, Mw = 6.9, Samos (Eastern Aegean Sea, Greece) Earthquake: Preparedness and Emergency Response for Effective Disaster Management*; Joint Report of National and Kapodistrian University of Athens and Earthquake Planning and Protection Organization; National and Kapodistrian University of Athens: Athens, Greece, 2020; pp. 1–53. [[CrossRef](#)]
195. Gill, J.C.; Malamud, B.D. Reviewing and visualizing the interactions of natural hazards. *Rev. Geophys.* **2014**, *52*, 680–722. [[CrossRef](#)]
196. Gill, J.C.; Malamud, B.D. Hazard interactions and interaction networks (cascades) within multi-hazard methodologies. *Earth Syst. Dyn.* **2016**, *7*, 659–679. [[CrossRef](#)]
197. Mavroulis, S.; Mavrouli, M.; Kourou, A.; Thoma, T.; Lekkas, E. Multi-Hazard Emergency Response for Geological Hazards Amid the Evolving COVID-19 Pandemic: Good Practices and Lessons Learned from Earthquake Disaster Management in Greece. *Sustainability* **2022**, *14*, 8486. [[CrossRef](#)]

Disclaimer/Publisher’s Note: The statements, opinions and data contained in all publications are solely those of the individual author(s) and contributor(s) and not of MDPI and/or the editor(s). MDPI and/or the editor(s) disclaim responsibility for any injury to people or property resulting from any ideas, methods, instructions or products referred to in the content.